Charles University

2nd Faculty of Medicine

&

The Czech Academy of Sciences

Institute of Experimental Medicine

Study programme: Neurosciences

Zuzana Kočí, MSc.

MESENCHYMAL STROMAL CELLS AND BIOLOGICAL SCAFFOLDS FOR NEURAL TISSUE REGENERATION

PhD. Thesis

Supervisor: Šárka Kubinová, PharmDr., PhD.

Prague, 2018

ABSTRACT

Despite tremendous progress in medicine, injuries of the adult central neural system remain without satisfactory solution. Regenerative medicine employs tissue engineering, cellular therapies, medical devices, gene therapy, or growth factors with the aim to bridge the lesion, re-establish lost connections and enhance endogenous repair in order to restore neural function.

The aim of my thesis was to evaluate therapeutic potential of two approaches, transplantation of human mesenchymal stromal cells (hMSCs) and biological scaffolds derived from extracellular matrix (ECM) for neural regeneration, particularly in models of spinal cord injury (SCI).

First, hMSCs from various sources - bone marrow (BM), adipose tissue (AT) and Wharton´s jelly (WJ) - were isolated and characterized *in vitro*. All cell types met the minimal criteria for MSC phenotype and displayed similar properties in terms of their surface marker expression, differentiation potential, migratory capacity, and secretion of cytokines and growth factors. On the other hand, the cell yield from WJ and AT was significantly higher, and MSCs isolated from these tissues proliferated better than from BM.

Therapeutic effect of intrathecal application of hWJ-MSCs was then evaluated in SCI compression model in rats. The effect of low (0.5 million) and high (1.5 million) dose of hWJ-MSCs in a single or repeated (3x) application was compared. We demonstrated that transplantation of single as well as repeated application of high cell dose had apparent beneficial effect on neural tissue repair and resulted in a better grey matter sparing and increased number of GAP43+ axons, reduced astrogliosis, and reduced expression of inflammatory and apoptotic markers. Significant recovery of functional outcome was reported in all cell-treated groups except for the single application of the low number of cells. We observed that the effect of hWJ-MSCs was augmented with the dosage and was further potentiated by repeated application.

In the third part of this project, we prepared biologic ECM hydrogels by decellularization of central nervous tissue (CNS: porcine brain and spinal cord) and non-CNS tissues (porcine urinary bladder and human umbilical cord) that were used alone and in combination with hWJ-MSCs to bridge the SCI lesion. Hydrogels from all ECM were characterized in terms of composition, mechanical and biological properties.

In vitro comparison of ECM hydrogels showed that despite the different origin, topography and composition, all ECM hydrogels similarly promoted the migration of hMSCs and differentiation of neural stem cells, as well as axonal outgrowth.

The effect of porcine tissue-derived spinal cord (SC) ECM and urinary bladder (UB) ECM hydrogels was evaluated *in vivo* after their injection into a hemisection cavity in rats. Both ECM hydrogels integrated well into the lesion and stimulated neovascularization and axonal ingrowth. Gene expression analysis revealed significant down-regulation of genes related to immune response and inflammation in both hydrogel types at 2 weeks post-SCI. However, no tissue specific effect was found for CNS-derived SC-ECM when compared to non-CNS UB-ECM. In addition, the combination of hWJ-MSCs with SC-ECM did not further promote ingrowth of axons and blood vessels into the lesion when compared with the SC-ECM hydrogel alone.

In conclusion, results from this project show that both hWJ-MSCs and ECM hydrogels represent promising ways which may contribute to neural tissue regeneration, and therefore, are strong candidates for translation into the clinical setting. We confirmed the beneficial effect of hWJ-MSCs in SCI and proposed repeated intrathecal application as convenient treatment approach. While hWJ-MSCs transplantation has already been transferred into the clinical trials, the production of ECM hydrogels needs to be further optimized for neural tissue applications especially in terms of their fast *in vivo* degradation.

Key words: regeneration, neural tissue, spinal cord injury, mesenchymal stromal cells, bone marrow, adipose tissue, Wharton´s jelly, extracellular matrix, hydrogel, umbilical cord

ABSTRAKT

Navzdory obrovskému pokroku v medicíně zůstává poranění centrálního nervového systému bez uspokojivého řešení. Regenerativní medicína využívá tkáňové inženýrství, buněčnou terapii, zdravotní protetiku, genovou terapii nebo růstové faktory s cílem přemostit lézi, opravit poškozená spojení a zlepšit endogenní regeneraci tak, aby došlo k obnově neurální funkce.

Cílem mé práce bylo zhodnotit terapeutický potenciál dvou přístupů, transplantace lidských mezenchymálních stromálních buněk (hMSC) a biologických hydrogelů získaných z extracelulární matrix (ECM) v regeneraci nervové tkáně u modelů míšního poranění.

První část práce je věnovaná charakterizaci hMSC z různých zdrojů – kostní dřeně (KD), tukové tkáně (AT) a Whartonova rosolu (WJ). Všechny typy buněk splnily minimální kritéria pro fenotyp MSC a vykazovaly podobné vlastnosti z hlediska exprese povrchových markerů, diferenciačního potenciálu, migrační kapacity a sekrece cytokinů a růstových faktorů. Pupečníková a tuková tkáň však vzhledem ke kostní dřeni poskytovaly významně vyšší výtěžky buněk a MSCs izolované z těchto tkání proliferovaly lépe než hBM-MSCs.

Terapeutický účinek intratekální aplikace hWJ-MSC byl posléze vyhodnocen na kompresním modelu míšního poranění u potkanů. Byl porovnán účinek nízké (0,5 milionu) a vysoké (1,5 milionu) dávky hWJ-MSC v jedné nebo opakované (3x) aplikaci. Jednorázová i opakovaná transplantace vysoké dávky buněk měla zjevný příznivý účinek na regeneraci nervové tkáně a vyústila ve větší zachování šedé hmoty a zvýšení počtu GAP43+ axonů, snížení astrogliózy, snížení exprese zánětlivých a apoptotických markerů. Významné obnovení funkčního výsledku bylo pozorováno ve všech buněčných skupinách s výjimkou jednorázové aplikace nízkého počtu buněk. Pozorovali jsme, že účinek hWJ-MSC se zvyšoval v závislosti od dávky a byl dále potencován opakovanou aplikací.

Ve třetí části tohoto projektu jsme připravili biologické ECM hydrogely decelularizací tkáně centrální nervové soustavy (CNS: prasečího mozku a míchy) a jiných tkání (prasečí močový měchýř a lidská pupeční šňůra). Tyto byly implantovány samostatně a v kombinaci s hWJ-MSCs, aby přemostili lézi míšního poranění. Hydrogely ze všech typů ECM byly charakterizovány z hlediska složení, mechanických a biologických vlastností.

In vitro srovnání ECM hydrogelů ukázalo, že i přes různý původ, topografii a složení mají všechny ECM hydrogely podobné biologické účinky na migraci hMSC, diferenciaci neurálních kmenových buněk a růst axonů.

ECM hydrogely připravené z prasečí míchy (SC) a močového měchýře (UB) byly hodnoceny *in vivo* po jejich implantaci do míšní hemisekce u potkanů. Oba typy ECM hydrogelů byly dobře integrovány do léze a stimulovaly neovaskularizaci a axonální růst. Analýza genové exprese prokázala významné snížení exprese genů souvisejících s imunitní odpovědí a zánětem u obou typů hydrogelů. Nebyl však prokázán benefiční účinek tkáňově specifického ECM hydrogelu izolovaného z SC. Kombinace hWJ-MSC s SC-ECM více nepodpořila vrůstání axonů a krevních cév do léze ve srovnání s implantací samotného hydrogelu.

Závěrem, výsledky této práce ukazují, že oba studované přístupy, transplantace hWJ-MSC i přemostění léze pomocí ECM hydrogelů mají pozitivní vliv na regeneraci nervové tkáně a jsou proto silnými kandidáty na translaci do klinického prostředí. Potvrdili jsme hypotézu, že opakované intratekální podání hWJ-MSC vedlo k potenciaci terapeutického efektu kmenových buněk po míšním poranění a tento léčebný postup je také vhodný pro klinickou praxi. Zatímco transplantace hWJ-MSC je již ověřována v klinických studiích, přípravu ECM hydrogelů je třeba dále optimalizovat, zejména pokud jde o jejich rychlou *in vivo* degradaci.

Klíčová slova: regenerace, nervová tkáň, míšní poranění, mezenchymální stromální buňky, kostní dřeň, tuková tkáň, Whartonův rosol, extracelulární matrix, hydrogel, pupečník

Prohlášení:

Prohlašuji, že jsem závěrečnou práci zpracovala samostatně a že jsem řádně uvedla a citovala všechny použité prameny a literaturu. Současně prohlašuji, že práce nebyla využita k získání jiného nebo stejného titulu.

Nesouhlasím s trvalým uložením elektronické verze mé práce v databázi systému meziuniverzitního projektu Theses.cz za účelem soustavné kontroly podobnosti kvalifikačních prací.

Declaration:

I declare that I have worked on the final thesis alone and that I have properly quoted and cited all the sources and literature used. Also, I declare that the work has not been used to obtain another or the same title.

I disagree with the permanent storage of the electronic version of my thesis in the database of the inter-university projects Thesis.cz that systematically checks the similarity of the qualification work.

In Prague, 20.4.2018

Mgr. Zuzana Kočí

Use this reference as:

KOČÍ, Zuzana. *Mesenchymal stromal cells and biological scaffolds for neural tissue regeneration.* Praha, 2018. 138 p., Ph.D. thesis. 2nd Faculty of Medicine, Charles University in Prague, Department of Biomaterials and Biophysical methods, Institute of Experimental Medicine, The Czech Academy of Sciences.

Thesis supervisor: Kubinová, Šárka.

Acknowledgements

I want to express my gratitude to my supervisor Dr Šárka Kubinová for her professional and personal leadership. Her ability to keep me motivated and not to lose the focus I appreciate very much.

I would also like to thank Prof Eva Syková who inspired me from the beginning of my PhD course and gave me great opportunities to grow.

My thanks belong to all my colleagues from the former Department of Neuroscience, which was later divided into Department of Biomaterials and Biophysical Methods and Department of Tissue Culture and Stem Cells for any kind of support. In this respect, I want to thank all technicians as well.

Last but not least, I am especially grateful to my broad family: my husband, my parents, my brothers, and my family in-law for their continuous support and belief. My dear friends, who were there for me at all times, deserve my gratitude as well.

CONTENTS

1 LIST OF ABBREVIATIONS

3D	Three-dimensional
Akt1	Serine/threonine-protein Kinase
Arg1	Arginase 1
hASC	Human Adipose Tissue-Derived Stromal Cells
ATP	Adenosine Triphosphate
BBB	Blood-brain Barrier
BBB test	Basso-Beattie-Breshnahan Openfield Locomotor Test
BDNF	Brain Derived Neurotrophic Growth Factor
B-ECM	Brain Derived Extracellular Matrix
hBMNC	Human Bone Marrow Mononuclear Cell Fraction
hBM-MSCs	Human Bone Marrow Mesenchymal Stromal Cells
bp	Base Pair
C	Carbon
Casp3	Caspase 3 (gene)
CD	Cluster of Differentiation
Ccl3 / MIP -1α	Macrophage Inflammatory Protein 1α
Ccl5 / RANTES	Chemokine (C-C Motif) Ligand 5
CNS	Central Nervous System
CM	Cell-cultured Conditioned Media
CS	Chondroitin sulphate
CXCR4	Chemokine (C-X-C Motif) Receptor Type 4
CXCL10 / IP-10	Chemokine (C-X-C Motif) Type 10
cDNA	Complementary Deoxyribonucleic Acid
sDNA	Single-strain DNA
dsDNA	Double-strain DNA
DRG	Dorsal Root Ganglion
ECM	Extracellular Matrix

EDTA	Ethylenediaminetetraacetic Acid
e.g.	For Example
EGF	Epidermal Growth Factor
ESCs	Embryonic stem cells
FACS	Fluorescence Activated Cell Sorting
FASP	Filter-aided Sample Preparation
FBS	Foetal Bovine Serum
bFGF	Basic Fibroblast Growth Factor
GAP43	Growth Associated Protein 43
Gapdh	Glyceraldehyde 3-phosphate Dehydrogenase (gene)
GDNF	Glial-Derived Neurotrophic Factor
GFAP	Glial Fibrillary Acidic Protein
GCF	Glial Growth Factor
G-CSF	Granulocyte Colony-stimulating Factor
GlcA	Glucuronic acid
GM-CSF	Granulocyte-macrophage Colony-stimulating Factor
HA	Hyaluronic acid
H&E	Haematoxylin-eosin
HGF	Hepatocyte Growth Factor
hMSCs	Human Mesenchymal Stromal Cells
HuCNS-SC	Human Foetal-Derived Neural Progenitor Cells
Hyp	Hydroxyproline
ChABC	Chondroitinase ABC
dH_2O	Deionized Water
Ig	Immunoglobulin
IHC	Immunohistochemistry
IDO	Indoleamine 2,3-dioxygenase
i.e.	That Is

ICAM-1 **/ CD54**	Intercellular Adhesion Molecule 1
IFNγ	Interferon Gamma
IGF-1	Insulin-like Growth Factor 1
IL	Interleukin
i.m.	Intramuscular
i.p.	Intraperitoneal
IP-10 / CXCL10	Interferon gamma-induced protein 10
iPSCs	Induced Pluripotent Stem Cells
Irf5	Interferon Regulatory Factor 5 (gene)
i.v.	Intravenous
i.t.	Intrathecal
LC-MS	Liquid Chromatography-Mass Spectrometry
LIF	Leukaemia Inhibitory Factor
M-CSF	Macrophage Colony-stimulating Factor
MAI	Myelin – Associated Inhibitors
MAG	Myelin-Associated Glycoprotein
MAP2	Microtubule Associated Protein 2
MCP1	Monocyte Chemoattractant Protein 1
MIP-1α	Macrophage Inflammatory Protein 1α
Mins	Minutes
MPSS	Methylprednisolone
Mrc1	Mannose Receptor C-Type 1 (gene)
mRNA	Messenger Ribonucleic Acid
MTCO2	Human Cytochrome C oxidase subunit II
N/A	Not Applicable
NCAM	Neural-cell Adhesion Molecule
NCSC	Neural Crest Stem Cell
Nestin	Type IV Intermediate Filament Protein

NF (70; 160)	Neurofilament (70; 160)
NG2	Chondroitin Sulphate Proteoglycan Neuron- glia Antigen 2; type of glial cells
NGF	Neuronal Growth Factor
NGFR / CD271 / p75	Nerve Growth Factor Receptor
NgR	Nogo-66 Receptor
NCS	Neural Stem Cells
NO	Nitric oxide
Nos2	Inducible Nitric Oxide Synthase 2 (gene)
Nrp-1	Neuropilin 1
NT3 / Sort1	Neurotrophin Type 3
OEC	Olfactory Ensheating Cell
OPC	Oligodendrocyte Precursor Cell
p75 / NGFR/ CD271	Nerve Growth Factor Receptor
PAN/PVC	Polyacrylonitrile/polyvinylchloride
PBS	Phosphate-Buffered Saline
PCL	Poly(ε-caprolactone)
PD	Population doubling
cPD	Cumulative Population Doubling
PDT	Population Doubling Time
PEDOT	Poly(3, 4-ethylendioxythiopene)
PEG	Polyethylene Glycol
PGA	Poly(glycolic acid)
PGE2	Prostaglandin E2
PHEMA	Poly(2-hydroxyethylmethacrylate)
PHPMA	Poly[N-(2-hydroxypropyl)methacrylate]
PlGF	Placental Growth Factor
PLA	Poly(lactic acid)

PLCL	Poly(lactic-co-caprolactone)
PLGA	Poly(lactic-co-glycolic acid)
PNN	Perineural Net
p.o.	Perorally
PP	Polypyrolle
ppm	Pars-per-million
P/S	Penicillin/Streptomycin
Ptgs2	Prostaglandin-endoperoxide Synthase 2 (gene)
PTFE	Poly(tetrafluoroethylene)
PVA	Polyvinyl Alcohol
PVDF	Polyvinylidene Fluoride
qRT-PCR	Quantitative Real-Time Polymerase Chain Reaction
RANTES / Ccl5	Regulated on Activation, Normal T-cell Expressed and Secreted
RECA	Anti-endothelial Cell Antibody
ROS	Reactive Oxygen Species
s.c.	Subcutaneous
SC-ECM	Spinal Cord-derived Extracellular Matrix
SCF	Stem Cell Factor
SCI	Spinal Cord Injury
SDF-1	Stromal Cell-derived Factor 1
SEM	Scanning Electron Microscope
Sort1 / NT3	Neurotrophin Type 3
SVF	Stromal Vascular Fraction
TCP	Tissue Culture Polystyrene
TE	Tissue Engineering
TNF-α	Tumour Necrosis Factor Alpha
Tn-R	Tenascin-R
TGF-α(β)	Transforming Growth Factor-alpha(beta)

TrkA(B, C)	Tropomyosin Related Kinase A (B, C)
UB-ECM	Urinary Bladder Extracellular Matrix
UC-ECM	Umbilical Cord Extracellular Matrix
VCAM-1 / CD106	Vascular cell adhesion molecule
VEGF-A	Vascular Endothelial Growth Factor A
Vimentin	Type III Intermediate Filament
hWJ-MSCs	human Wharton´s Jelly Mesenchymal Stromal Cells
Wnt	Wingless/int-1

2 INTRODUCTION

2.1 REGENERATION

Regeneration is a survival mechanism that allows an organism to restore lost and damaged tissues or organs with identical structure and function. This inherent capacity of organisms is subject of a study of the Regenerative Medicine field, which aims to recapitulate regenerative processes in order to restore tissue function that has been damaged by trauma, disease or birth defects (Naranjo et al. 2016). The tools to realize these outcomes are tissue engineering (TE), cellular therapies, medical devices, gene therapy and soluble molecules (Fig. 1). Moreover, combinations of these approaches can amplify the healing process.

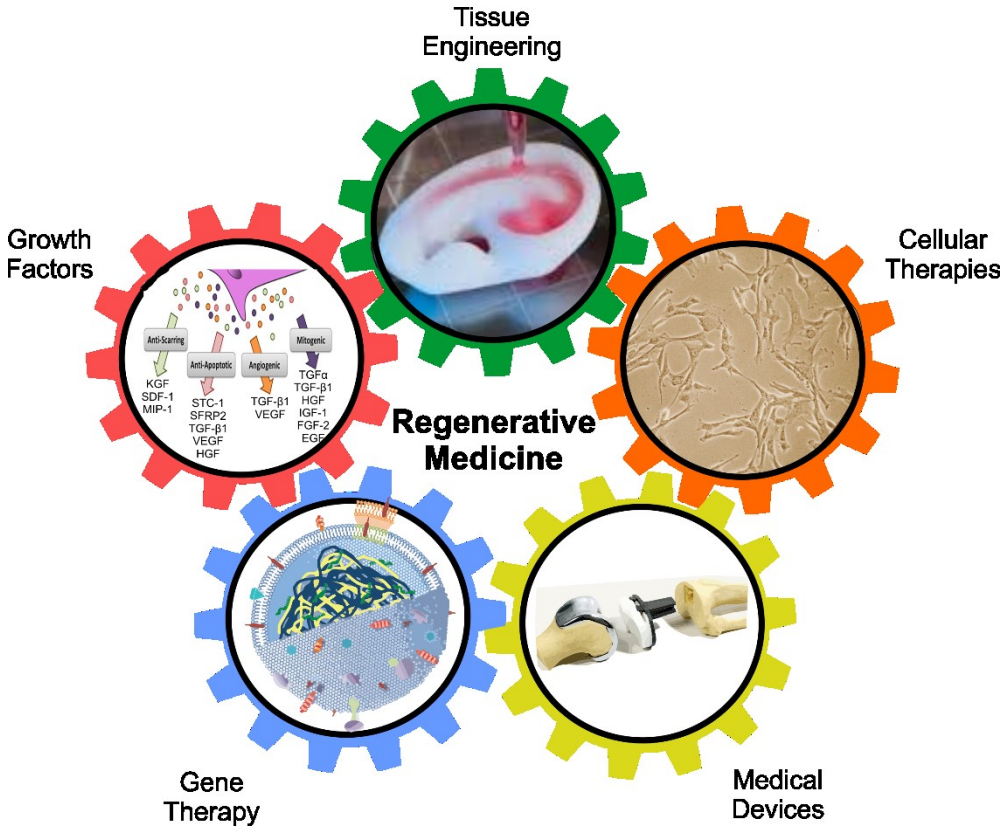

Fig. 1. Tools of Regenerative Medicine field. Indidual pictures taken from (clockwise) http://www.avensonline.org/blog/1045.html, human mesenchymal stromal cell culture, https://safis-solutions.com/regulatory-compliance/medical-devices-2/, https://www.intechopen.com/books/gene-therapy-tools-and-potential-applications/cancer-gene-therapy-key-biological-concepts-in-the-design-of-multifunctional-non-viral-delivery-syst, https://www.intechopen.com/books/advanced-techniques-in-bone-regeneration/stem-cells-for-bone-regeneration-role-of-trophic-factors.

2.2 THE SPINAL CORD

The spinal cord is one of two constituents of the Central Nervous System (CNS). It relays afferent and efferent signals and connects the brain to the periphery. Spinal cord is a centre for coordinating reflexes and contains reflex arcs and central pattern generators.

The spinal cord lies inside vertebral canal, surrounded by its meninges – dura mater, arachnoidea and pia mater. It begins from medulla oblongata, just above the C1 vertebral lever and ends at the L1-L2 intervertebral space; in between we distinguish cervical, thoracic, lumbar and sacral segments of the spinal cord. From here, long lumbar and sacral nerve roots extend to form the cauda equina. The spinal cord is made of 31 segments from which one pair of sensory nerve root and one pair of motor nerve root branches. The nerve roots then merge into bilaterally symmetrical pairs of spinal nerves.

2.2.1 Gross spinal cord anatomy

On a cross section of the spinal cord, a grey matter has distinct butterfly shape and three pairs of horns can be distinguished: ventral horns contain motoric neuronal bodies; dorsal horns contain sensory neuronal bodies and lateral horns contain visceral neural cell bodies. Apart from neural cell bodies, grey matter houses the terminal synapses of axons from other areas, dendrites and glial cells. In the centre, there is central canal - an extension of the fourth brain ventricle that contains cerebrospinal fluid. Grey matter is surrounded by white matter with sensory (ascending) and motor (descending) myelinated axons, which constitute tracts connecting periphery to CNS (Fig. 2). Sensory (ascending) tracts deliver information about fine touch, pressure, vibration, temperature, pain, and crude touch to the brain. Three major sensory tracts are these: posterior columns - fasciculus gracilis and fasciculus cuneatus, spinothalamic and spinocerebellar tract. Descending tracts deliver the information from the brain to the periphery. Functionally, descending tracts can be divided into two major groups: pyramidal - corticospinal and corticobulbar (innervates non-oculomotor cranial nerves, not shown in the picture) – tracts for voluntary control of the musculature, and extrapyramidal – reticulospinal, vestibulospinal, rubrospinal, tectospinal – tracts for automatic control of the musculature such as muscle tone, balance and posture.

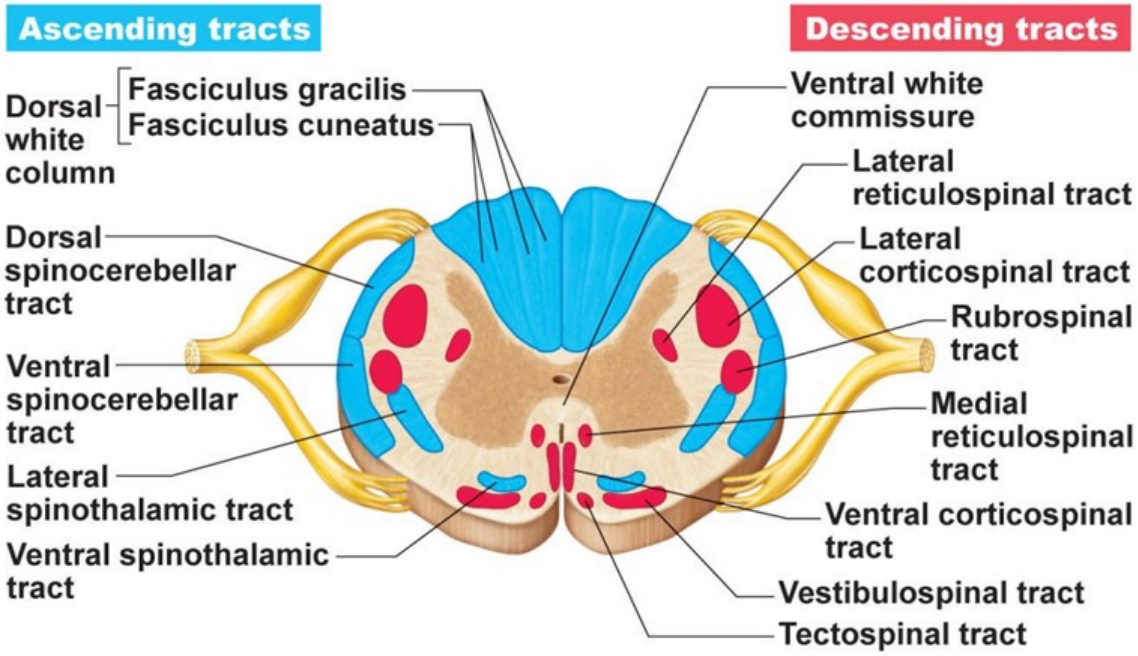

Fig. 2. Simplified scheme to show the position of the main ascending and descending spinal cord tracts. Illustration from http://lexusorganics.com/blog/descending-ascending-tracts-of-the-brain/.

At the base of branching of spinal nerves lie dorsal root ganglia (DRGs), also known as spinal ganglia or posterior root ganglia. DRGs form an important connection to CNS. Each DRG consists of cell bodies of primary afferent neurons that bring the sensory information from the periphery to the spinal cord. Fibres heading toward the periphery leave the ganglion through the spinal nerve – where they run together with fibres of motoneurons.

Motoneurons carry information from the CNS to organs, muscles and glands. The interface between a motor neuron and muscle fibre is a specialized synapse called the neuromuscular junction. Upon adequate stimulation, the motor neuron releases neurotransmitters that bind to postsynaptic receptors and trigger a response in the muscle fibre which leads to muscle movement.

2.2.2 Spinal cord injury (SCI)

Spinal cord injury (SCI) is temporary or permanent damage of the spinal cord, usually caused by trauma. The typical SCI patient is a male in his productive age around 15-35 years old injured in a car accident, fall, or sport accident (Medicine 2011). SCI causes loss of muscle function, sensation or autonomic function in parts of the body that are below the lesion. Patients after SCI might experience symptoms from incontinence to complete paralysis depending on the location and severity of spinal cord lesion.

2.2.2.1 Primary injury

The immediate damage happens within a few seconds after the primary insult. The spinal cord is damaged directly by mechanical shearing or stretching, or indirectly by a pressure of fractured bone, both of which cause bleeding, intravenous thrombosis and oedema. Damage to the vasculature results in ischaemia and a production of free radicals and reactive oxygen species (ROS). Necrosis and oxidative stress create ion imbalance and block neural transmission. Intracellular components from damaged cells and excitatory neurotransmitters (glutamate) further harm neurons in the lesion proximity. Given the high vascularity and metabolic demands, the grey matter suffers in this stage more harm than the white matter (Kwon et al. 2004).

2.2.2.2 Secondary injury – acute phase

Acute phase sets 2-48 hours after primary insult and develops into spinal shock (Fig. 3). Pathologic changes spread concentrically from the centre of the lesion. Loss of oxygen perpetuates necrotic cell death. Without proper vasculature cells cannot produce enough adenosine triphosphate (ATP) that maintains the membrane integrity. Cell membranes disrupt, and lysosomal enzymes, together with intracellular ions and neurotransmitters are released into extracellular space. The continuous axonal depolarization from increased glutamate leads to massive increase in intracellular Ca^{2+} that triggers cell death. The ion imbalance – mainly an increase of extracellular K^{+}, ROS, neurotoxic glutamate disrupt the blood-brain barrier (BBB), and allow infiltration of immune cells (Rowland et al. 2008; Tator and Fehlings 1991). The inflammatory reaction caused by leukocytes, macrophages and other immune cells is two-fold – helps to clean the lesion site from cell debris, but on the other hand increases production of inflammatory cytokines and prolongs activation of immune cells that hamper endogenous regeneration. Axonal damage is further pronounced by the disruption of myelin sheath, causing irreversible damage to the white matter.

2.2.2.3 Secondary injury – subacute phase

Subacute phase follows after 2 days till 2 weeks post injury. Hostile environment causes hypertrophy and activation of astrocytes and other glial cells (*e.g.* NG2 glia). In order to limit the harmful events, they surround the lesion side and produce extracellular molecules – chondroitin and keratin sulphate proteoglycans – which form a dense glial scar and hinder the proliferation and migration of neural cells across the lesion (Fig. 3) (Fawcett and Asher 1999). Damaged axons degenerate in both, anterograde and retrograde direction from the lesion site (Eva and Fawcett 2014).

2.2.2.4 Secondary injury – chronic phase

The chronic phase of SCI develops after several weeks after the initial insult (Fig. 3). The patient´s neurological status is stabilized (Christensen and Hulsebosch 1997; McDonald and Belegu 2006), however, on the cellular level, apoptosis, glial scar turnover, axonal demyelination and cyst formation occurs (Christensen and Hulsebosch 1997).

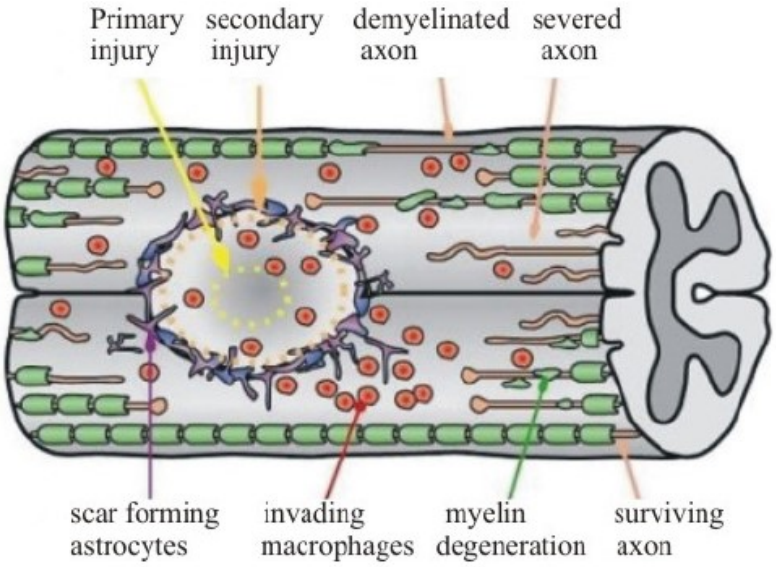

Fig. 3. Physiological events after spinal cord compression. Drawing by Sven Möllers. (Dalton PD and Mej J. 2009).

2.2.3 Endogenous regeneration

The first notice about a regeneration capacity of adult neural tissue comes from the work of Josef Ferdinand Rosenthal (1817 – 1887) and Jan Evangelista Purkyně (1787 - 1867). In his dissertation that contains results and illustrations from Purkyně (Frankenberger 1954), Rosenthal describes *formation granulosa* – granular bodies which were present in embryonal as well as adult tissues and, which as authors presumed, supply lost cells throughout the life (Chvatal 2014).

However, for a long time it had been accepted that once development has ended, the growth and regeneration of neural tissue is stopped irrevocably. Only in 1962, scientist Joseph Altman changed this belief when he reported neurogenesis in mammalian cerebral cortex (Altman 1962) and hippocampus (Altman and Chorover 1963), and his findings were later confirmed by Michael Kaplan and Shirley Bayer (Bayer 1982).

Today, we know, that although limited, endogenous regeneration occurs in both, CNS and peripheral nervous system. Axonal sprouting, neural plasticity and neurogenesis are inherent regenerative properties of neural tissue that to some extend help to overcome the impact of SCI (Huebner and Strittmatter 2009).

Axonal sprouting is very limited as axons lack appropriate components (growth factors and permissive extracellular matrices) and are inhibited by a presence of inhibitory molecules in the lesion. Two major factors contribute to failure of axonal regrowth: myelin – associated inhibitors (MAI) and molecules synthetized by the cellular components of the glial scar (Blesch and Tuszynski 2009; Filbin 2003; Low et al. 2008; Profyris et al. 2004).

MAI, as for example Myelin-associated glycoprotein (MAG), oligodendrocyte myelin glycoprotein (OMGP) and Nogo-A, bind to the growth cone receptor on axons: Nogo-66 receptor (NgR) – and trigger a molecular cascade that eventually results in a collapse of the growth cone. Therefore, MAI inhibit axonal regrowth in the early phase after SCI (Profyris et al. 2004).

Later on, inhibitory molecules such as chondroitin sulphate proteoglycans (CSPGs), chondroitin sulphate proteoglycan neuron-glia antigen 2 (NG2), neurocan, brevican, phosphacan and versican, especially their side chains (Tang et al. 2003), contribute to the formation of a glial scar that serves as a chemical and physical barrier to axonal regrowth (Jones et al. 2003; Murakami and Ohtsuka 2003; Profyris et al. 2004). Netrin, semaphorin and tenascin are other components of the glial scar that have both inhibitory and regenerative effects on axonal regrowth. Tenascin inhibits neurite outgrowth, but can also bind CSPGs and prevents them from forming a glial scar. Netrin and semaphorins are known as axonal guidance molecules during development (Profyris et al. 2004).

Neural plasticity is the capacity of neurons to rearrange their structure and function to adjust to normal development or injury or disease and can be spontaneous or activity-dependent (Dunlop 2008). Appropriate induction and guidance of activity-dependent spinal cord plasticity by rehabilitation support motor function restoration. Spontaneous plasticity is believed to be responsible for improvements in neurological return, respiratory and sexual function (Anderson et al. 2007; Blesch and Tuszynski 2009). However, it is randomly oriented, and may have complications such as increased muscle tonus, autonomic dysreflexia, neuropathic pain and osteoporosis (Blesch and Tuszynski 2009; Dunlop 2008; Christensen and Hulsebosch 1997). Spontaneous plasticity is therefore not always beneficial (Dunlop 2008).

Neurogenesis is a process of gaining new neurons from stem cell that was described in certain parts of the spinal cord - ependymal zone surrounding central canal (Hugnot and Franzen 2011) and subpial white matter zone (Knerlich-Lukoschus et al. 2010). In fact, there is an evidence that after SCI ependymal cells increase 50-fold their proliferation potential (Stenudd et al. 2015), traffic to the injury site (Cizkova et al. 2007) and develop into neurons (Alvarez-Buylla et al. 2008), glial cells associated with scar tissue as well as oligodendrocytes that re-myelinate axons (Meletis et al. 2008).

All above mentioned mechanisms of endogenous repair are important for their stabilization effect; however, they do not have the capacity to functionally repair the damaged spinal cord.

2.2.4 Standard treatment of patients after SCI

After stabilization of patients in the acute phase (within 3-10 hours), an anti-inflammatory agent – e.g. methylprednisolone (MPSS) is administered. The rationale of using MPSS for acute SCI is questioned recently; it is not only expensive (Karsy and Hawryluk 2017), but also it does not significantly improve the neurological deficit. In higher doses, its application is associated with increased morbidity and mortality (Breslin and Agrawal 2012). Some studies though have shown that MPSS has neuroprotective effect and prevent secondary damage of the spinal cord (Kwon et al. 2004).

Generally, patients should start with rehabilitation as early as possible to evoke activity-dependent neuroplasticity. Symptomatic treatment involves pain relief and management of spasticity and other complications (Baptiste and Fehlings 2007). Nevertheless, available pharmacologic intervention is not capable to restore lost function after SCI.

2.2.5 Clinical trials SCI patients

Various drugs and molecules were tested pre-clinically in terms of their neuroprotective and neuroregenerative effects after SCI. Based on promising results obtained in pre-clinical studies, following human clinical trials were also performed, however, their results were ambiguous.

Nowadays (Oct 2017), 694 studies for spinal cord injured patients are listed in clinicaltrials.gov website. Among tested interventions are devices (e.g. motorized bicycle exercise training, ReWalk^{TM}), virtual training, physiotherapy, medical drugs used for other indications (dalfampridine, lithium, selenium, vit E), new medical drugs (ES135, KAI-1678, Cethrin/BA-210, AC105, HP184), biological agents (various stem cells – described in Stem Cell section) or even acupuncture and hypnosis (www.clinicaltrials.gov).

As promising neuroprotective agents for patients with SCI were tested, *e.g.* tirilazad mesylate (Bracken et al. 1997), naloxone (Bracken et al. 1990), tryrotropin-releasing hormone (TRH) (Pitts et al. 1995), minocycline (Casha et al. 2012), granulocyte colony-stimulating factor (G-CSF) (Karsy and Hawryluk 2017; Pan et al. 2008), riluzole (Schwartz and Fehlings 2001), or gacyclidine (Hirbec et al. 2001).

2.2.6 Experimental treatments

In preclinical research, advanced therapies aim to target various aspects of the complex pathophysiology after SCI, such as neuroprotection, remyelination, enhancement of axonal growth, or reduction of glial scarring.

One of the strategies how to improve functional recovery after SCI is blocking of MAI molecules. NgR blocks all three MAI molecules and has been shown to promote corticospinal tract sprouting and behavioural recovery after SCI (Borrie et al. 2012).

Another strategy how to reduce inhibitory environment is enzymatic digestion of the CSPG present in glial scar with the use of chondroitinase ABC (ChABC). ChABC has been shown to promote axonal regeneration and encouraged functional recovery after SCI (Anderson et al. 2009; Tester and Howland 2008). Moreover, digestion of CSPG affects perineuronal nets (PNN) which enhance neural plasticity and lead to morphological and functional improvement (Kwok et al. 2008).

Other pharmacological interventions target enhancement of axonal growth. Administration of growth factors, e.g. epithelial growth factor (EGF) and basic fibroblast growth factor (bFGF) stimulates the proliferation of ependymal cells and showed improved locomotor function after SCI injury in rats (Fahmy and Moftah 2010). Other stimulating growth factors include brain derived neurotrophic growth factor (BDNF), vascular endothelial growth factor (VEGF), stromal derived factor 1 (SDF-1), tropomyosin related kinase B (TrkB), neuropilin 1 (Nrp-1), chemokine (C-X-C motif) receptor type 4 (CXCR4) and nitric oxide (NO) (Ohab et al. 2006).

Given the complexity of SCI, no single repair strategy has been repeatedly successful in promoting full functional recovery. Therefore, combination of above mentioned molecules, growth factors, stem cells and biomaterials (both are discussed further) will probably have synergic effect on SCI (Kubinova and Sykova 2012).

2.2.7 Experimental models of SCI

To evaluate new experimental treatment *in vivo*, the animal models are inevitable.

Animal models help to better understand the pathophysiology after SCI and to test safety and potential effect of various experimental therapies. As SCI model are used small (mice and rat) as well as medium and large sized mammals (cats, dogs or pigs).

The most frequently used model for exploring the neuroprotective strategies for SCI is contusion and compression model. It can be achieved by various methods, including weight-drop model (Allen 1911), or its modification - NYU impactor (Gruner 1992), aneurysmal clamp compression (Rivlin and Tator 1978) or electromagnetic model compression (Behrmann et al. 1992). In our laboratory, we use balloon compression (Fig. 4A) as it produces uniform size of lesion and closely mimics the form of injury which occurs in clinical practice (Vanicky et al. 2001).

To investigate axonal regeneration, models of either complete transection or hemisection (Fig. 4B) are utilized (Hultborn and Malmsten 1983; Zingale 1989). Both models are suitable for biomaterial testing as there is a cavity after surgical removal of spinal cord tissue. Models of chemically induced SCI include injection of excitotoxic quisqualic acid (Yezierski et al. 1998) and photochemical lesion (Verdu et al. 2003).

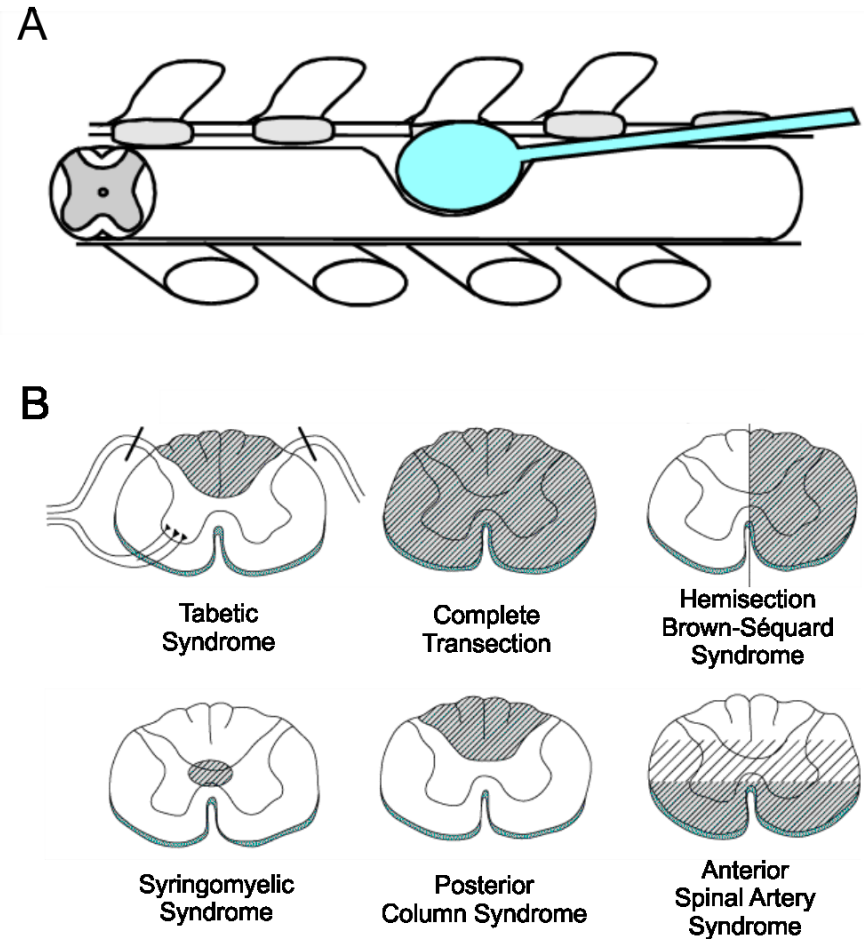

Fig. 4. A) Schematic illustration of balloon compression model of spinal cord injury (SCI). Spinal cord compression is performed by inflation of a balloon catheter (in blue) for 5 minutes (mins) at the thoracic vertebra 8 (Th8) spinal level. B) schematic illustration of different versions of spinal cord hemisection adopted from Ropper and Samuels: Adams & Victor´s Principles of Neurology 9th Edition: http://www.accessmedicine.com.

To assess neurological recovery in SCI models, various locomotor and sensory tests have been developed.

The most often used locomotor evaluation is the open field test that is rated according to a scale developed by Tarlov and Klinger (Kwok et al. 2011) and the Basso, Beattie, Bresnahan test (BBB test) (Basso et al. 1995). BBB test is nowadays used across laboratories making data comparable and unambiguous. Other locomotor tests include the cylinder rearing test, the horizontal ladder test, the catwalk, flat beam walk, or rotarod (Djerbal et al. 2017; Van Meeteren et al. 2003). An automated method for acquiring movement parameters during walking on a ladder beam, over ground walking, wading and swimming is presented *e.g.* by TSE MotoRater System (Bad Homburg, Germany). By detecting the precise position of joints and video recording of their movement from the left and right side and from below at the same time it allows an objective kinematic evaluation of animal movements.

The sensory function is then evaluated with the use of thermal nociception assessment by plantar test or sensitivity to mechanical stimulus using von Frey hair of fibres.

2.3 STEM CELLS

Stem cells are an emerging treatment for SCI. They are primitive, undifferentiated cells that possess a capacity of a self-renewal and can differentiate into multiple cell types. Stem cells can be classified by their differentiation potential and tissue source (Fig. 5).

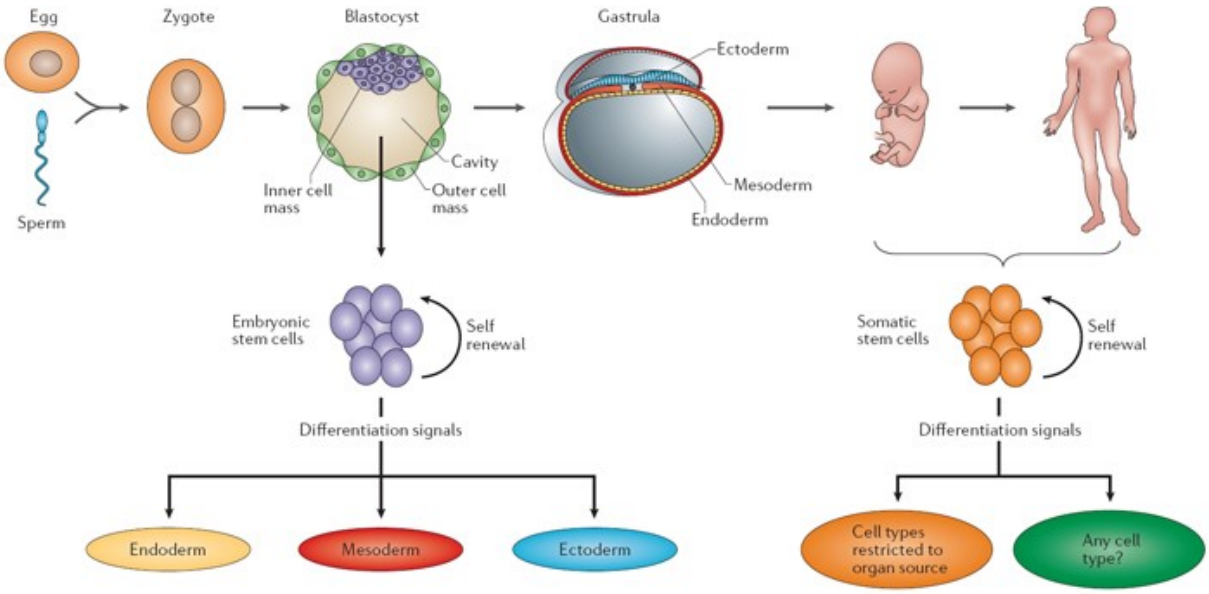

Fig. 5. Different stem cell types from different sources. Adapted from Chial (2008) Gene-based therapeutic approaches. Nature Education 1(1):210.

The most potent are **totipotent stem cells** formed within 1-3 days or embryogenesis after first few divisions of a fertilized egg – in zygote. Totipotent stem cells have the capacity to create an entire organism as they differentiate into embryonic and extra-embryonic cell types (Mitalipov and Wolf 2009).

Pluripotent stem cells lost their ability to form the whole organism, still, they can differentiate into all three germ layers – endoderm, mesoderm and ectoderm (Caplan 1991).

Embryonic stem cells (ESCs) are pluripotent stem cells derived from the inner cell mass within blastocyst (Fig. 5). ESCs have enormous therapeutic potential, but might be rejected by a host organism (Chan et al. 2014), or form tumours; and their isolation is constrained with ethical and legal issues (Caplan 1991). To prevent from tumour formation, they are differentiated into desired cell type. For example, hESCs can be differentiated into motor neurons or oligodendroglial progenitors [reviewed in Peng et al. (2010)]. This strategy was used in phase I clinical trial conducted by Geron Corporation (Menlo Park, CA, USA) where hESC-derived oligodendroglial progenitor cells (GRNOPC1) were utilized in patients with SCI. In spite of good safety profile and no serious adverse events, this study was terminated in November 2011

due to financial reasons. In 2013 Geron´s ESCs division was acquired by biotechnology company Asterias Biotherapeutics, Inc. (Fremont, CA, USA) which started a phase I/II clinical trial (NCT02302157) using oligodendrocyte progenitor cells (AST-OPC1) for subacute SCI in 2014.

Pluripotent stem cells can also be derived from adult differentiated cells without any ethical constrains. A recent breakthrough by Yamanaka in 2006 enabled to gain iPSCs from adult mice fibroblasts by genetic reprogramming, introducing four factors Oct3/4, Sox2, c-Myc, and Klf4 (Takahashi and Yamanaka 2006). Pluripotency has been then induced also in human fibroblasts (Takahashi et al. 2007). iPSCs have become an invaluable source of cells for disease modelling, drug testing and developmental studies. However, before their translation into clinical practice, their safety must be confirmed and transfection efficacy improved.

Foetal stem cells (Fig. 5) are adult stem cells (also called somatic stem cells), with a narrower differentiation potential. Neural stem cells (NSCs), can differentiate into main phenotypes of neural system, therefore hold a great promise for SCI (Salazar et al. 2010). Human foetal-derived neural progenitor cells (HuCNS-SC) were utilized in two phase II clinical trials (NCT01321333, NCT02163876) conducted by StemCells Inc. (Newark, CA, USA) for treatment of patients with SCI. However, both studies were terminated for financial reasons in 2015. The interim data analysis revealed overall motor improvement in patients treated with HuCNS-SC, but the magnitude of the effect did not justify its expensive continuation. Currently, safety of human spinal cord-derived NSCs (HSSC) transplantation for the treatment of chronic SCI is being evaluated in a phase I study (NCT01772810) sponsored by Neuralstem Inc. (Germantown, MD, USA). Autologous neural stem cells with a three-dimensional (3D) biomatrix are tested in a phase I/II clinical trial sponsored by Federal Research Clinical Center of Federal Medical & Biological Agency (Moscow, Russia).

Multipotent mesenchymal stromal cells (MSCs, Fig. 5) are adult (or somatic) stem cells with potential to differentiate into cells of a certain layer – mesoderm that later differentiates into hematopoietic and connective tissue. MSCs were firstly described in bone marrow (BM) by Friendenstein (Friedenstein et al. 1968). Currently, there are more than 35 clinical trials evaluating safety and efficiency of MSCs in the treatment of SCI (Callera and do Nascimento 2006; Geffner et al. 2008; Park et al. 2005; Sykova et al. 2006).

Tissue progenitors can be found in virtually every tissue and are pre-determined to differentiate into the mature tissue cells thus serving for tissue maintenance and repair.

2.3.1 Mesenchymal stromal cells (MSCs)

MSCs are the most frequently used stem cells. According to the International Society for Cellular Therapy (ISCT) position paper (Dominici et al. 2006), MSCs represent a population of cells that:

i) are plastic-adherent;

ii) have positive surface marker expression of CD105, CD73, CD90 while lacking the expression of CD45, CD34, CD14 or CD11b, CD79α or CD19 and HLA-DR;

iii) display multipotent differentiation potential demonstrated as the ability to differentiate into osteoblasts, adipocytes and chondrocytes *in vitro.*

2.3.1.1 MSC sources

BM-MSCs were the first discovered MSCs type and still remain a gold standard in stem cell therapies. hBM-MSCs are usually obtained from iliac crest BM and expanded in a standard cell culture. Adipose tissue (AT) obtained from liposuction serves as an alternative and richer source of MSCs (ASCs) (Zuk et al. 2001; Strioga et al. 2012). MSCs could also be found in neonatal tissue – umbilical blood or cord tissue (Wharton´s jelly MSCs, WJ-MSCs) (Troyer and Weiss 2008), placenta (Gronthos et al. 2001) and amniotic fluid.

Other MSCs sources present skin, synovial fluid, periosteum, dental pulp, hair follicles, intestine, and others.

Different subtypes of stem cells can be isolated and expanded *in vitro* or can be applied as a non-concentrated mixture of stem cells – e.g. BMNC, or stromal vascular fraction from adipose tissue (SVF). Different types of MSCs may share the main mesenchymal features but also differ in expression profile, differentiation capacity or cytokine production (Strioga et al. 2012).

2.3.1.2 Mode of action with the focus on neural repair

The effect of MSC transplantation have been evaluated in various neural tissue injuries or neurodegenerative diseases. After transplantation, MSCs enhanced neural cell survival and neural tissue repair (Geffner et al. 2008; Meirelles Lda et al. 2009; Neuhuber et al. 2005; Parr et al. 2007; Ruzicka et al. 2013; Zhao et al. 2002) acting through various modes that can be classified into two main mechanisms of action:

i) *direct interaction* – as replacement units that engraft, differentiate (Acquistapace et al. 2011; Caplan and Dennis 2006) or influence immune cells by direct contact (Puissant et al. 2005);

ii) *indirect interaction* – by which they produce chemokines, cytokines and growth factors with paracrine and autocrine function (Caplan and Dennis 2006).

The latter mode of action is likely to be responsible for the therapeutic effect of MSCs as many studies confirmed beneficial effect even when only MSC-conditioned media alone was applied (Kinnaird et al. 2004).

2.3.1.2.1 Direct interaction of MSCs with host tissue

Engraftment of MSCs in the host tissue

MSCs are known to migrate to injured sites and this property has been attributed to the expression of growth factor, chemokine and extracellular matrix receptors on their surface (Meirelles Lda et al. 2009). When engrafting to the host tissue, MSCs adhere in the lesion site and replace missing cells (Caplan and Dennis 2006). MSCs have been showed to engraft into spinal cord (Ruzicka et al. 2013) and other tissues such as: marrow stroma (Muguruma et al. 2006), heart tissue (Thiele et al. 2004) and wound bed (Wu et al. 2007).

Differentiation of MSCs in vitro and in vivo

According to ISCT Minimal criteria (Dominici et al. 2006), MSCs have capacity to differentiate into bone, cartilage and adipose tissue *in vitro.* Also, it has been shown that MSCs can differentiate into other mesodermal tissue as such as skeletal muscle (Dezawa et al. 2005), tendon (Kuo and Tuan 2008), myocardium (Shim et al. 2004), smooth muscle and endothelium (Oswald et al. 2004). Some *in vitro* studies confirmed even greater differentiation plasticity, that is, trans-differentiation into cells of ectodermic origin such as neurons (Krampera et al. 2007), or neuron-like cells (Arboleda et al. 2011; Ding et al. 2007; Kadam et al. 2009; Ma et

al. 2005), or cells of endodermic origin, for example epithelial cells (Paunescu et al. 2007), insulin producing cells (Timper et al. 2006), and hepatocytes (Sato et al. 2005).

Despite promising initial results in neural tissue repair, the *in vitro* (Krampera et al. 2007) and *in vivo* (Peran et al. 2011) neuron-like cells differentiation capacity of MSCs has been recently re-evaluated (Caplan 2017; Parr et al. 2007; Zhao et al. 2002). Trans-differentiation into neuron-like MSCs might result into characteristic neuronal markers, however, functional properties in terms of ion channels and excitability were not confirmed (Parr et al. 2007; Zhao et al. 2002). Currently accepted explanation of functional recovery of neural tissue after MSCs transplantation is based on their paracrine effect rather than direct trans-differentiation.

Anti-inflammatory effect & Immunomodulation

Anti-inflammatory and immunomodulatory effects of MSCs have been recently extensively studied. In direct interaction with the immune system cells, MSCs suppress T-cell (CD4+ and CD8+) responses by arresting them in G0/G1 phase of the cell cycle as a result of cyclinD2 and Ki67 downregulation and p27kipl upregulation (Kaplan et al. 2011; Rehman et al. 2004; Siegel et al. 2009). One of the mechanisms is contact between T-cells and antigen presenting cells and MSCs, or expression of negative co-regulatory molecules B7-H1, B7-H4, or HLA-G on the surface of MSCs (Kaplan et al. 2011).

2.3.1.2.2 Indirect interaction of MSCs with host tissue

MSCs produce an array of bioactive factors that support cell survival, modulate immune reaction, stimulate angiogenesis, mitosis and differentiation of endogenous stem cells (Caplan and Dennis 2006). MSCs secretome also includes components of extracellular matrix (ECM) such as fibronectin, laminin, collagen and proteoglycans (Devine and Hoffman 2000). An overview of MSCs trophic effects is displayed in Fig.6. In fact, recently it has been suggested to re-name MSCs to Medicinal Signalling Cells in order to more accurately reflect the fact that these cells home to the site of the injury and secrete bioactive factors that support regeneration (Caplan 2017).

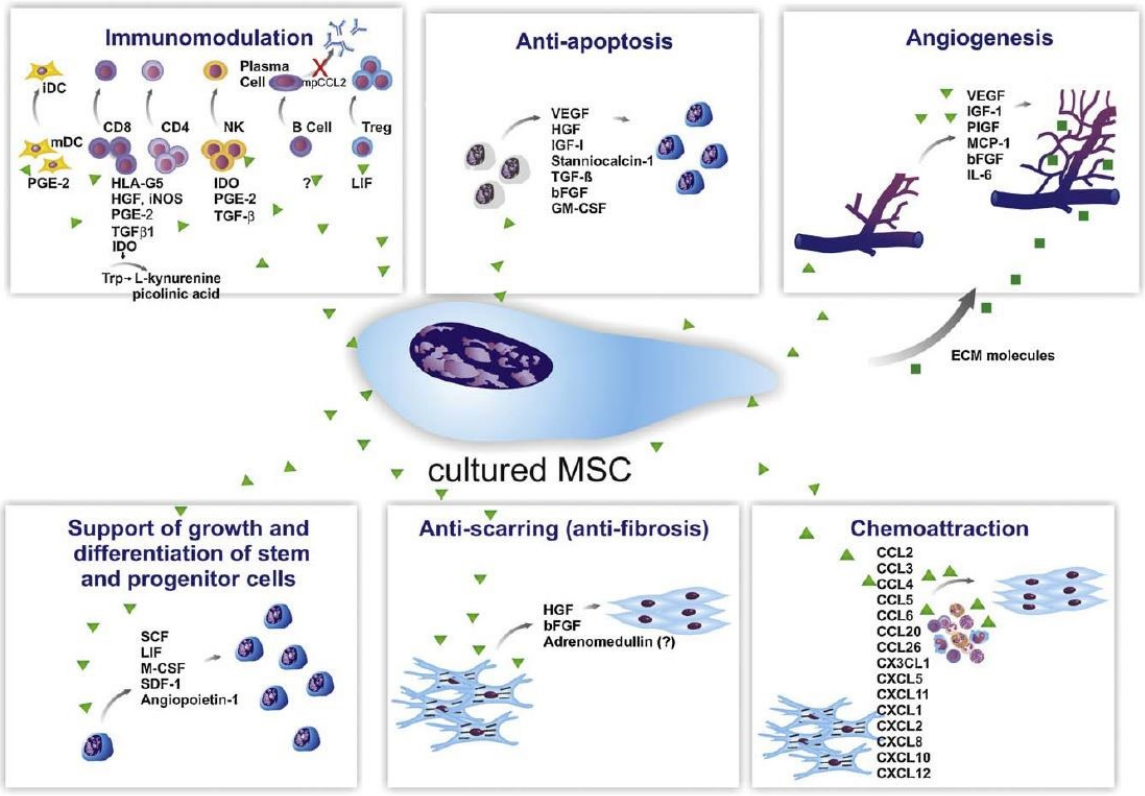

Fig. 6. Overview of MSCs trophic effects. Adapted from Meirelles Lda et al. (2009).

Anti-apoptotic properties

MSCs support survival of neurons after SCI by expressing the pro-survival gene Akt1 (Noiseux et al. 2006). Anti-apoptotic effect is enhanced by the production of VEGF, hepatocyte growth factor (HGF), insulin-like growth factor 1 (IGF-1) and monocyte chemoattractant protein 1 (MCP1) which inhibit the death of endothelial cells cultured under hypoxic conditions and promote the formation of capillary-like structures *in vitro* (Meirelles Lda et al. 2009; Murphy et al. 2013; Rehman et al. 2004).

Factors that support mitosis, proliferation and differentiation of other cells

In order to support haematopoiesis, MSCs produce factors that support mitosis such as macrophage colony-stimulating factor (M-CSF), granulocyte-macrophage colony-stimulating factor (GM-CSF), and interleukin (IL) – 6 (Haynesworth et al. 1996).

Moreover, MSCs secrete various neurotrophic factors that promote axonal regeneration, glial scar reduction and neural outgrowth (Neuhuber et al. 2005; Park et al. 2010a). Such factors include nerve growth factor (NGF), BDNF (Lu et al. 2005), neurotrophin – 3 (NT-3), NT-4/5.

Other supportive factors include stem cell factor (SCF), leukaemia inhibitory factor (LIF), HGF, IGF-1, placental growth factor (PlGF), EGF, and angiogenic factors such as bFGF, VEGF

and angiopoietin-1. MSCs also produce chemoattractant molecules including SDF-1, chemokine (C-C motif) ligand 5 (Ccl5/ regulated on activation, normal T-cell expressed and secreted - RANTES), transforming growth factor-alpha (TGF-α), TFG-β, MCP1, macrophage inflammatory protein (MIP-1α), E-selectin, and IL-8 (Hoffmann et al. 2002; Meirelles Lda et al. 2009).

Anti-inflammatory effect & Immunomodulation

MSCs act as immune modulators and have the capacity to interact with, influence or even profoundly affect the *in vivo* functions of most effector cells involved in an innate or adaptive immunity (Di Nicola et al. 2002). Prior to that, MSCs need to be stimulated, either by direct cell to cell contact (Glennie et al. 2005) with T-cells or indirectly by interferon gamma (IFN-γ), tumour necrosis factor alpha (TNF-α; both produced by activated T-cells) (Jones et al. 2003) or IL-1, IL-2, IL-12 (Murphy et al. 2013).

MSCs inhibit proliferation and function of naïve and memory $CD4^+$ and $CD8^+$ T-cells (Di Nicola et al. 2002; Glennie et al. 2005), promote regulatory T-cell expansion and enhance their immunosuppressive activity (Zhao et al. 2010). Also, they supress natural killer cells (NK cells), B-cells (Glennie et al. 2005), monocytes, macrophages and dendritic cells (Jiang et al. 2005; Murphy et al. 2013).

Secreted prostaglandin E2 (PGE2) is a central mediator of MSCs immunomodulating effects. Other immunomodulatory factors include TGF- β1, LIF, nitric oxide (NO), indoleamine 2,3-dioxygenase (IDO), IL-4, IL-6, IL-10, IL-1 receptor antagonist and soluble TNF- α receptor (Murphy et al. 2013).

By reducing INF-γ and increasing IL-4 and IL-10 secretion, MSCs indirectly restore the T1/T2 imbalance and shift the phenotype of macrophages towards M2 phenotype which has been shown to promote anti-inflammatory environment, regeneration and tissue remodelling (Murphy et al. 2013).

2.3.2 hMSCs in clinical practice

Currently, hMSCs are extensively used in autologous or allogeneic manner in various clinical applications. The regenerative potential of MSCs have been already demonstrated in SCI (Callera and do Nascimento 2006; Deda et al. 2008; Geffner et al. 2008; Park et al. 2005; Sykova et al. 2006; Yoon et al. 2007), brain injury or stroke (Chen et al. 2001; Li et al. 2002; Menasche and Vanneaux 2016), injured myocardium (Orlic et al. 2001; Rota et al. 2007), lung fibrosis (Menasche and Vanneaux 2016), heart failure (Menasche and Vanneaux 2016; Shiota and Itaba 2016), liver diseases (Shiota and Itaba 2016), bone defects (Sponer et al. 2016) or critical limb ischaemia (Dubsky et al. 2014). Immunomodulatory function of MSCs was used in the treatment of graft versus host disease (GvHD) (Lysak et al. 2016), rheumatoid arthritis, osteoarthritis and Crohn´s disease (Caplan 2009).

2.4 BIOMATERIALS

Biomaterials are increasingly utilized for SCI treatment not only to bridge the lesion but also as carriers of cells and therapeutic agents.

It is widely accepted that a suitable biomaterial for *in vivo* applications must fulfil basic criteria:

i) be biocompatible – have zero toxicity, promote cell adhesion, proliferation and differentiation, degrade into non-toxic products,

ii) have controlled degradation rate – biomaterial´s degradation kinetics and tissue regeneration should match,

iii) display mechanical properties similar to those of the tissue to be repaired,

iv) have open network of pores – to allow fluid and nutrient exchange,

v) allow the host cell infiltration and new tissue replacement.

To develop such material, researchers try to mimic the biological and mechanical properties of the cell microenvironment seen *in vivo.* Numerous materials, both synthetic and natural, biodegradable and non-biodegradable have been proposed for SCI (Pego et al. 2012). A special form of biomaterials is represented by hydrogels.

2.4.1 HYDROGELS

Hydrogels are polymers with 3D crosslinked networks that allows a high integration of water. Hydrogels can be prepared from synthetic or natural materials. High versatility and biocompatibility enables their usage for drug or cell delivery or as a part of composite biomaterials (Annabi et al. 2014).

In view of the irregular lesion that occurs in the SCI, hydrogels seem to be the most fitting material – they can be easily cast into various shapes or injected directly for *in situ* gelation and provide a scaffold through which nerves can regenerate (Straley et al. 2010).

To enable 3D ingrowth of cells, it is critical to create a porous structure. When a pore diameter is comparable to the cell size – 10-40 μm (Schwartz and Fehlings 2001), these hydrogels are termed *macroporous* (or *superporous*), smaller pore size hydrogels are called *microporous.* A macroporous structure of a hydrogel can be achieved for instance by cryogelation, lyophilization, or gelation of the polymer in the presence of ammonium oxalate needles (Pan et al. 2008) or needle-like sodium acetate crystals (Bracken et al. 1990) which resulted in porous structure within the hydrogel. An uprising method of hydrogel preparation is a 3D printing (Gomes et al. 2017).

Self-assembly injectable hydrogels were developed to mimic ECM structure. These include self-assembling peptides (SAP) (Yamaguchi 2000) and peptide amphiphiles (Bollini et al. 2013). These engineered peptides have a defined composition and are easy to manufacture and there is a possibility of scale-up production and commercialisation (Straley et al. 2010). An example of commercialized SAP is BDPuraMatrix^{TM} (3D Matrix, Inc., Cambridge, MA).

2.4.1.1 Synthetic scaffolds for SCI

Synthetic preparation of a scaffold allows the control of physical and biological properties to better predict and modulate scaffold´s behaviour *in vivo*. Synthetic materials have tuneable mechanical properties, but lack biological activity. Both degradable and non-degradable materials are developed for SCI repairs (listed in Table 1).

Among *synthetic biodegradable* polymers belong poly(α-hydroxyacids), as *e.g.* poly(lactic acid) (PLA), poly(glycolic acid) (PGA), poly(ε-caprolactone) (PCL), and their copolymers poly(lactic acid-co-glycolic acid) (PLGA) and poly(lactide-co-caprolactone) (PLCL) (Hejcl et al. 2008; Straley et al. 2010; Tsai et al. 2004; Woerly et al. 2008). Some of them have already been approved by FDA for short gaps in human peripheral nerves (Table 1).

Non-degradable synthetic materials include silicone, polyacrylonitrile/polyvinylchloride (PAN/PVC), and cross-linked polymers based on methacrylate hydrogels such as poly(2-hydroxyethyl methacrylate) (PHEMA), poly[N-(2-hydroxypropyl)methacrylate] (PHPMA) (Hejcl et al. 2008; Straley et al. 2010; Tsai et al. 2004; Woerly et al. 2008). Both, PHEMA and PHPMA hydrogel can be prepared to mimic the mechanical properties of the soft spinal cord tissue.

Other non-degradable synthetic materials that are often used are poly(ethylene glycol) (PEG), poly(vinyl alcohol) (PVA), and polyacrylamide (PAM).

Synthetic biomaterials for neural TE	
Biodegradable	Non-biodegradable
PLA*	silicone
PGA*	PAN/PVC
PLGA	PHEMA†
PLCL	PHPMA†
PCL*	PTFE[#]
	PVA*
	PVDF[#]
	PEDOT[#]
	PP[#]

*Table 1. List of synthetic scaffolds for neural tissue engineering (TE): poly(lactic acid) (PLA), poly(glycolic acid) (PGA), poly(lactic acid-co-glycolic acid) (PLGA), poly(lactide-co-caprolactone) (PLCL), poly(ε-caprolactone) (PCL), polyacrylonitrile/polyvinylchloride (PAN/PVC), poly(2-hydroxyethyl methacrylate) (PHEMA), poly[N-(2-hydroxypropyl)methacrylate] (PHPMA), poly(tetrafluoroethylene) (PTFE), polyvinyl alcohol (PVA), polyvinylidene fluoride (PVDF), polypyrolle (PP), poly(3,4-ethylendioxythiophene) (PEDOT). *scaffolds approved by Food and Drug Agency (FDA, USA); † hydrogels, # electrically active materials. Based on review Pego et al. (2012) and Straley et al. (2010).*

However, wider using of synthetic materials is hampered by their low biocompatibility. Cell adhesion properties of synthetic materials might be enhanced in various ways; for example, by modification of their chemical composition, the net charge of the surface (Hejcl et al. 2009) and the balance between the hydrophilic and hydrophobic domains.

Other modifications to increase cell attachment include introduction of ECM proteins by pre-coating or their immobilization. These proteins are for instance fibronectin-derived RGD (Arg-

Gly-Asp) or other fibronectin subunits (Raposo and Stoorvogel 2013), laminin-derived peptides YIGSR (Tyr-Ile-Gly-Ser-Arg), IKVAV (Ile-Lys-Val-Ala-Val) (Pan et al. 2008), cholesterol (Kubinova et al. 2009) and others (Gunn et al. 2005). Commercially available is Neurogel^{TM} - a microporous PHPMA hydrogel functionalized with the RGD peptide that has been reported to promote tissue ingrowth, angiogenesis and axonal regeneration (Woerly et al. 2008).

2.4.1.2 Natural scaffolds

Naturally-derived scaffolds are biodegradable, have enhanced biocompatibility and better tissue adherence and therefore are generally preferred for neural tissue repair (Annabi et al. 2014). On the other hand, their batch-to-batch variability, or in some cases induction of immunogenic reactions might be a limiting factor.

Natural materials used for SCI repair include collagen (Yoshii and Constantine-Paton 2010), fibrin (Taylor et al. 2004), hyaluronic acid (Park et al. 2010b), agarose (Gros et al. 2010), alginate (Prang et al. 2006), silk fibroin (Shen et al. 2010), poly(β- hydroxybutyrate) (Novikova et al. 2008) and chitosan (Bozkurt et al. 2010) (Table 2). Other naturally occurring polymers include gelatine, elastin, chondroitin sulphate or heparin. A special type of naturally derived material utilized for neural tissue repair presents biological scaffolds that consists of structural proteins of the ECM (Crapo et al. 2014).

Natural biomaterials for neural TE	
Name	Main constituent
collagen	Hyp
fibrin	Ca^{2+}, α-D-mannose, D-glucosamine
hyaluronic acid	D-glucuronic acid, N-acetyl-D-glucosamine
agarose	D-galactose, 3,6-anhydro-L-galactopyranose
alginate	β-D-mannuronate, α-L-guluronate
fibroin	$(Gly\text{-}Ser\text{-}Gly\text{-}Ala\text{-}Gly\text{-}Ala)_n$
PHB	poly(β- hydroxybutyrate)
chitosan	polysaccharide chitin
ECM	collagen, GAGs

Table 2. List of natural scaffolds used as scaffolds for SCI repair. Poly(β- hydroxybutyrate) (PHB), glycine (Gly),GAGs (glycosaminoglycans), serine (Ser), alanin (Ala), hydroxyproline (Hyp). Based on review Pego et al. (2012) and Straley et al. (2010).

The degradation of naturally derived hydrogels is usually adjusted by cross-linking agent that covalently bonds to polymer chain and creates stable hydrogels (Pego et al. 2012). Such example is a covalent cross-linking of chitosan with dialdehydes or glutaraldehyde (Straley et al. 2010).

2.5 EXTRACELLULAR MATRIX (ECM)

ECM is 3D fibrillary structure secreted by the cells which provides structural framework as well as spatial and biochemical cues that influences cell fate, maintains cell homeostasis and acts on their behaviour (Crapo et al. 2011; Keane et al. 2015). Forming ECM is a dynamic process and can be seen throughout the development and also in adult tissue during healing and fibrosis. ECM stores a wide range of growth factors, which are released as response to changes in physiological conditions. This allows rapid and local growth factor-mediated activation of cellular functions without *de novo* synthesis.

Cells bind to ECM by specific cellular adhesion molecules known as integrins. Through signal transductions, mediated by integrins and other cell surface receptors, ECM can regulate cell adhesion, migration (Tran and Damaser 2015), proliferation (Bracken et al. 1997), gene expression (Caplan 1991), differentiation (Lai et al. 2011) and even apoptosis (Flamm et al. 1985).

The ECM plays a crucial role in maintaining the structural integrity of all tissues, including nervous system where it influences neurons, glia, inflammatory cells and other cell types.

2.5.1 CNS ECM

Each tissue has its specific ECM composition and topology that is generated during the development through dynamic and reciprocal, biochemical and biophysical interactions with cellular components. CNS ECM contains high amounts of proteoglycans (Casha et al. 2012), hyaluronic acid (Pitts et al. 1995), laminin (Karsy and Hawryluk 2017), fibronectin (Hirbec et al. 2001) and tenascins (Tadie 2005). In addition to water, negatively charged proteoglycans retain growth factors that instruct CNS in development and also aid to regeneration. Some of these proteins, or their specific domains are utilized to increase biocompatibility of synthetic materials intended for neuronal repair.

2.5.2 Structure of the ECM

ECM components are produced intracellularly and are secreted via exocytosis (Hirano and Mooney 2004). ECM contains three classes of molecules (Fig. 7).

i) *Structural proteins*: collagen, elastin

ii) *Glycosaminoglycans (GAGs)*: carbohydrate polymers

a. **Proteoglycans:** heparan sulphate, chondroitin sulphate, keratan sulphate

b. **Non-proteoglycan polysaccharide**: hyaluronic acid

iii) *Adhesive glycoproteins* to attach cells to matrix: fibronectin and laminin

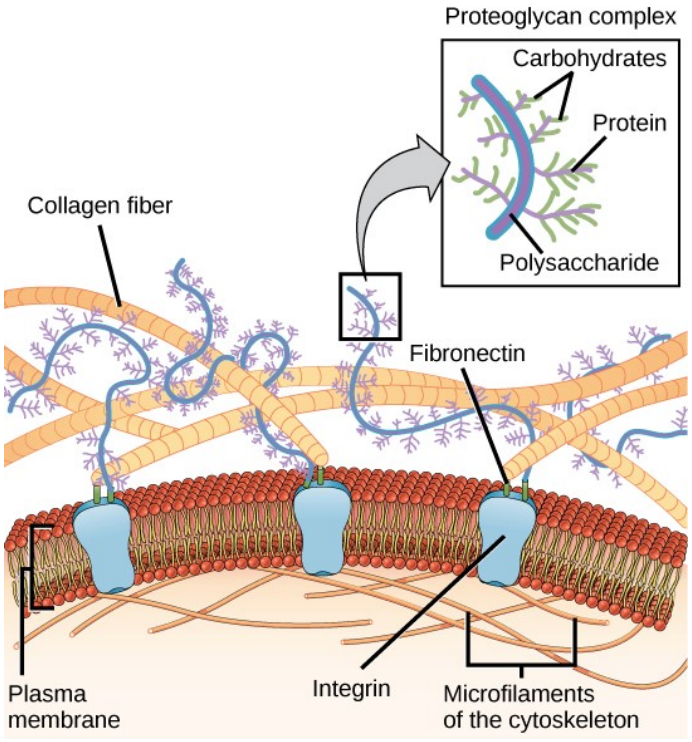

Fig. 7. Depiction of extracellular matrix components. Adapted from http://cnx.org/contents/GFy_h8cu@10.53:rZudN6XP@2/Introduction.

2.5.2.1 Structural proteins

Collagen is the most abundant protein in the ECM consisting of amino acids that intertwine together to form triple helices which conform to elongated fibrils. Characteristic for collagen is the high hydroxyproline (Hyp) content. Collagen is exocytosed from the cells in its precursor form of procollagen, which is then cleaved by proteases to allow assembly. In CNS, collagen is present in meninges and vasculature. Different collagen types are distinguished based on types of structure they form:

- *Fibrillar collagens:* type I, II, III, V, XI
- *Non-fibrillar*
    - *Fibril associated Collagens with Interrupted Triple helices (FACIT):* type IX, XII, XIV, XIX, XXI
    - *Short chain:* type VIII, X
    - *Basement membrane:* type IV

- *Multiple Triple Helix Domains with Interruptions (Multiplexin):* type XV, XVIII
- *Membrane Associated Collagens with Interrupted Triple Helices (MACIT):* type XIII, XVII
- *Other:* type VI, VII, XIII

Elastin is composed of small amino acids such as glycine, valine, alanine and proline. It is synthetized by fibroblasts and smooth muscle cells and released in their precursor form of a tropoelastin. Elastin gives elasticity to tissues – particularly blood vessels, lungs, skin and ligaments.

2.5.2.2 Proteoglycans

Proteoglycans are composed of GAG chains covalently linked to a specific protein core. Their heterogeneity is caused by the diversity of core proteins as well as variation in GAG chains. GAG chains are sulphated polysaccharides composed of repeating disaccharide units of hexuronate (glucuronate or iduronate) and hexosamines (glucosamine or galactosmine). Proteoglycans have a net negative charge that attracts positively charged Na^{2+} and attracts water, thus keeping ECM hydrated. Proteoglycans also store growth factors, *e.g.* IGF-1, lipoprotein receptor related protein 1, and TGFβ, epidermal growth factor receptor (EGFR), EGF, bFGF, VEGF, or keratinocyte growth factor (KGF), HGF, PDGF (Long et al. 1986). Proteoglycans form PNN surrounding neuronal cells and can regulate neuronal plasticity (Yamaguchi 2000). Also they play a role in neurodegenerative disorders such as Alzheimer´s disease, Parkinson´s disease and prion disease (Kwok et al. 2008) as they may aggregate with pathologic intracellular fibrils (Holmes et al. 2013).

Chondroitin sulphate (CS) is the most abundant GAG in the CNS matrix. It can be also found in tendons, ligaments and aorta and is responsible for their tensile strength. The basic CS disaccharide subunit is composed of glucuronic acid (GlcA) and N-acetylgalactosamine. Sulfation of CS significantly affects its affinity to various signalling molecules and thus can influence pathological processes during development and in adulthood (Djerbal et al. 2017). CS sulfation takes place on carbon (C-) 2 or C-3 on the GlcA residue and C-4 or C-6 on the N-acetylgalactosamine residue. Chondroitin 4 -sulphate is the most prominent CS-GAG found in adult CNS and also after injury (*e.g.* in glial scar after SCI) and it has been shown to exhibit a strong negative guidance in the neurons (Fawcett and Asher 1999; Kwok et al. 2011). On the

other hand, chondroitin 6-sulphate may in fact be beneficial for neural regeneration (Kwok et al. 2011).

Heparan sulphate is a linear polysaccharide consisting of various sulphated disaccharide units, the most common is GlcA and N-acetylglucosamine. It is found abundantly in basement membranes and attaches to multi-domain proteins such as perlecan, agrin and collagen XVIII. Heparan sulphate has a wide range of biological activities including developmental processes, angiogenesis, blood coagulation and tumour metastasis that are exerted through localizing of the growth factors to particular sites (Smith et al. 2015). Heparan sulphate acts as low affinity receptor binding bFGF (Reuss and von Bohlen und Halbach 2003), HGF, VEGF, IL-8 and INF-γ (Sadir et al. 1998).

Keratan sulphate is a linear polysaccharide with repeating galactose and N-acetylglucosamine units. Apart from CNS, keratan sulphate is present also in cornea, cartilage, and bones. Keratan sulphate participates in CNS development as well as in the glial scar formation and potent inhibitor of neurite growth (Silver and Miller 2004).

2.5.2.3 Hyaluronic acid

Hyaluronic acid (HA) is a linear polymer of non-sulphated N-acetylglucosamine and GlcA disaccharide units. During the development of the CNS, HA is produced by cells in the neuronal tube and notochord; it plays a vital structural role in the formation of brain ECM (Bignami et al. 1993). HA has been viewed as a space filling substance due to its capacity to absorb significant amounts of water. It also has the ability to resist compression by providing a counteracting turgor force thanks to swelling. Apart from CNS, HA could be found in load-bearing joints and interstitial gel (Bignami et al. 1993). HA regulates embryonic development, healing process, inflammation and tumour development though its specific transmembrane receptor CD44 (Bignami et al. 1993). Together with link proteins, SC proteoglycans, and tenascin-R (Tn-R), HA forms the PNN that is known to play a direct role in the control of CNS plasticity (Kwok et al. 2011).

2.5.2.4 Cell adhesive glycoproteins

Fibronectin is a glycoprotein composed of two trimers – each consisting of three different polypeptide chains – that are connected through disulphide bonds. Each subunit contains domains which binds fibronectin to collagens, GAG, proteoglycans and cell integrins and causes cell adhesion and facilitates cell movement. Fibronectin interacts with subset of

developing neurons and regulates neural differentiation (Reuss and von Bohlen und Halbach 2003).

Laminin is found in basal membrane and forms web-like structures around the blood vessels that resist tensile forces and assist cell adhesion (Erickson and Couchman 2000). During development, laminin is present in basal laminae along neural crest migratory pathways, in sensory ganglia, early dorsal and ventral roots and in the marginal zones of the CNS that are regions of cell migration and axonal elongation (Rogers et al. 1989). After injury, laminin is associated with growth cones of regenerating axons (Barros et al. 2011).

2.5.3 ECM scaffolds

To utilize beneficial effect of ECM on tissue regeneration, ECM can be extracted from virtually any tissue by a simple method of decellularisation (Fig. 8). In this process, using physical and mechanical methods, detergents, organic solvents or enzymatic digestion cells are removed from tissues or organs. Decellularized ECM can be prepared in a form of a solid fibrillary matrix, sheet or powder, or it can be solubilized by pepsin digestion (pH<2) to form a hydrogel (Fig. 8) (Badylak et al. 2009). The concept of cell removal from tissues was described as early as in 1975 (Meezan et al. 1975), but was not broadly introduced until the late 1980s (Badylak et al. 1989).

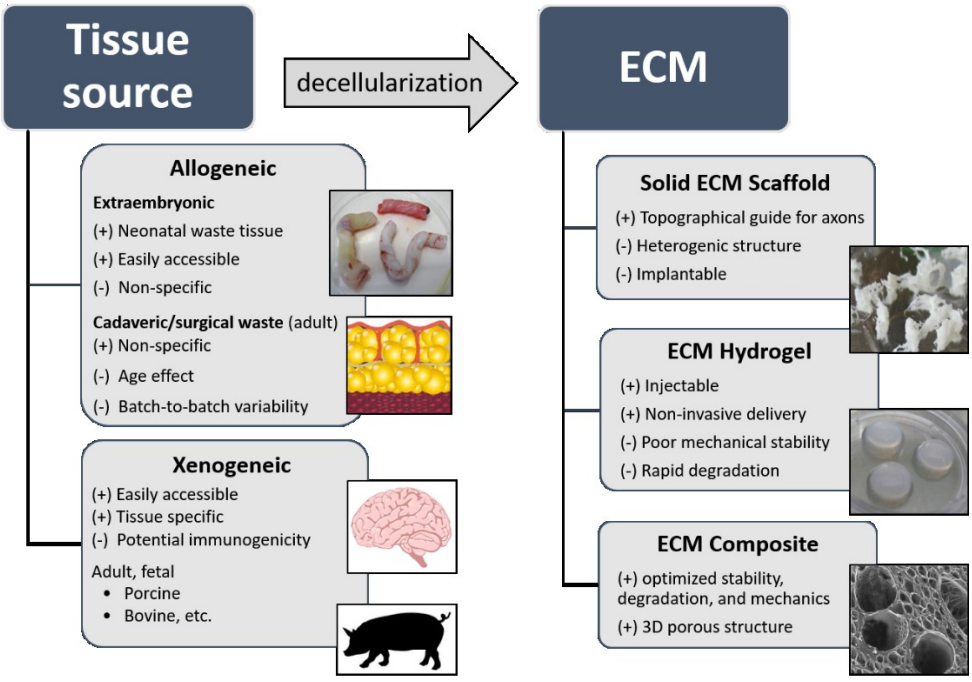

Fig. 8. A scheme of extracellular matrix (ECM) preparation, types of tissue sources used for ECM extraction and ECM properties after decellularisation.

2.5.4 Clinical utilization of ECM scaffolds

Using biologic scaffolds composed of ECM has many advantages – they possess 3D structure, low immunogenicity, complex biomolecular composition, retention of growth factors and other chemical cues (DeQuach et al. 2011; Wolf et al. 2012). Their therapeutic effect is based on their ability to establish tissue remodelling by modulation of the immune response and stimulation of endogenous repair – so called constructive remodelling (Badylak et al. 2009). By degradation, ECM not only allow gradual replacing by anatomical appropriate and functional tissue, but also they reveal cryptic proteins for cell attachment and release chemoattractant factors that recruit host progenitor cells (Badylak et al. 2009). Furthermore, ECM scaffolds can be used as cell carriers and provide stimulatory niche for the transplanted implant.

Numerous allogenic as well as xenogeneic ECM materials are currently commercially available and have been utilized for the treatment of many patients with encouraging results (Badylak 2014; Badylak et al. 2009; Long et al. 1986).

ECM from porcine urinary bladder (UB), spinal cord (SC), brain (B) (Medberry et al. 2013), porcine intestinal submucosa, porcine or bovine dermis, pericardium, heart valves, basement membrane and stroma of the liver, and Achilles tendon (Long et al. 1986) have already been tested in clinical practice for non-CNS tissue reconstruction including peripheral nerve, myocardium, muscles, blood vessels, valves, oesophagus, dura mater, cornea, bones, skin but also whole organs such as lungs, kidney, liver and heart among others.

Commercially available for human use are *e.g.* cross-linked human dermis (Alloderm^{TM}) and purified bovine type I collagen (Contigen^{TM}).

However, there are only few studies evaluating the therapeutic potential of ECM scaffolds for SCI repair (Meng et al. 2014; Wang et al. 2015).

2.5.5 Modification of ECM

Modification of ECM by chemical or non-chemical means allows to tune their physical, mechanical or immunogenic properties. Chemical cross-linking methods use for instance aldehyde or carbodiimide (Bouhadir and Mooney 1998) or natural cross-linking agent – genipin (Inostroza-Brito et al. 2017). Photochemical crosslinking occurs in a mixture of macromers and photoinitiator and after their exposure to the light source (ultraviolet – UV or visible light) (Parr et al. 2007).

3 HYPOTHESES AND STUDY AIMS

1) Human mesenchymal stromal cells (hMSCs) isolated from Wharton´s jelly (hWJ-MSCs) are comparable with other cell types, such as adipose tissue-derived MSCs (hASCs) and bone marrow MSCs (hBM-MSCs).

   Aim 1) to characterize and compare hMSCs from Wharton´s jelly, bone marrow and adipose tissue *in vitro* in terms of their tissue yield, proliferation, population doubling, and expressions of surface markers, differentiation and characterization of their secretome.

2) Intrathecal (i.t.) transplantation of hWJ-MSCs has beneficial effects on spinal cord injury (SCI) repair in rats and this effect is dose-dependent.

   Aim 1) to transplant hWJ-MSCs into the SCI and evaluate their effect using histochemical, behavioural and gene expression analysis. To compare different dosage (0.5 or 1.5 x 10^6 hWJ-MSCs), single and repeated (3x) application of hWJ-MSCs.

3) Extracellular matrix (ECM) can be isolated from the human umbilical cord (UC), solubilized to the form of a hydrogel and is suitable for neural repair.

   Aim 1) to prepare ECM hydrogels from human umbilical cord (UC-ECM), porcine urinary bladder (UB-ECM), porcine brain (B-ECM) and spinal cord (SC-ECM) and characterize them in terms of composition, mechanical properties and *in vitro* biocompatibility and neurotrophic properties.

4) CNS –derived ECM scaffolds are suitable for SCI repair and reveal tissue specific effect.

   Aim 1) to compare CNS and non-CNS derived ECM hydrogels in a model of spinal cord hemisection in rats.

   Aim 2) to evaluate ECM scaffolds in 3D culture as carriers for cell delivery.

4 METHODS

4.1 Cell culture

4.1.1 MSC isolation

hWJ-MSCs were derived from umbilical cords (UC) which were obtained from healthy full-term neonates after spontaneous delivery at University Hospital Pilsen (Pilsen, Czech Republic). About 10-15 cm of UC were stored in sterile PBS with antibiotic-antimycotic solution (PBS+AA; Sigma-Aldrich, St. Louis, Missouri, USA) at 4°C and transported to our laboratory within 24 hours. After washing several times in PBS+AA and 10% Betadine (Egis Pharmaceuticals, Budapest, Hungary), blood vessels were removed from the interior of the cord. The WJ tissue was chopped into small pieces (1-2 mm^3) and weighed. One gram of cut tissue was immersed in the solution of 0,26 U/ml Liberase™ (Roche Custom Biotech, Mannheim, Germany) and 1 mg/mL hyaluronidase (Sigma) at 37°C with constant stirring for 2 hours. After enzymatic digestion, nucleated cells were centrifuged at 450×g for 10 minutes (mins) and cultured under standard conditions.

Human BM was obtained from the iliac crest of healthy donors, that were either subjects in a clinical trial (study sponsor Bioinova, Ltd., Prague, Czech Republic) or undergoing an orthopaedic surgery (in University Hospital Motol, Prague, Czech Republic) for different than BM related problem. BM harvesting was performed under local or central anaesthesia.

To isolate hMSCs, BM was applied on Gelofusine® (B. Braun, Melsungen AG, Germany) and mononuclear fraction was seeded on plastic flasks ($7 \times 10^4 – 1.4 \times 10^5$ cells/cm^2; TPP Techno Plastic Products AG, Trasadingen, Switzerland) and allowed to adhere. Non-adherent cells were removed after 24 and 48 hours by replacing the media. Adherent cells were cultured under standard conditions.

Human AT samples were obtained from healthy volunteers who underwent liposuction procedures for aesthetic reasons (Prague aesthetic clinic, Prague, Czech Republic). The lipoaspirate was repeatedly washed in phosphate-buffered saline (PBS, IKEM, Prague, Czech Republic) and enzymatically digested by collagenase (0.3 PzU/mL, Collagenase NB 6 GMP, Serva Electrophoresis GmbH, Heidelberg, Germany) at 37°C, centrifuged at 450×g for 5 mins, and the cells were cultured under standard conditions.

All donors of human tissues and cells provided their written informed consent prior any intervention and all the studies using human tissues or cells were approved by the local ethics committee. Human tissues and cells were donated anonymously.

4.1.2 MSC proliferation

All hMSCs were cultured at 37°C in a humidified atmosphere containing 5% CO_2 in enriched MEM Alpha Lonza Walkersville Inc. Maryland, USA) media containing platelet lysate (5%; Bioinova, Ltd.) and gentamicin (10 µg/ml; Gentamicin Lek®; Lek Pharmaceuticals, Ljubljana, Slovenia). The media was changed twice a week. After reaching near-confluence, cells were harvested by a Trypsin/EDTA solution (Life Technologies, Carlsbad, California, USA), and cell yield in the first passage was recorded. Cells were then seeded again onto a fresh plastic surface at a density 5 x 10^3 cells/cm^2.

At each passage, population doubling time (PDT; 1) and population doubling (PD; 2) was calculated according these formulas:

$$PDT = (t_2\text{-}t_1) \cdot \frac{\log 2}{\log\left(\frac{number\ of\ cells\ at\ t2}{number\ of\ cells\ at\ t1}\right)} \quad (1)$$

$$PD = \frac{\log(number\ of\ harvested\ cells) - \log(number\ of\ seeded\ cells)}{\log 2} \quad (2)$$

4.1.3 MSC migration and proliferation assay

To perform migration assay, xCELLigence® RTCA DT Instrument (Acea Biosciences Inc. San Diego, CA, USA) was used. Prior migration assay, cells were left for 24 hours in a media without appropriate supplements (platelet lysate). On the experiment day, medium with SDF-1 (20 ng/mL, Sigma) was placed into a lower chamber of CIM-Plate 16, and hMSCs were then pipetted into the upper chamber (10^5 cells in 100 µL of media without supplements). Recorded impedance signal at 6 hours was normalized to migration towards supplement-free media and was then used to assess the rate of cell migration. The assay was repeated five times.

To determine *in vitro* proliferation, cells were seeded into a 96-well plate 5 x 10^3 cells/cm^2 in 100 mL media. Cell proliferation was measured using WST-1 assay (Roche) after 1, 3, 7, and 14 days of the culture. Ten microliters of WST-1 reagent was added to each well containing 100 mL culture media, and the plates were incubated for 2 hours at 37°C. The absorbance was measured using a Tecan Spectra plate reader (Tecan, Switzerland) at 450 nm. The assay was repeated five times.

4.1.4 MSC surface marker expression

Suspension of 2 x 10^6 MSCs from the third passage was resuspended in PBS and incubated with appropriate antibodies against different cluster of differentiation (CD) cell surface molecules for 20 mins at room temperature. Flow cytometry analysis was performed using a FACS sorter (FACSAria™, Becton Dickinson, San Jose, California). The antibodies used against human antigens were as followed: CD10, CD14, CD44, CD34, CD105, CD106, HLA-DR+DP (Exbio, Vestec, Czech Republic); CD29, CD73, CD90, CD271, CD31, CD45, CD146, HLA-ABC (BD Pharmingen, San Jose, California, USA); CD133 (Miltenyi Biotec, Bergisch Gladbach, Germany), CD235a (Dako, Glostrup, Denmark), VEGFR2 (BioLegend, San Diego, California), and monoclonal anti-human fibroblast (Sigma) conjugated with secondary antibody anti-mouse IgM (Exbio). Data analysis was performed using BD FASCDiVa software (BD Biosciences, San Diego, California, USA).

4.1.5 Multipotent differentiation of MSCs

Cells in the third passage were used for multilineage differentiation according to standard differentiation protocols.

Adipogenic differentiation

hMSCs were seeded into six-well tissue-culture plates at a density of 8 x 10^4 cells/well and treated with media consisting of MesenCult®, 10% foetal bovine serum (FBS), 1% Penicillin/Streptomycin (P/S™), 1 µM dexamethasone, 0.5 mM 3-isobutyl-1-methylxanthine, 0.1 mM indomethacin and 10 µg/mL insulin (all from Sigma). After two weeks in the culture, the cells were fixed with 4% paraformaldehyde in PBS and stained with Oil-Red-O to detect lipid droplets.

Osteogenic differentiation

hMSCs were seeded into six-well tissue-culture plates at a density of 3 x 10^4 cells/well. The next day, cells were treated with media consisting of MesenCult®, 10% FBS, 1% P/S™, 0.1 µM dexamethasone, 10 mM β –glycerolphoshate and 0.1 mM L-ascorbic acid (Sigma). After two to three weeks of the culture, the cells were fixed and stained with Alizarin Red S to detect calcium-rich deposits.

Chondrogenic differentiation

hMSCs 2.5 x 10^5 were transferred into conical tubes, centrifuged and cultivated as pellets in a media consisting of MesenCult®, 1% ITS Universal Culture Supplement Premix (BD

Biosciences, Bedford, Massachusetts, USA), 1% P/S™, 0.1 μM dexamethasone, 0.05 mM L-ascorbic acid, and 10 ng/mL hTGF-β (Millipore, Billerica, Massachusetts, USA). After three to four weeks the pellets were stained with Alcian blue to detect acid mucopolysaccharides.

4.1.6 Secretome analysis of MSCs

Production of chemokines, cytokines and growth factors was assessed from all hMSCs cell-cultured conditioned media (CM). For each cell type, we pooled three donors in a cell culture. Pooled hMSCs were cultured in a media with addition of ITS supplement alone or ITS supplement plus addition of inflammatory cytokines: IFNγ (10 ng/mL) and TNFα (10 ng/mL). CM were collected after 24 hours from confluent cultures. Then, CM was centrifuged at 440×g for 5 mins at 4°C and stored at -80°C before being used for bead-based cytokine array ProcartaPlex (eBioscience, San Diego, CA, USA) multiplex immunoassay for simultaneous detection of these analytes: bFGF, BDNF, EGF, HGF, VEGF-A, IL-6, IL-12, IL-1 receptor antagonist (IL-1RA), IFNα, MCP1, SDF-1, Interferon gamma-induced protein 10 (IP-10/CXCL10), RANTES, ICAM-1 and VCAM-1. The analysis was performed using a Lumniex SD (Bio-Rad, Hercules, CA, USA) instrument and R software (Vienna, Austria).

4.2 ECM hydrogels

4.2.1 Tissue decellularisation and preparation of ECM hydrogels

Porcine urinary bladders (UB), spinal cords (SC) and brains (B) were obtained from an abattoir (Český Brod, Czech Republic); the age of the animals was 6 months. ECM hydrogels were prepared according to previously described protocols (Crapo et al. 2012; Medberry et al. 2013). Human UC were obtained from healthy full-term neonates after spontaneous delivery at University Hospital Pilsen. About 10-15 cm of umbilical tissues were frozen (>16 hours at -20°C), aseptically transported into the laboratory, and subsequently thawed and transversely cut into pieces (< 0.5 cm length). Tissue pieces were agitated in 0.1 M PBS bath (48 hours at 120 rpm, 4°C). The PBS bath was exchanged three to five times before the tissue pieces were soaked in 0.02% trypsin/0.05% EDTA (120 mins at 120 rpm, 37°C, Sigma) and afterwards in a 0.1% peracetic acid in 4.0% ethanol bath (120 mins at 300 rpm; Penta, Prague, Czech Republic) and in a series of PBS and deionized water (dH_2O) soaks. Finally, tissue pieces were lyophilized for 24 hours (FreeZone® 2.5, Labconco Corporation, Kansas City, MO, USA) and powdered (Mini-Mill Cutting Mill, Thomas Scientific, Swedesboro, NJ, USA). For the *in vivo* application, the powdered ECM was sterilized in ethylene oxide at 37°C overnight.

To prepare the hydrogel, powdered ECM samples were solubilized with 1.0 mg/mL pepsin in 0.01 M HCl (Sigma) at a concentration of 10 mg ECM/mL, and stirred at room temperature for 48 hours to form a pre-gel solution (pH ~ 2). The pepsin-HCl ECM solution was neutralized to pH 7.4 with 0.1 M NaOH, isotonically balanced with 10x PBS, and diluted with 1x PBS to the final concentration of 8 mg/mL, which allows *in vivo* gelation (Ghuman et al. 2016). To form the hydrogel, the neutralized pre-gel was placed in 37°C for ~ 45 mins.

4.2.2 ECM hydrogel characterization

4.2.2.1 Nanoscale topography of ECM hydrogels

The surface topography of the UC-ECM, UB-ECM, SC-ECM and B-ECM hydrogels was analysed by scanning electron microscopy (SEM) mode. Briefly, a gel was placed on the glass slide, fixed in cold 2.5% glutaraldehyde (Electron Microscopy Sciences, Hateld, PA, USA) for 24 hours and washed in PBS. Hydrogels were then dehydrated in a graded series of alcohol, followed by subsequent chemical drying with hexamethyldisilazane (Sigma). The dried samples were cut to expose their inner structure and used for SEM studies. Micrographs were taken using a FEI Quanta 3D FEG scanning electron microscope at an acceleration voltage of 2 kV, to prevent charging of unconductive samples. ImageJ (Rasband, W.S., U.S. National Institutes of Health; Bethesda, MD) software was used for image processing and micrograph quantification. Using special plugin for ImageJ (FibrilTool) (Boudaoud et al. 2014), image analysis was performed in terms of anisotropy score calculation.

4.2.2.2 Efficiency of tissue decellularisation

The absence of cell nuclei in decellularized tissues was proved by haematoxylin-eosin (H&E) staining. The nuclei were stained using DAPI. Double–strain DNA (dsDNA) was isolated from native and decellularized tissue according to the manufacturer´s instructions (DNeasy® Blood&Tissue Kit, Qiagen, Hilden, Germany), and quantified using a spectrophotometer (NanoPhotometer™ P-Class, Munich, Germany). DNA content was normalized to the initial dry weight of the samples. For each native and decellularized tissue, the assay was repeated 3 times. Base pair length of residual DNA was determined on 2% agarose gel (Sigma) containing 0.5% SYBR Safe DNA Gel Stain (Thermo Fisher Scientific, Walham, MA, USA) and visualized with ultraviolet transillumination, using a reference 50-base pair (bp) ladder (Cleaver Scientific, Warwickshire, UK).

4.2.2.3 Immunohistochemical analysis of decellularized ECM

To visualize the content of acid mucopolysaccharides, collagen, laminin and fibronectin, the decellularized ECM were fixed in 4% paraformaldehyde in PBS and embedded in paraffin blocks. Sections of 5 µm thickness were mounted onto slides, deparaffined and stained with Alcian blue (pH 2.5; all acid mucosubstances, blue or greenish blue) together with Weigert's iron haematoxylin (nuclei, black) and Van Gieson staining (acid fuchsine in saturated aqueous picric acid; collagen, red). Also, the immunohistochemistry using primary antibodies against collagen I (mouse monoclonal IgG1, clone COL-1, 1:1000), laminin (rabbit polyclonal IgG, 1:200), and fibronectin (rabbit polyclonal IgG, 1:200, all from Abcam) was performed. Goat anti-mouse IgG conjugated with AlexaFluor 488 (1:400) for collagen, goat anti-rabbit IgG conjugated with AlexaFluor 488 (1:400) for fibronectin and goat anti-rabbit IgG conjugated with AlexaFluor 594 (1:400) for laminin (all from Life Technologies, Eugene, OR, USA) served as secondary antibodies. Images were taken using LEICA CTR 6500 microscope (Leica Microsystems, Wetzlar, Germany).

4.2.2.4 Collagen and glycosaminoglycan quantification in ECM hydrogels

The collagen content in ECM hydrogels was assessed using colorimetric assay Sircol™ Insoluble Collagen Assay Kit (Biocolor Ltd., UK). Sulphated glycosaminoglycan (sGAG) concentrations in ECM hydrogels were determined using the Blyscan Sulfated Glycosaminoglycan Assay Kit (Biocolor). Absorbance of the samples was recorded at 555 nm for collagen, and at 656 nm for sGAG content, using Tecan-Spectra plate reader (Tecan, Männedorf, Switzerland). All assays were performed according to the manufacturer's recommended protocol from three independent samples measured in triplicates. The collagen and sGAG content was normalized to the initial dry weight of the samples.

4.2.2.5 Mass spectrometry analysis of UC and UC-ECM

Samples of native UC tissue (n = 2) and UC-ECM (n = 3) were processed for liquid chromatography-mass spectrometry (LC-MS) analysis. Native UC was homogenized and powdered. Powdered native UC and UC-ECM were solubilized and processed by filter-aided sample preparation (FASP) method (Wisniewski et al. 2009). Proteins were alkylated, digested by trypsin on filter unit membrane and resulting peptides mixtures were analysed on LC-MS system (RSLCnano and Orbitrap-Elite, ThermoFisher Scientific). Data were processed using Proteome Discover software (version 1.4, ThermoFisher Scientific) with Mascot and Sequest searching engines. Percolator was used for post-processing of search results. Quantification

using protein area calculation in Proteome Discoverer was used to calculate the percentage and pars-per-million (ppm) values within each sample.

4.2.2.6 Rheometry of ECM hydrogels

Dynamic oscillatory shear tests were used to investigate the viscoelastic properties of ECM hydrogels. ECM hydrogels were subjected to a sinusoidal deformation in a 40 mm parallel plate rheometer (AR-G2, TA Instruments, New Castle, DE, USA) at 1 Pa stress and 10°C, to determine their mechanical response (displacement or strain) as a function of time. A dynamic time sweep was run with the parameters of 5% strain, 1 rad/s (0.159 Hz), and increasing the temperature from 10°C to 37°C, to induce gelation as indicated by a sharp increase and plateau phase of the storage modulus (G'). The assay was repeated three times with three independent samples in triplicates.

4.2.2.7 Turbidity gelation measurement of ECM hydrogels

The turbidimetric gelation kinetics were determined on a spectrophotometer (Infinite® 200 Pro, Tecan), which was pre-heated to 37°C. ECM hydrogel samples (8 mg/mL) were kept on ice at 4°C until 100 µL were pipetted into each well of a 96 well plate, and inserted into a spectrophotometer. Absorbance was measured at 405 nm every 10 mins for 100 mins. Normalized absorbance, time to reach 50% and 95% maximal absorbance were determined as $t_{1/2}$ and t_{95} (Gelman et al. 1979). The lag time (t_{lag}) was defined as the point where a line representing the slope at log $t_{1/2}$ intersects the turbidimetry baseline with 0% absorbance. The gelation rate (S) was defined as the slope of the linear region of the gelation curve. The measurements were repeated three times with three independent samples in triplicates.

4.2.3 *In vitro* characterization of ECM hydrogel on cell culture

For *in vitro* characterization of ECM hydrogel, hMSCs, human neural stem cells and dorsal root ganglia (DRG) explant cultures were used.

4.2.3.1 hMSCs culture

hBM-MSCs, hASCs and hWJ-MSCs were obtained, cultured under standard conditions and their surface markers were determined as described above.

4.2.3.2 Human neural stem cell culture

A conditionally immortalized human foetal neural stem cell line SPC-01 (NSCs) was generated from 8 week old human foetal spinal cord as described previously (Pollock et al. 2006). Cells

were cultured in tissue-culture flasks, freshly coated with laminin (10 μg/mL) in DMEM/F12 (Gibco, Life Technologies, Grand Island, NY), supplemented with human serum albumin (0.03%, Baxter Healthcare Ltd., Norfolk, UK), human apo-transferrin (100 μg/mL), putrescine DiHCl (16.2 μg/mL), human recombinant insulin (5 μg/mL), progesterone (60 ng/mL), L-glutamine (2 mM), sodium selenite (40 ng/mL), 4-OHT (100 nM) (all from Sigma), human EGF (20 ng/mL) and human bFGF (10 ng/mL, PeproTech, London, UK) and primocin 100 μg/mL (InvivoGen, San Diego, CA, USA), at 37°C and 5% CO_2 in a humidified atmosphere.

4.2.3.3 Cell growth and proliferation

To determine *in vitro* hMSCs proliferation, ECM hydrogels were placed into a 96-well plate (90 μL/well) and seeded with cells (5 x 10^3 cells/cm^2 in 100 μL media). hMSCs seeded on wells without hydrogel (TCP) served as a control. hMSC proliferation was measured using WST-1 assay on 1, 3, 7 and 14 days of the culture. 10 μL of WST-1 reagent was added to each well containing 100 μL culture media, and the plates were incubated for 2 hours at 37°C. The absorbance was measured using a Tecan-Spectra plate reader at 450 nm. Each type of hydrogel was seeded in triplicate. Six independent experiments of three hydrogel batches were performed for each hydrogel type.

The morphology of the hMSCs grown on the hydrogels was examined by immunofluorescent staining for actin filaments. After fixation in 4% paraformaldehyde in PBS for 15 mins, the cells were washed with PBS and stained with Alexa-Fluor 568 phalloidin (1:400, Molecular Probes, Eugene, Oregon, USA); the nuclei were visualized using DAPI fluorescent dye (1:1000).

NSC growth and differentiation was analysed after their seeding (10^5/cm^2) on laminin coated coverslips or ECM hydrogel disks formed inside a cylindrical mould with a diameter 0.8 cm (Scaffdex, Tampere, Finland). After 7 and 14 days of the culture, the cells were fixed in 4% paraformaldehyde in PBS for 15 mins, washed with PBS and stained using AlexaFluor 568 phalloidin. Next, the immunohistochemical staining against light neurofilaments (70 kDa) using mouse monoclonal IgG1 (NF70, 1:400; clone DA2, Merck-Millipore, Billerica, MA, USA) and mouse monoclonal IgG against microtubule-associated protein 2 (MAP2, 1:1000; clone AP20, Millipore) were performed. The nuclei were visualized using DAPI fluorescent dye (1:1000). Images were taken using confocal microscope Zeiss LSM 5 DUO (Carl Zeiss, MicroImaging GmbH, Jena, Germany).

4.2.3.4 Cell migration towards ECM hydrogels

To assess the chemotactic capacity of ECM hydrogels for hMSCs, xCELLigence® RTCA DP Instrument was used to perform Cell Invasion and Migration Assay. ECM hydrogels (6% v/v solutions in media without supplements) were placed into a lower chamber of CIM-Plate 16, and hBM-MSCs, hASCs and hWJ-MSCs (10^5 cells in 100 µL of media without supplements) were than pipetted into an upper chamber. The impedance signal was reduced when cells adhered to the microporous membrane in order to migrate towards ECM hydrogels. As a positive control SDF-1 (20 ng/mL, Sigma) was used; culture medium without supplements served as a negative control. Recording was performed as described above. The assay was repeated five times.

4.2.3.5 Dorsal root ganglia explant culture

Dorsal root ganglia (DRGs) were extracted from four 3-5 days old Wistar rats. Briefly, the spinal cords were dissected and DRGs from low thoracic and lumbar parts were isolated, placed in cold Hank's Balanced Salt Solution without Ca^{2+}/Mg^{2+} solution (Invitrogen), and cleaned of peripheral nerve processes. DRG explants were then placed on ECM hydrogels or Matrigel (Matrigel® Growth Factor Reduced Basement Membrane Matrix, Phenol Red-Free, Corning, New York, USA) in 24-well plates, and cultured in Neurobasal medium (Invitrogen) supplemented with 2% B27 (Life Technologies), 2 mM L- glutamine (Invitrogen), 0.5% NGF (50 ng/mL, PeproTech), uridine (17.5 µg/mL, Sigma) and primocine (2 µL/mL, PeproTech) in a humidified atmosphere at 37°C and 5% CO_2. The medium was changed every 3 days. After 7 days of culture, DRGs were fixed with 4% paraformaldehyde in PBS for 10 mins and stained for anti-NF160 antibody (clone NN18, 1:200, Sigma), AlexaFluor 488 secondary antibody (1:200, Invitrogen), and cell nuclei (DAPI, 1:1000). Fluorescent images were taken using Leica fluorescent microscope (Leica DMI 6000B) and TissueGnostic software (TissueGnostics GmbH, Vienna, Austria). The neurite extension area and the longest neurite length were determined using a special plugin for ImageJ (NeuriteJ) (Torres-Espin et al. 2014). The assay was repeated three times for each hydrogel.

4.3 Experiments on animal models

All animal experiments were performed in accordance with the European Communities Council Directive of 22nd of September 2010 (2010/63/EU) regarding the use of animals in research and were approved by the Ethics Committee of the Institute of Experimental Medicine (IEM), Czech Academy of Sciences (Prague, Czech Republic).

4.3.1 Transplantation of hWJ-MSCs into a rat model of SCI

As an experimental model, the adult Wistar male rats were used. All the animals were approximately 10 weeks old with the weight varying between 275-305g (n = 90). First group of animals (n = 47) surviving 9 weeks was used for behavioural testing, histological, immunohistochemical and quantitative real-time polymerase chain reaction (qRT-PCR) analysis. Second group of animals (n = 39) was used for qRT-PCR evaluation 4 weeks after SCI and was not included in behavioural testing. Additional four animals in two groups (n = 4) were used for evaluation of surviving cells two weeks after transplantation of 0.5 and 1.5 x 10^6 hWJ-MSCs. For the transplantation, cells in the third passage were used.

4.3.1.1 Spinal cord injury model

Surgical procedure was performed in operating theatre under the standard conditions. Under antibiotic prophylaxis and proper anaesthesia and analgesia, the skin on the animal´s back was incised and paravertebral muscles were separated at the level of thoracic vertebra Th7 - Th12 and laminectomy of Th10 was performed. A sterile 2-french Fogarty catheter was carefully inserted into the epidural space until the centre of the balloon rested on level of Th8. The balloon was rapidly inflated with 15 µl saline and kept for 5 mins. Then, the balloon was deflated and removed, and muscles and skin were sutured by single non-absorbable stitches. During the procedure, the animal's body temperature was kept at 37°C with a heating pad. The lesioned animals were assisted in feeding and urination until they had recovered sufficiently to perform these functions on their own. The animals received antibiotics for 7 days to prevent postoperative infections and were allowed to feed and drink *ad libitum*.

Cyclosporine A (10 mg/kg, i.p.; Sandimmun, Novartis, Basel, Switzerland) was administered to all animals a day before intended application of human cells and throughout the whole study. Under the short-time general anaesthesia (described above) hWJ-MSC were transplanted intrathecally on 7th, 14th and 21st day after the SCI. Animals were divided into 5 groups with variable treatment (Table 3).

Group	Nb. of hWJ-MSCs	Days after SCI	Animals for behavioural testing	Animals for qRT-PCR	Animals for cell surival
1.	0.5 x 10^6	7	12	5	2
2.	1.5 x 10^6	7	9	5	2
3.	Triple 0.5 x 10^6	7, 14, 21	8	5	
4.	Triple 1.5 x 10^6	7, 14, 21	7	5	
5.	0	7, 14, 21	11	5	

Table 3. Animal groups with variable treatment. Human Wharton´s jelly mesenchymal stromal cells (hWJ-MSC) were administered in 50 µL saline.

4.3.2 *In vivo* testing of ECM hydrogels

4.3.2.1 Injection of UC-ECM hydrogels into a rat photothrombotic lesion as a model of focal cerebral ischaemia

To test the biocompatibility of UC-ECM hydrogel *in vivo*, a focal brain photochemical lesion was created in the motor cortex in rats. Eight male Wistar rats (330 ± 30 g) were maintained at 22°C on a 12-hour light/dark schedule and given water and food *ad libitum*. To create the defect, the animal was placed into the stereotactic apparatus under isoflurane (3%) anaesthesia and the scalp was incised in the midline; the pericranial tissue was dissected to expose the bregma. Focal cerebral ischaemia was performed according to Anderova et al. (2006) as follows: Bengal Rose (Sigma) was injected via the right femoral vein (0.08 g/mL saline; 1µL/g), and the skull was illuminated above the primary motor cortex (2 mm rostral and 2 mm dextrolateral to the bregma) with a fibre optic bundle of a cold light source (KL 1500 LCD; Zeiss) for 10 mins. The skin overlying the cranium was then sutured.

Seven days after the focal cerebral ischaemia, a small opening in the lesion site was drilled into the scull of the animal and 10 µL of UC-ECM (n = 4) or saline (n = 4) were injected into the lesion (in a depth of 2 mm) using a Hamilton syringe (Hamilton Company, Bonaduz, Switzerland) and stereotactic apparatus.

4.3.2.2 Injection of SC-ECM and UC-ECM hydrogels into a rat hemisection as a model of SCI

Male Wistar rats (250–300 g) underwent a hemisection at the level of the Th8. The neutralized and isotonically balanced liquid pre-gel solution of SC-ECM and UB-ECM hydrogels (8 mg/mL), were acutely injected into the spinal cord defect after hemisection and allowed to gelate *in situ*, followed by histological evaluation after 2, 4 and 8 weeks after the implantation (n = 5 per group, per time point). The surgery was performed under adequate pentobarbital anaesthesia (60 mg/kg). The animals received local injections of mesocain (0.3 mL s.c. at the surgery site) in addition to general anaesthesia, as well as gentamicin (0.05 mL i.m., Sandoz, Prague, Czech Republic) and atropine (0.2 mL, atropine solution 1:5; both from BB Pharma, Prague Czech Republic) injections. First, a microsection of the skin was made at the level of Th8 spinal processes using scalpel. Then the laminectomy of Th8 was performed using rongeur and the dura was incised with capsulotomy scissors. A 2 mm long spinal cord segment of volume ~ 6 mm^3 was dissected using delicate tissue scissors to generate a hemisection cavity. Then the dissected segment was removed using a small piece of cellulose and fine forceps. Aforementioned instruments were purchased from Medicon® (Tuttingen, Germany). The dura mater was sutured with 10/0 monofil unresorbable thread (B Braun, Aesculap, Melsungen, Germany), and the hydrogels were injected into the cavity in a single injection using an Omnican®Insulin syringe for U-100 Insulin (B Braun, Melsungen, Germany). The muscles and skin were sutured with 4/0 monofil unresorbable thread (4/0 Chirmax, Prague, Czech Republic), and the animals were housed in cage and provided with food and water *ad libitum*. In the control SCI group (n = 4) the hemisection defect was filled with saline and dura was sutured.

To evaluate the potential of ECM hydrogels as a cell vehicle, the SC-ECM hydrogels were mixed with hWJ-MSCs (n = 4; 0.5 x 10^6 cells per 0.2 mL; ~ 1.5 x 10^4 cells) prior to their implantation into the hemisection cavity. This animal group received a daily injection of the immunosuppressant cyclosporine A (10 mg/kg, i.p.), azathioprine (2 mg/kg, p.o.; Imuran, Apen Europe GmbH, Bad Oldesloe, Germany) and methylprednisolone (2 mg/kg, i.m; Solu-Medrol, Pfizer, Puurs, Belgium) to prevent the rejection of the transplanted cells.

4.4 Evaluation of animal studies

4.4.1 Behavioural testing

4.4.1.1 BBB test

The BBB test was used to assess the function recovery and locomotor abilities in SCI studies where hWJ-MSCs were transplanted. The scale (0- 21) represents sequential recovery stages and categorizes combinations of rat joint movement, hind limb movements, stepping, forelimb and hind limb coordination, trunk position and stability, paw placement and tail position. In BBB test, rats were placed on the floor surrounded by boundaries making the rectangular shape. Results were evaluated as: 0 indicated complete lack of motor capability and 21 indicated the best possible score (healthy rat). Measurement was performed before SCI and then every week for the 8 weeks starting the first week after SCI.

4.4.1.2 Rotarod test

Rotarod unit machine (Ugo Basile, Comerio, Italy) was used to test advanced degree of motor coordination of the limbs. Ability to balance on a rotating rod was recorded. Each animal was taught this task one week before surgery and then every two weeks – 2nd, 4th, 6th and 8th week after SCI. Animals were placed on a rotating rod at a fixed speed of 10 rpm before surgery and 5 rpm after surgery and were left to walk for 60 seconds. There were four trials per day within five consecutive days. Between trials there was always 5 mins break. The latency to fall off the rod onto a floor was measured.

4.4.1.3 Beam walk test

In the flat beam test, we tested ability to cross a 1m long narrow beam with a flat surface. Rats were placed on the beginning of the beam whereas on the other side the escape box was placed. The latency and the trajectory to traverse the beam were recorded by a video tracking system (TSE-Systems Inc., Bad Homburg, Germany) for a maximum of 60 seconds. Performance of locomotor coordination was evaluated using a 0-7 point scale modified from Metz and Whishaw (Metz and Whishaw 2009). All animals were firstly trained in this task before surgery and then tested every week starting the second week after SCI.

4.4.2 Tissue processing, histology and immunohistochemistry

4.4.2.1 Analysis of SCI lesion transplanted with hWJ-MSCs

Under deep anaesthesia, 9 weeks after the SCI, all animals were sacrificed and transcardially perfused with a phosphate buffer solution (250 mL), followed by a 4% paraformaldehyde

solution in a phosphate buffer (250 mL). The spinal cord was dissected and removed from the spinal column and embedded in a paraffin wax. Serial cross-sections (5 μm thick cut at 1 mm intervals) were obtained by microtome within a 2 cm-long segment around the centre of the lesion. Samples of five animals from each group (fifteen cross-sections in total - 7 sections cranially and caudally to the centre of the lesion) were stained using specific markers and observed under Axioskop 2 plus microscope (Zeiss, Oberkochen, Germany) and analysed with ImageJ software (NIH, Bethesda, MD, USA).

Following attributes were assessed: the total volume of spared white and grey matter using Cresyl violet and Luxol fast blue staining, the extent of the glial scar using CY3-conjugated primary antibody against glial fibrillary acidic protein (GFAP, Sigma), newly sprouted axons were using a primary antibody against growth associated protein 43 (GAP43, Millipore) and survival of the transplanted cells at 2 weeks after the surgery using HuNu ((Millipore).

4.4.2.2 Analysis of UC-ECM hydrogels injected into a rat photothrombotic lesion

Animals were sacrificed 24 hours after the UC-ECM implantation. The brains were removed, fixed in 4% paraformaldehyde for 10 days and cut in frozen mode (local temperature -24°C). Coronal slides, 40 μm thick, were stained for cell nuclei with DAPI (1:1000), mouse monoclonal IgG1 to CD68 (ED1; 1:150, Abcam), goat polyclonal IgG to CD206 (c-20; 1:250, Santa Cruz, Heidelberg, Germany) or mouse monoclonal IgG1 to collagen I (1:1000, COL-I, Abcam) diluted in 0.1 M PBS containing goat (or donkey – depending on the host organism of secondary antibodies) serum (1:10 both; Sigma) and Triton X-100 (0.1%) overnight in 4ºC. Staining solution lacking Triton-X was used only in the case of extracellular anti-collagen staining. As secondary antibodies, goat anti-mouse IgG conjugated with AlexaFluor 594 (1:400) for collagen I, donkey anti-mouse IgG conj. with AlexaFluor 488 (1:400) for CD68 and donkey anti-goat IgG conj. with AlexaFluor 594 (1:400;) for CD206 (all from Life Technologies) were used.

Fluorescent images were taken using confocal microscope Zeiss LSM 5 DUO. The relative number of macrophages in the hydrogel area was determined from three randomly selected sections using a 20x objective and ImageJ software.

4.4.2.3 Analysis of SCI lesion implanted with SC-ECM and UB-ECM

At 2, 4 and 8 weeks after hydrogel injection, the animals were deeply anesthetized with an i.p. injection of overdose pentobarbital and perfused with PBS followed by 4 % paraformaldehyde

in 0.1 M PBS. The spinal cord was left in bone overnight, then removed and post fixed in the same fixative for at least 1 week. A 3 cm long segment of the spinal cord containing the lesioned site was dissected out, and a series of 40 µm thick longitudinal sections was collected. H&E staining was performed using a standard protocol. For immunohistological analysis we used antibodies against neurofilaments (NF 160, 1:200), endothelial cells (RECA-1, 1:500), astrocytes (Cy3-conjugated mouse GFAP, 1:200; all from Sigma), Schwann cells (p75, 1:200), serotonin-positive axons (R-SERO, 1:100), oligodendrocytes (OSP, 1:1000), macrophages (ED1, 1:100), M1 macrophages (CD86, Cy5-conjugated donkey anti-rabbit IgG-PerCp-Cy5,5, 1:2500), human mitochondria (MTCO2, 1:250; all from Abcam), M2 macrophages (CD206, 1:250), axonal growth cone (GAP43, 1:100; all from Santa Cruz, Heidelberg, Germany). Alexa Fluor® 488- conjugated goat anti-mouse IgG (1:200), Alexa Fluor® 594- conjugated goat anti-mouse IgG (1:200) and Alexa Fluor® 488- conjugated donkey anti-goat IgG (1:700) were used as secondary antibodies. The nuclei were visualized by using DAPI (Invitrogen) fluorescent dye. Fluorescent micrographs were taken using AxioCam HRc Axioscop 2 Plus fluorescent microscope (Zeiss, Jena, Germany) and LSM 510 DUO laser scanning confocal microscope.

For axonal and vessel analysis, multiple images across the entire lesion were taken using a 20x objective. Five images from each sample were selected and the total area of the axons (NF160 staining) and blood vessels (RECA staining) within the lesion area was outlined using ImageJ software and divided by the area of the lesion to determine the percentage of the lesion that was occupied by new axons or vasculature.

4.4.3 qRT-PCR analysis

qRT-PCR was used to evaluate the changes in expressions of target genes in SCI lesion transplanted with hWJ-MSCs, UB-ECM, SC-ECM and hWJ-MSCs laden SC-ECM hydrogel.

Messenger ribonucleic acid (mRNA) was isolated from paraformaldehyde-fixed frozen tissue sections of injured spinal cord around the centre of the lesion using the High Pure RNA Paraffin Kit (Roche, Penzberg, Germany), following the manufacturer's recommendations. The mRNA amount was quantified using a spectrophotometer (NanoPhotometer™ P-Class, München, Germany). The isolated mRNA was reverse transcribed into cDNA using Transcriptor Universal cDNA Master (Roche, Penzberg, Germany) and thermal cycler (T100™ Thermal Cycler, Bio-Rad). The qRT-PCR was carried out in a final volume of 10 µL containing cDNA solution, TagMan® Gene Expression Assays (Life Technologies, Carlsbad, CA, USA) and

FastStart Universal Probe Master (Roche, Manheim, Germany). Primers that were used to detect changes in gene expression are listed in Table 4.

qRT-PCR was performed on StepOnePlus™ Real Time PCR cycler (Life Technologies). Amplifications run under the same cycling condition: two mins at 50°C, 5 mins at 95°C, followed by 40 cycles of 15 seconds at 95°C, one min at 60°C.

All samples were run in duplicate and a negative control was included in each array. Results were analysed with StepOnePlus® software. Gene expression level was normalized using house-keeping gene - glyceraldehyde-3-phosphate dehydrogenase (*Gapdh)* as a reference gene. Relative quantification of gene expression was calculated using the $\Delta\Delta C_t$ method.

Target gene	TagMan® Gene Expression Assays
Gapdh	*Rn01775763_g1*
Casp3	*Rn00563902_m1*
Gfap	*Rn00566603_m1*
Cd86	*Rn00571654_m1*
Irf5	*Rn01500522_m1*
Mrc1	*Rn01487342_m1*
Cd163	*Rn01492519_m1*
Fgf2	*Rn00570809_m1*
Gap43	*Rn01474579_m1*
Vegfa	*Rn01511601_m1*
Sort1 / Nt3	*Rn01521847_m1*
Nos2	*Rn00561646_m1*
Arg1	*Rn00566603_m1*
Ccl3 / MIP-1α	*Rn01464736_g1*
Ccl5 /RANTES	*Rn00579590_m1*
Ptgs2	*Rn01483828_m1*
Il2	*Rn00587673_m1*
Il6	*Rn01410330_m1*
Il12b	*Rn00575112_m1*

Table 4. TagMan® Gene Expression Assays. Glyceraldehyde-3-phosphate dehydrogenase (Gapdh), caspase 3 (Casp3), glial fibrillary acidic protein (Gfap), interferon regulatory factor 5 (Irf5), mannose receptor C-type 1 (Mrc1), macrophage scavenger receptor (Cd163), fibroblast growth factor (Fgf2), growth associated protein 43 (Gap43), vascular endothelial growth factor (Vegfa), neurotrophin type 3 (/Sort1/Nt3), inducible nitric oxide synthase 2 (Nos2), arginase 1 (Arg1), macrophage inflammatory protein 1α (Ccl3/MIP-1α), chemokine (C-C motif) ligand 5 (Ccl5/RANTES), prostaglandin-endoperoxide synthase 2 (Ptgs2), interleukin 2 (Il2).

4.5 Statistical analysis

All data are presented as mean ± standard error mean. Data were analysed using GraphPad Prism (San Diego, CA, USA) or SigmaStat 3.1 (Sistat Software Inc., San Jose, CA, USA) using appropriate statistical method. For statistical evaluation of PDT, student non-paired t-test was used. For statistical evaluation of cell yield, proliferation, migration, PD, flow cytometry, cytokine production, comparison of groups treated with hWJ-MSCs and saline, ECM hydrogel *in vitro* and *in vivo* evaluation and gene expression statistical evaluation, one-way analysis of variance (ANOVA) with Tukey´s multiple comparison *post hoc* analysis was used. To compare the results in time, two-way ANOVA was used. Two-way repeated measurement ANOVA with Student-Newman-Keuls *post hoc* pair-to-pair test was used to compare the behavioural results between the groups, grey/white matter sparing and GFAP positive area of glial scar. Statistical significance level was set at a *p*-value of $p<0.05$ (significant), $p<0.01$ (very significant) and $p<0.001$ (highly significant).

5 Part 1: hMSCs Isolation, Expansion and *In Vitro* Characterization

5.1 Introduction

hMSCs represent a useful therapeutic approach for neural regeneration. After their initial discovery in BM, they have been isolated and characterized from a wide variety of adult and foetal tissues (Caplan 2007).

The source of hMSCs is an important factor to consider as it determines the behaviour, expression of their surface markers, differentiation potential and secretome production of MSCs (Hass et al. 2011). Each of the hMSCs sources has its own merits and limitations; and deeper investigation of their properties could help to choose the right hMSCs source for individual clinical applications.

In an adult human, BM and AT are sites where hMSCs are most prevalent. hBM-MSCs are often designated as the gold standard, but their isolation is accompanied by an invasive and painful procedure with a risk of infection. hASCs are usually isolated from a surgical waste – lipoaspirate. However, in indicated cases there might be small amount of adipose tissue for ASCs isolation. hMSCs from BM and AT are used in both autologous and allogeneic clinical applications.

Human umbilical cord tissue – Wharton´s jelly (WJ) is an appealing source for hMSCs isolation – it is easily accessible, non-invasive, ethical and does not bear age- and disease- related alterations. Moreover, it was suggested that hWJ-MSCs have improved proliferative capacity (Troyer and Weiss 2008) and life span. They have been reported to be more primitive (Amable et al. 2014), possess low immunogenicity (Zhou et al. 2011), and higher differentiation potential in comparison to MSCs derived from adult sources (Hass et al. 2011).

5.2 Aim of the study

In this study, we optimized a method for isolation of hMSCs from WJ and compared their properties to hBM-MSCs and ASCs *in vitro* in terms of cell yield, migration potential, proliferation, population doubling (PD), cumulative PD (cPD), PD time (PDT), expression of surface markers, differentiation potential and secretion of cytokines and growth factors.

5.3 Results

5.3.1 Cell yield

Cell yield was assessed as the number of the cells in the first passage that was normalized to millilitre (mL) or gram (g) of tissue. The highest number of cells was isolated from WJ, followed by AT. From both sources, significantly more hMSCs were isolated when compared to BM (Fig. 9). This observation corresponds to findings from other reports (Amable et al. 2014; Murphy et al. 2013; Zuk et al. 2001).

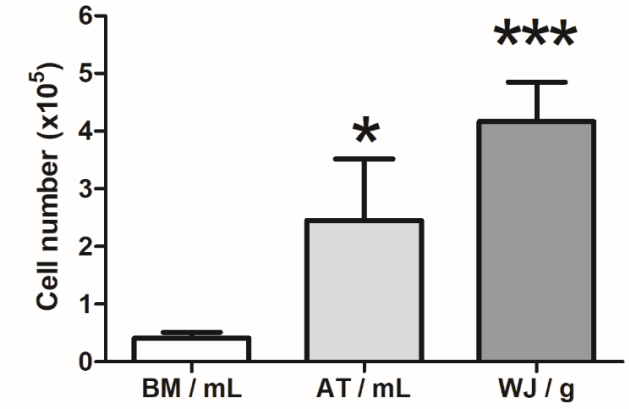

*Fig. 9. Cell yield expressed as a number of cells in the first passage. Adipose tissue (AT, n=7) and Wharton's jelly tissue (WJ, n=7) provide significantly higher amount of MSCs compared to bone marrow (BM, n=7). Data are shown as mean ± standard error mean. *p<0.05, ***p<0.001.*

5.3.2 Population doubling time (PDT)

PDT is a period of time required for the cell population to double in number. The lower the PDT, the higher is the proliferation capacity of the cell culture. PDT was calculated in each passage for all cell types. hWJ-MSCs displayed the lowest PDT during the first five passages. In the third passage, hWJ-MSCs PDT was significantly lower than the hASCs PDT (Table 5). hWJ-MSCs PDT was significantly lower than hBM-MSCs PDT in passage 2 (2P), 3P, 4P, 10P and 11P. hASCs displayed significantly lower PDT than hBM-MSCs in 6P, 8P, 10P and 11P.

When looking at the whole study time (1P-11P), PDT of hASCs and hWJ-MSCs remained relatively stable, as opposed to PDT of hBM-MSCs which significantly increased in time (Table 5). Of note, from seven hBM-MSCs cultures, only four could be expanded until 11P, which might have resulted in inhomogeneity of PDT across the passages (especially in 5P).

hMSC PDT (in hours)					
	2P	3P	4P	5P	6P
hBM-MSCs	68.3±13.1 n = 7	71.8±10.3 n = 6	99.0±21.9 n = 6	130.6±78.6 n = 6	81.1±23.9 n = 5
hASCs	43.7±5.9	48.6±8.3 ††	56.3±20.9	34.8±8.3	25.9±2.6 *
hWJ-MSCs	29.5±3.8 **	27.4±3.4 ***	25.4±3.8 **	24.2±3.5	33.5±5.6

hMSC PDT (in hours)					
	7P	8P	9P	10P	11P
hBM-MSCs	81.1±29.3 n = 5	81.1±27.5 n = 5	92.9±27.6 n = 5	105.1±39.1 n = 4	174.5±40.0 n = 4
hASCs	33.9±3.6	28.7±2.9 *	43.4±5.9	39.3±3.7 *	39.3±2.7 **
hWJ-MSCs	40.4±5.5	38.7±6.0	41.9±8.1	44.1±2.2 *	49.8±23.8 *

*Table 5. Population doubling time (PDT) of human mesenchymal stromal cells (hMSCs) from bone marrow (BM, n = according to table), adipose tissue (ASCs, n = 7) and Wharton´s jelly (WJ, n = 7) in hours in each passage. Data are shown as mean ± standard error mean. Statistical analysis using unpaired student t-test. *p<0.05, **p<0.01, ***p<0.001 versus hBM-MSC, †† p<0.01 versus hASCs.*

5.3.3 Cumulative population doubling (cPD)

PD presents a number of doublings that the cell population has undergone since initial seeding. cPD was calculated as number of PD at every passage added to the total of previous PDs. cPD tends to increase in cell cultures with high proliferation capacity.

The highest cPD in the first three passages as well as during the whole study time (1P-11P) was found for hWJ-MSCs. While hWJ-MSCs and hASCs PD was maintained or even increased with passage, PD of hBM-MSCs decreased in time (Fig. 10). hBM-MSCs reached a plateau in cPD at 8P indicating they did not further proliferate, while hASCs and hWJ-MSCs continued in proliferation and increased their cPD throughout the study period - up to 11P. This confirms a relative long-term proliferation and low senescence of hWJ-MSCs and hASCs.

When comparing to hBM-MSCs, cPD of hWJ-MSCs was significantly higher in all passages from 3P (p<0.001). When comparing hASCs to hBM-MSCs cPD, it was significantly higher in all passages from 4P (p<0.01, resp. p<0.001; Fig. 10). Significantly higher cPD of hWJ-MSCs than hASCs was then found in the 2P and 7P (p<0.05).

A

	hMSC PD									
	2P	3P	4P	5P	6P	7P	8P	9P	10P	11P
hBM-MSCs	2.37±0.35	2.03±0.16	1.59±0.40	1.69±0.47	1.50±0.33	2.04±0.51	1.82±0.62	1.65±0.62	0.85±0.76	1.0±0.51
hASCs	2.57±0.21	3.24±0.35	2.99±0.47	4.80±0.36	3.52±0.22	2.94±0.47	3.18±0.22	3.03±0.22	3.51±0.23	3.28±0.28
hWJ-MSCs	3.37±0.31	3.99±0.40	3.71±0.22	4.13±0.23	4.13±0.32	4.23±0.30	3.50±0.37	3.81±0.29	3.54±0.04	3.63±0.05

B

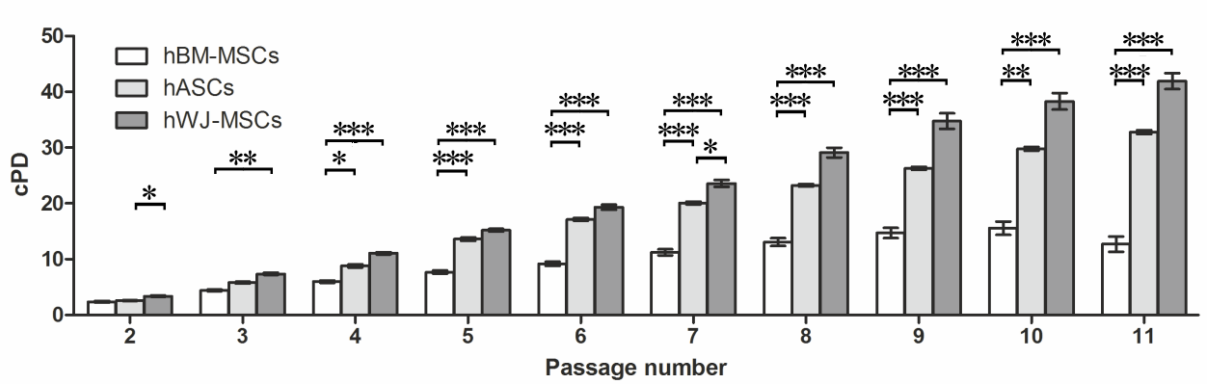

*Fig. 10. Analysis of proliferation of human mesenchymal stromal cells (hMSCs) from bone marrow (BM, n = 7), adipose tissue (hASCs, n = 7) and Wharton´s jelly (WJ, n = 7). (A) hMSCs population doubling (PD) calculations in each passage for all cell types. (B) hMSCs cumulative population doubling (cPD) determined as PD at each passage added to PD of the previous passages. Data are shown as mean ± standard error mean. *p<0.05, **p<0.01, ***p<0.001.*

5.3.4 Migration and proliferation assay

Migratory capacity is one of the essential hMSCs properties that enables their trafficking and thus allows them to act in the lesioned site. hMSCs were reported to migrate towards a variety of chemokines, *e.g.* SDF-1.

In a transwell culture, we confirmed the trafficking capacity of all hMSCs to migrate towards SDF-1. The migration rate did not differ between individual cell types (Fig. 11A).

Proliferation of hMSCs in a monolayer culture is exponential. To depict the cell growth within one passage, cells were analysed in a proliferation assay using WST-1 reagent. hWJ-MSCs proliferated more in the first 3 days in culture. Later, hASCs proliferation increased, while the proliferation of hBM-MSCs still remained slow. At the day 7, the proliferation of hWJ-MSCs and hASCs were significantly higher than the proliferation of hBM-MSCs (both $p<0.05$). At the day 7, however, hWJ-MSCs proliferation reached plateau and did not increase further due to contact inhibition (cells were not passaged in between). hASCs proliferated until the 14th

day, but the proliferation was low. At day 14, hBM-MSCs reached the proliferation of hWJ-MSCs and hASCs (Fig. 11B).

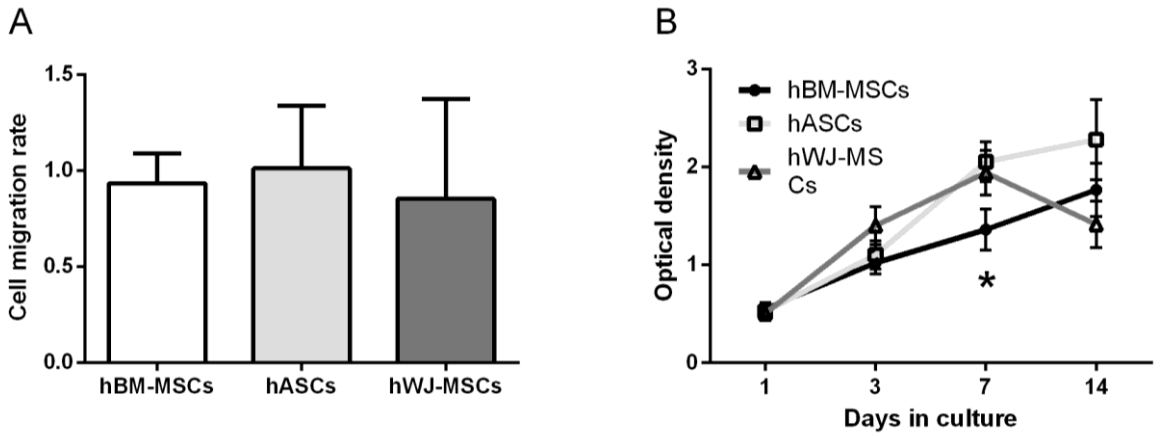

*Fig. 11. Analysis of migration and proliferation of human mesenchymal stromal cells (hMSCs) in 3rd passage. (A) Migration capacity of hMSCs from bone marrow (BM, n = 5), adipose tissue (hASCs, n =5) and Wharton´s jelly (WJ, n = 5) towards chemokine SDF-1 at 6 hours using xCELLigence Instrument. (B) Proliferation of hMSCs in time in a standard culture using WST assay (n = 5). Data are shown as mean ± standard error mean. *p<0.05.*

5.3.5 Cytometric analysis

Cytometric analysis of CD markers showed that all types of hMSCs fulfil the ISCT minimal criteria for mesenchymal cell phenotype (Dominici et al. 2006). All hMSCs revealed plastic adherence, shared fibroblast-like morphology (not shown) and a non-haematopoietic phenotype characterized by lacking markers such as CD14, CD34, CD45 and CD133 and expressing CD105, CD73, CD90 and human leukocyte antigen (HLA) class I (HLA-ABC) but not HLA class II (HLA-DR+DP, Fig. 12).

The most obvious difference was seen in the expression of CD106 – the positive expression was seen in hBM-MSCs but not in hASCs and hWJ-MSCs as reported also elsewhere (De Ugarte et al. 2003; Zuk et al. 2001).

hWJ-MSCs showed moderate expression of CD146 that was significantly higher when compared to hASCs and also moderate expression of CD235a that was significantly higher when compared to both, hASCs and hBM-MSCs.

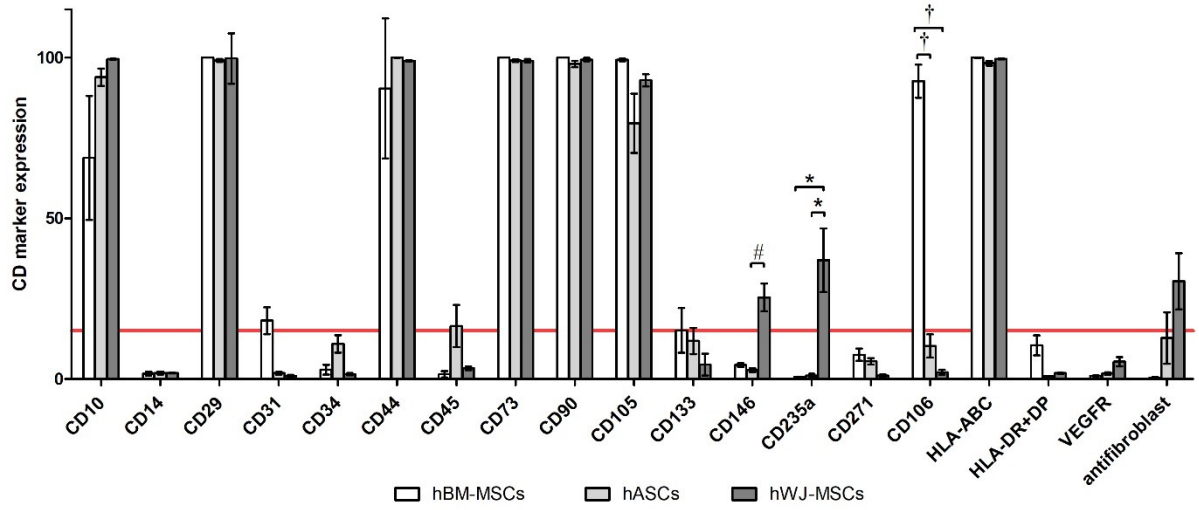

*Fig. 12. Flow cytometry analysis of the surface markers of three types of human mesenchymal stromal cells (hMSCs) from bone marrow (BM, n = 7), adipose tissue (ASCs, n = 7), and Wharton´s jelly (WJ, n = 7). Red line shows the distinction between the negative and positive expression and was set for our conditions at the 15% level. Data are shown as mean ± standard error mean. *p<0.05; #p<0.01; †p<0.001.*

5.3.6 Multi-lineage differentiation potential

hMSCs were differentiated into osteoblasts, adipocytes and chondrocytes by using appropriate differentiation media and protocols (Fig. 13). All hMSCs differentiated into adipocytes and chondrocytes. hBM-MSCs and hASCs differentiated under standard conditions into osteoblasts. On the other hand, osteo-differentiation could be performed only in freshly isolated hWJ-MSCs after longer differentiation period (4-5 weeks), while cryopreserved hWJ-MSCs did not differentiate into osteoblasts.

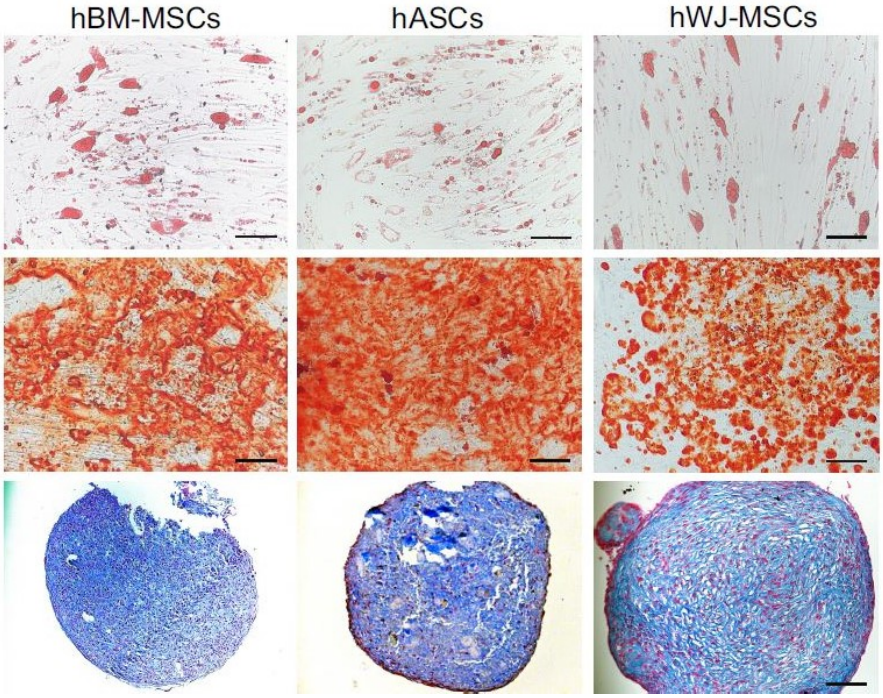

Fig.13. Multipotent differentiation of human mesenchymal stromal cells (hMSCs) from bone marrow (BM), adipose tissue (ASCs) and Wharton´s jelly (WJ). Differentiation into adipocytes illustrated by Oil-Red-O staining (first row), osteoblasts illustrated by Alizarin Red S staining (middle row) and chondrocytes illustrated by Alcian blue staining (bottom row). The scale represents 100 µm.

5.3.7 Secretome analysis

In view or recent findings, hMSCs´ secretome plays a key role in the MSCs action. Production of cytokines, growth factors, chemokines and cell adhesion molecules were determined using bead- based cytokine assay from conditioned media of unstimulated and stimulated hMSCs by inflammatory cytokines: IFNγ (10 ng/mL) and TNFα (10 ng/mL).

After inflammatory stimulation, high levels of IL-6 were found in hBM-MSCs CM, followed by hWJ-MSCs and hASCs CM. We also detected IL-12 and IFNα in CM of stimulated hBM-MSCs, hASCs and hWJ-MSCs. IL1RA secretion was seen in CM of stimulated hASCs and hBM-MSCs, but not in hWJ-MSCs (Fig. 14).

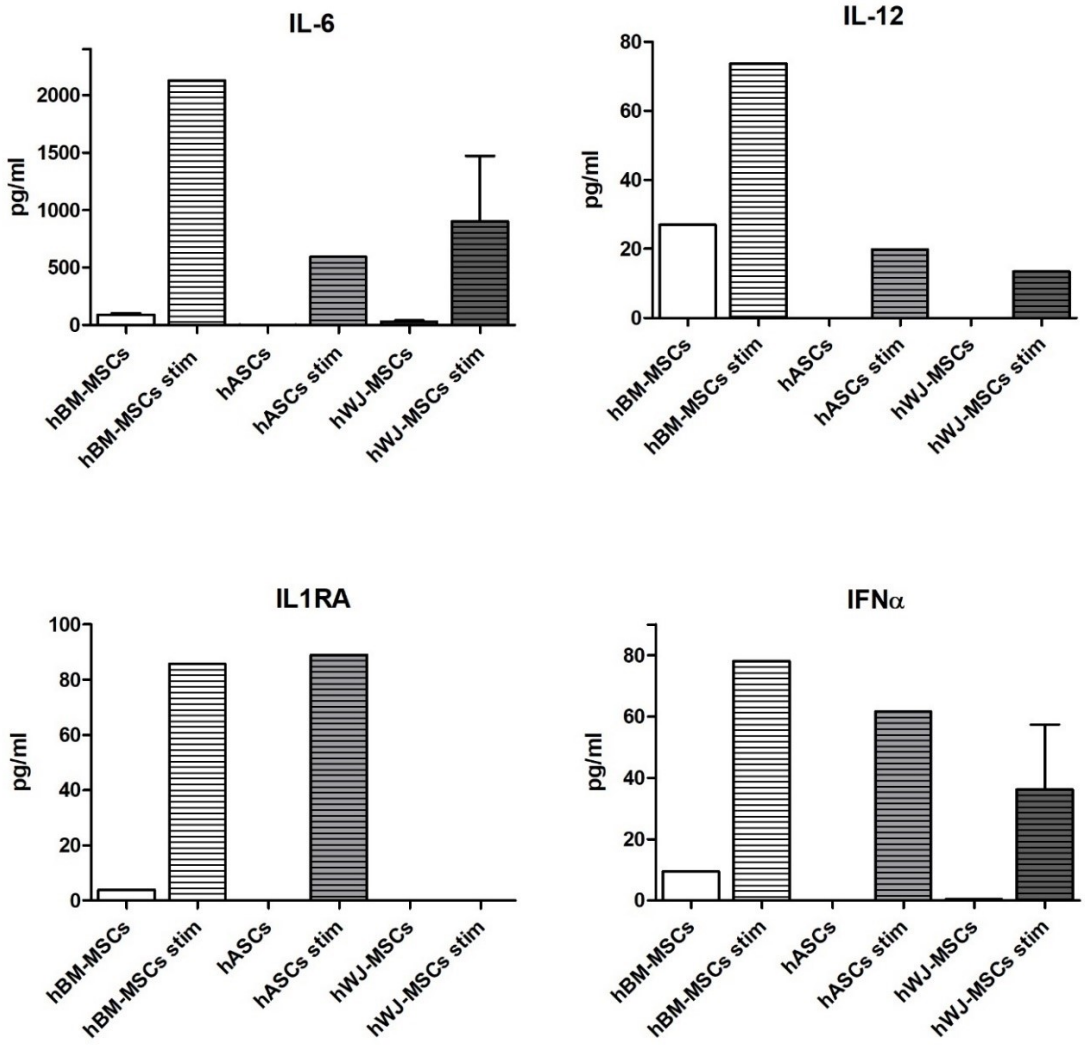

Fig. 14. Production of selected cytokines by human mesenchymal stromal cells (hMSCs) from bone marrow (BM), adipose tissue (ASCs) and Wharton´s jelly (WJ). Interleukin 6 (IL-6), IL-12, IL-1 receptor antagonist (IL1RA), interferon alpha (IFNα). hMSCs pooled from three donors were grown in media without or with inflammatory cytokines (stim): interferon gamma (IFNγ, 10 ng/mL) and tumour necrosis factor alpha (TNFα, 10 ng/mL). Data are presented as mean from a double measurement.

Regarding growth factor secretion, all cell types expressed HGF and BDNF, both in higher amounts in hWJ-MSC CM. VEGF-A was increasingly expressed by non-stimulated hBM-MSCs, in a less amount by hASCs, but not by hWJ-MSCs. Inflammatory stimulation enhanced secretion of bFGF and EGF, while no effect was found in secretion of HGF, BDNF or VEGF-A (Fig. 15).

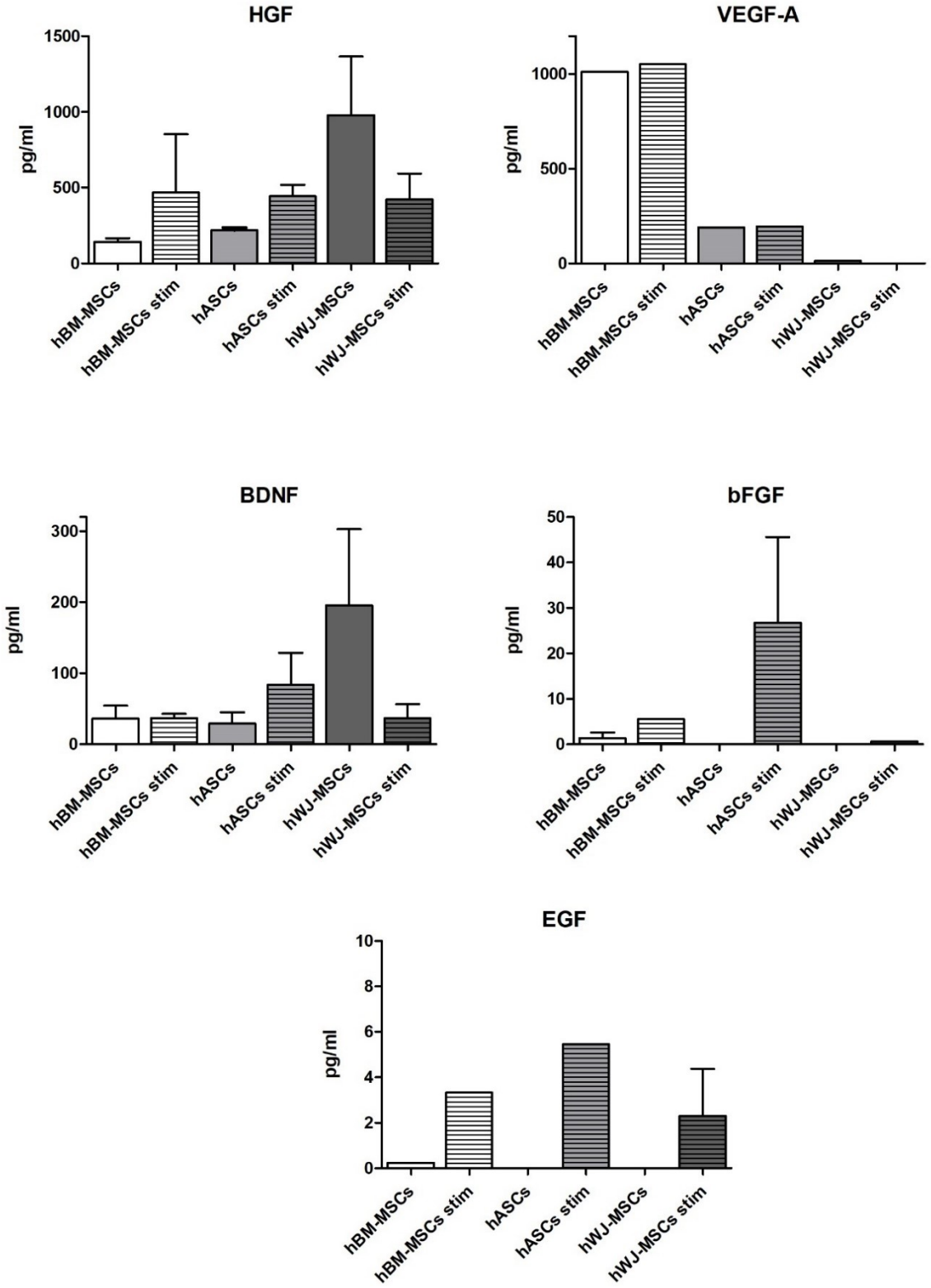

Fig. 15. Production of selected growth factors by human mesenchymal stromal cells (hMSCs) from bone marrow (BM), adipose tissue (ASCs) and Wharton´s jelly (WJ). Hepatocyte growth factor (HGF), vascular endothelial growth factor A (VEGF-A), brain-derived neurotrophic factor (BDNF), basic fibroblast growth factor (bFGF), epithelial growth factor (EGF). hMSCs were pooled from three donors and grown in media supplemented with ITS alone or ITS plus addition of inflammatory cytokines (stim): interferon gamma (IFNγ, 10 ng/mL) and tumour

necrosis factor alpha (TNFα, 10 ng/mL). Data are presented as mean from a double measurement of conditioned media.

All MSCs produced high levels of chemokines. SDF-1 was produced in all cell types, irrespectively of cytokine stimulation. Production of MCP1 and RANTES was increased after inflammatory cytokine stimulation. On the other hand, IP-10 was only produced after exposure to inflammatory cytokines (Fig. 16).

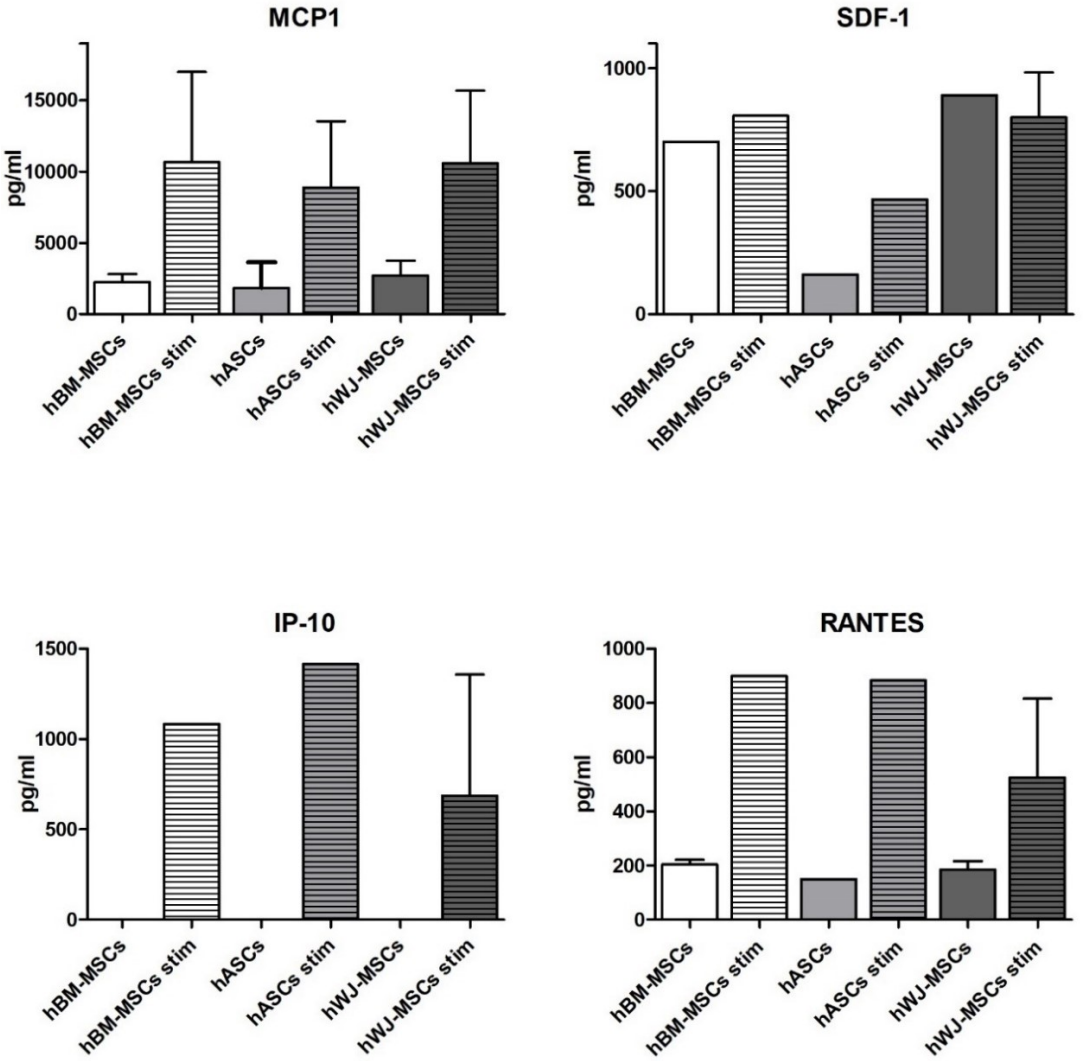

Fig. 16. Production of selected chemokines by human mesenchymal stromal cells (hMSCs) from bone marrow (BM), adipose tissue (ASCs) and Wharton´s jelly (WJ). Monocyte chemoattractant protein 1 (MCP1), stromal cell-derived factor1 (SDF-1), interferon gamma-induced protein 10 (IP-10), regulated on activation, normal T-cell expressed and secreted protein (RANTES). hMSCs were pooled from three donors and grown in media without or with addition of inflammatory cytokines (stim): interferon gamma (IFN γ, 10 ng/mL) and tumour necrosis factor alpha (TNFα, 10 ng/mL). Data are presented as mean from a double measurement.

We detected also secretion of cell adhesion molecules, namely ICAM-1 and VCAM (CD106). Expression of ICAM-1 was found highest in stimulated hWJ-MSCs, while VCAM-1 expression was only detected in stimulated cells and expressed in higher amounts in hBM-MSCs. The high expression of VCAM-1 (CD106) by hBM-MSCs corresponds with its positive surface marker expression (Fig. 17).

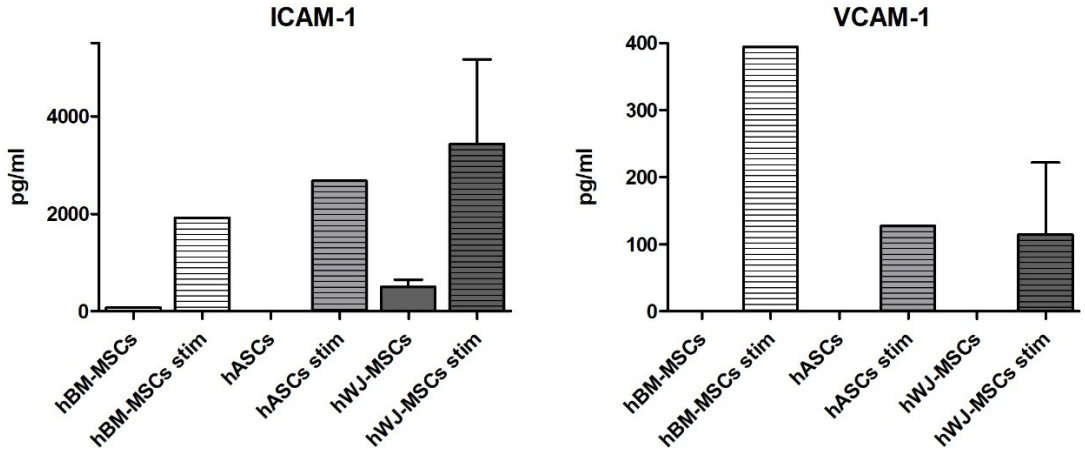

Fig. 17. Production of selected cell adhesion molecules by human mesenchymal stromal cells (hMSCs) from bone marrow (BM), adipose tissue (ASCs) and Wharton´s jelly (WJ). hMSCs were pooled from three donors and grown in media without or with addition of inflammatory cytokines (stim): interferon gamma (IFN γ, 10 ng/mL) and tumour necrosis factor alpha (TNFα, 10 ng/mL). Data are presented as mean from a double measurement.

5.4 Conclusion

We optimized a method for hWJ-MSCs isolation and confirmed that hWJ-MSCs met the basic criteria for mesenchymal stem cell phenotype, displayed a high proliferation rate, and migration capacity. hWJ-MSCs secreted a number of pro-inflammatory and anti-inflammatory cytokines, chemokines, cell adhesion molecules and neurotrophic growth factors, some of them could be enhanced by *in vitro* inflammatory stimulation. hWJ-MSCs are intended for allogeneic application, therefore, their immunomodulatory capacity and *in vivo* therapeutic potential should be assessed prior their wider utilization.

6 Part 2: Intrathecal Transplantation of hWJ-MSCs in the SCI

6.1 Introduction

Stem cell transplantation have become increasingly utilized in both preclinical and clinical research as promising strategy for the treatment of SCI. The beneficial effects of stem cells on neural repair are multifactorial, in synergy they may act as a cellular bridge which can replace neural cells, secrete cytokines and growth factors, modulate the immune response, inhibit the scar formation and protect neurons.

In terms of stem cell source, our findings (Chapter 5) confirm that hWJ-MSCs are efficient source of hMSCs. They were first described by McElreavey et al. (1991). Apart from being isolated by completely non-invasive way, their other advantage is that they are not influenced by age or disease of the donor. They have been found to have greater expansion capacity, faster growth *in vitro* (Troyer and Weiss 2008), are less mature (Amable et al. 2014) and express less MHC-II thus might show less immunogenicity compared to other MSC types (Zhou et al. 2011). hWJ-MSCs were therefore selected as suitable source of hMSCs for *in vivo* testing in the SCI compression model in rats.

hWJ-MSCs are increasingly evaluated in various clinical trials including also the SCI and their safety has already been confirmed (Cheng et al. 2014). However, there are many questions that remain unanswered at the basic research level, *e.g.* the right cell dose and frequency of their application.

6.2 Aim of the study

Our aim was to evaluate the effect of intrathecally transplanted hWJ-MSCs in a low (0.5×10^6) and a high (1.5×10^6) dose administered in a single or repeated (3x) application in the treatment of the SCI in rats. For the assessment, histochemical, behavioral and gene expression analysis were used.

6.3 Results

6.3.1 Cell culture

hWJ-MSCs mesenchymal phenotype, multipotent differentiation potential and proliferation capacity were confirmed in the Chapter 5.

6.3.2 Behavioural analysis

6.3.2.1 BBB test

Recovery of the hind limb locomotor function was evaluated every week immediately after SCI. BBB test score was calculated as a mean value from scores of both legs (Fig. 18A). One week after SCI all tested animals had severe paraparesis or paraplegia. No differences between groups were observed.

At 2 weeks after SCI, a significant difference in BBB test score was observed in a group treated with single dose of 1.5 x 10^6 hWJ-MSCs and a control group ($p<0.05$). From the 3rd week after SCI, rats treated with 1.5 x 10^6 and 3x 0.5 x 10^6 and 3x 1.5 x 10^6 hWJ-MSCs performed significantly better than control group and animals treated by 0.5 x 10^6 ($p<0.05$, $p<0.001$). No significant difference between the control group and 0.5 x 10^6 hWJ-MSCs group was recorded (Fig. 18A).

By the end of the 9th week after the SCI, animals in the groups with repetitive treatment achieved effective weight support of their body when standing, or walking (Fig. 18A).

6.3.2.2 Rotarod test

Due to severity of the lesion and limited recovery no significant differences were observed between the groups (Fig. 18B).

6.3.2.3 Beam walk test

Most of the rats showed minimal ability to cross the beam and balanced at the beginning of the beam (Fig. 18C).

Animals treated by 3x 1.5 x 10^6 hWJ-MSCs performed significantly better when compared to other groups. For the first three weeks, animals treated with 0.5 x 10^6 hWJ-MSCs achieved significantly better results than the control group, but in subsequent weeks they gradually worsened and the significant difference was lost. This was probably caused by weight gaining, lack of motivation and fear of falling of the beam (Fig. 18C).

Time to cross the beam (maximally for 60 seconds) was also measured. During the pre-training healthy rats were able to cross the beam in approximately 3.0 seconds (Fig. 18D). Measurements were performed weekly starting 2 weeks after SCI. At 2 weeks after SCI none of the rats was able to cross the beam and move from the start line. In the following weeks a significant improvement was observed between the rats treated by 3x 1.5 x 10^6 hWJ-MSCs and the other groups. Best score was achieved at 6 weeks in the group 3x 1.5 x 10^6 hWJ-MSCs, when rats traversed the beam in average time 34.9 ± 7 seconds (Fig. 18D).

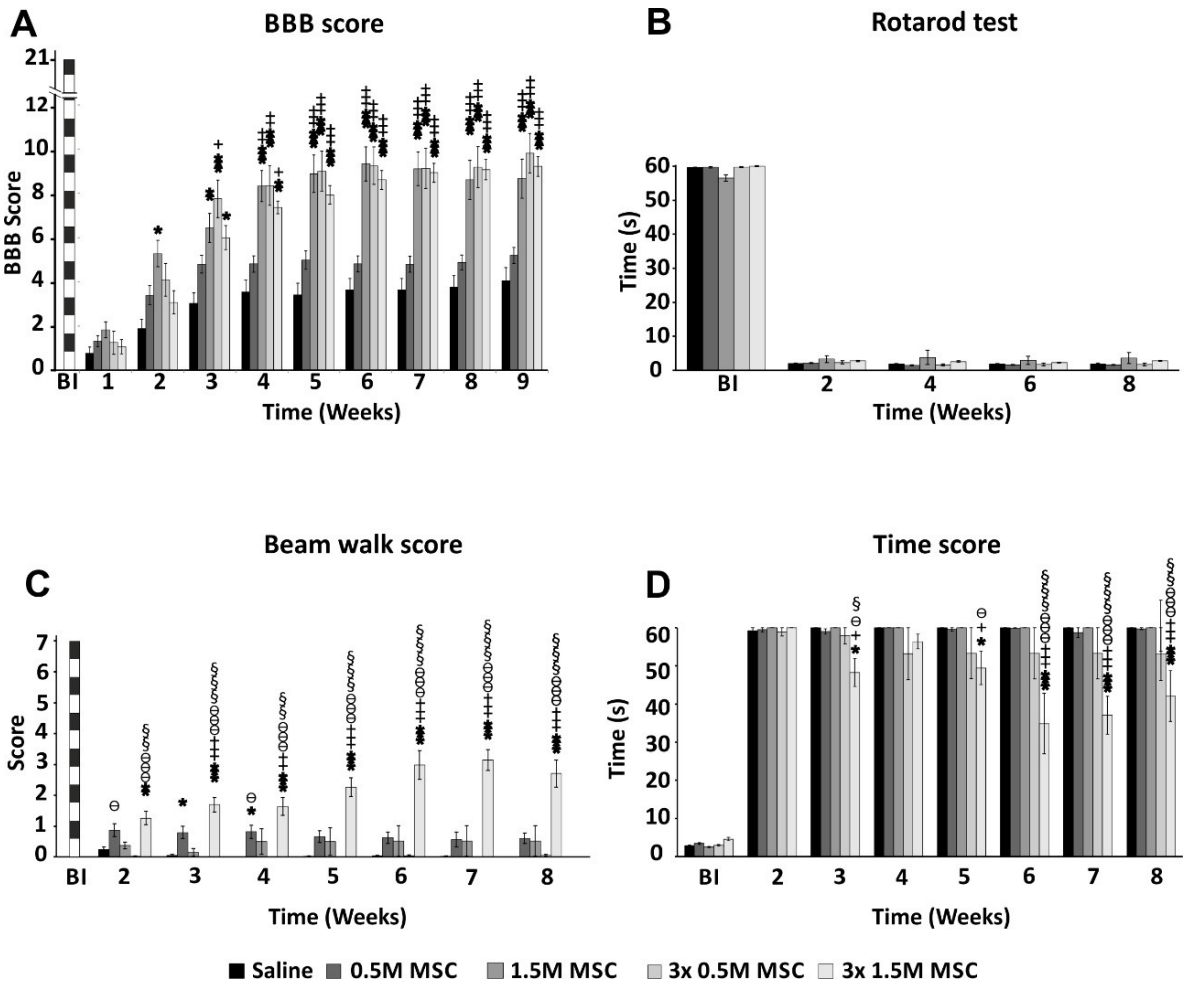

*Fig. 18. Recovery of locomotor functions following human Wharton´s jelly mesenchymal stromal cell (hWJ-MSCs) transplantation after spinal cord injury (SCI). (A) Locomotor skills of saline- or hWJ-MSCs-treated rats are illustrated using the Basso, Beattie, and Bresnahan open field locomotor test (BBB test score), (B) rotarod test, (C) beam walk score and (D) time score. Data are shown as mean ± standard error mean. Statistical analysis using two-way ANOVA, * p<0.05 versus saline; ** p<0.01 versus saline; *** p<0.001 versus saline; + p<0.05 versus 0.5 x 10^6 hWJ-MSCs; +++ p<0.001 versus 0.5 x 10^6 hWJ-MSCs; § p<0.05 versus 3x 0.5 x 10^6 hWJ-MSCs; §§ p<0.01 versus 3 x 0.5 x 10^6 hWJ-MSCs; §§§ p<0.001 versus 3x 0.5 x 10^6 hWJ-MSCs; ɵ p<0.05 versus 1.5 x 10^6 hWJ-MSCs; ɵɵɵ p<0.001 versus 1.5 x 10^6 hWJ-MSCs. BI = before injury.*

6.3.3 Histology and immunohistochemistry analysis

6.3.3.1 Grey and white matter sparing

Total area of spared grey/white matter was measured on the fifteen (5 μm thick) cross sections of the spinal cord 9 weeks after the SCI (7 sections cranially and caudally to the centre of the lesion). Values were averaged and compared to the control, which was set as a 100%. A significant difference in conserving the grey matter was observed between the group 3x 1.5 x 10^6 hWJ-MSCs and a control group (Fig. 19A, $p<0.05$) and a strong trend was observed when compared to the group of 0.5 x 10^6 hWJ-MSCs ($p = 0.051$). Comparison of the white matter sparing showed no significant difference between the groups (Fig. 19B). Similarly to the grey matter, significantly more white matter sparing was observed in the centre of the lesion and in surrounding tissue in animals treated with 1.5 and 3x 1.5 x 10^6 hWJ-MSCs when compared to the control group and rats treated with 0.5 x 10^6 hWJ-MSCs.

6.3.3.2 Astrogliosis and distribution of protoplasmic astrocytes

The area of the glial scar formed around the central cavity is presented as a ratio of GFAP-CY3 positive staining to the whole section (Fig. 19C). Groups treated by 3x 1.5 x 10^6, 3x 0.5 x 10^6 and 1.5 x 10^6 hWJ-MSCs had significantly smaller GFAP positive area around the main cavity compared to the control group. Group treated by 0.5 x 10^6 hWJ-MSCs showed no significant difference compared to saline treated rats.

Also, the number of protoplasmic astrocytes was counted (Fig. 19D). Rats treated by 3x 0.5 x 10^6, 1.5 x 10^6 and 3x 1.5 x 10^6 hWJ-MSCs had significantly lower number of protoplasmic astrocytes compared to the control group.

6.3.3.3 Axonal sprouting

Axonal sprouting was determined as a number of GAP43+ fibres. Number of GAP43+ fibres per section was counted manually. Values were averaged and compared to the control, which was set as a 100%. A significant effect of the cell treatment was not only dose dependent, but further improved after repeated application (Fig. 19E). Treatment with the lowest dose – 0.5 x 10^6 hWJ-MSCs had zero or minimal effect on axonal sprouting (102 ± 4%). In the other cell-treated groups, however, the number of positive fibres gradually increased with number of grafted cells (1.5 x 10^6 hWJ-MSCs 140 ± 4%). In addition, repeated application had significantly stronger effect compared to a single dose (3x 0.5 x 10^6 hWJ-MSCs 168 ± 10%; and 3x 1.5 x 10^6 hWJ-MSCs 212 ± 18%; $p<0.05$).

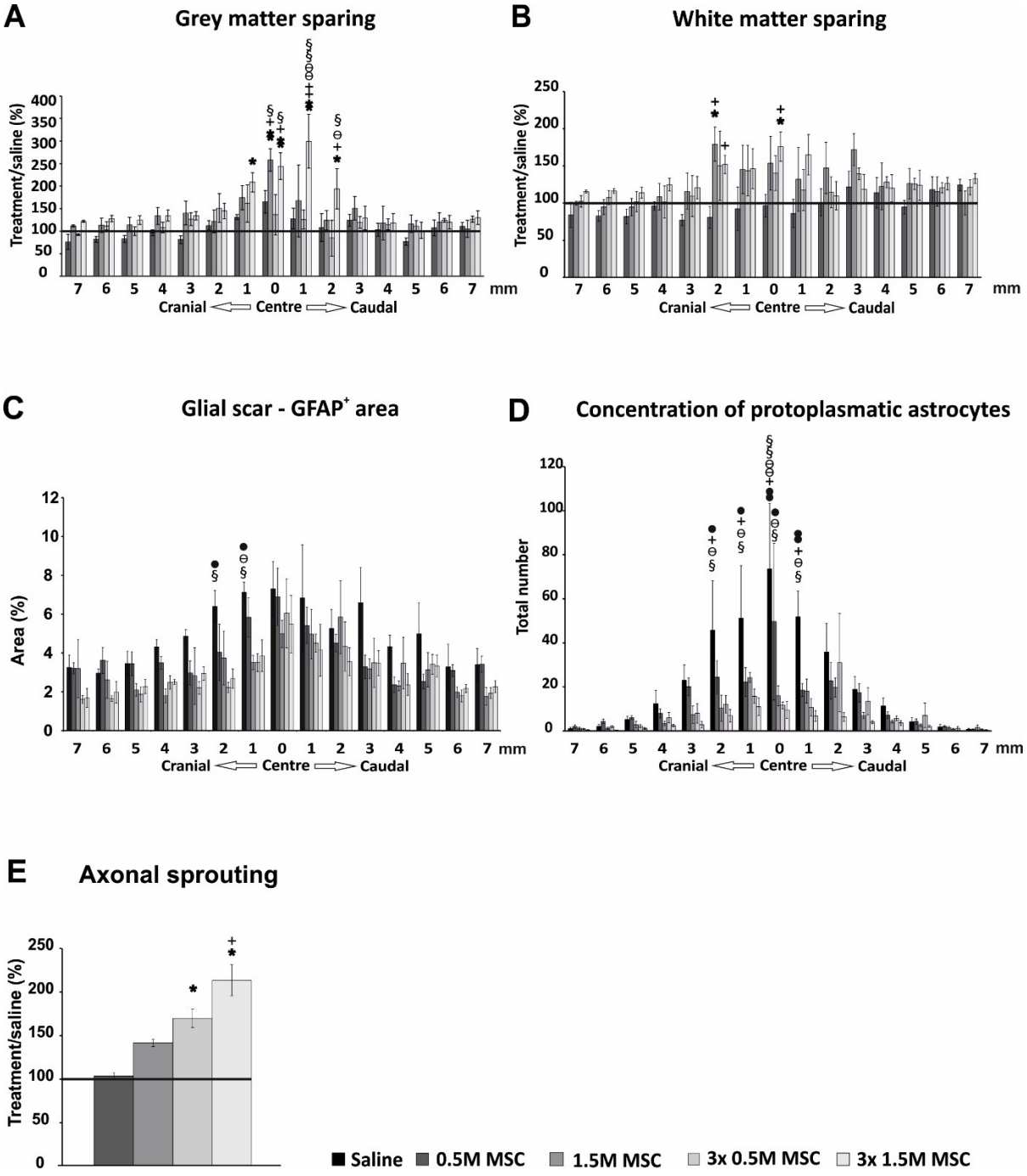

Fig. 19. Immunohistochemical and histological analysis 9 weeks after spinal cord injury (SCI) treated with human Wharton´s jelly mesenchymal stromal cells (hWJ-MSCs). (A) Analysis of grey matter sparing. (B) Analysis of the white matter. (C) Glial fibrillary acidic protein cyanine (GFAP-CY3) positive area showing the glial scar formation around the central cavity. (D) Average number of protoplasmic astrocytes near the centre of the lesion, (E) The average number of growth associated protein 43 (GAP43+) fibres. Data are shown as mean ± standard error mean. Statistical analysis using two-way repeated measurement ANOVA, $p<0.05$ versus saline; ** $p<0.01$ versus saline; *** $p<0.001$ versus saline; + $p<0.05$ versus 0.5 x 10^6 hWJ-MSCs; ++ $p<0.01$ versus 0.5 x 10^6 hWJ-MSCs; § $p<0.05$ versus 3x 0.5 x 10^6 hWJ-MSCs; §§ $p<0.01$ versus 3x 0.5 x 10^6 hWJ-MSCs; ɵ $p<0.05$ versus 1.5 x 10^6 hWJ-MSCs; ɵɵ $p<0.01$ versus 1.5 x 10^6 hWJ-MSCs; ● $p<0.05$ versus 3x 1.5 x 10^6 hWJ-MSCs; ●● $p<0.01$ versus 3x 1.5 x 10^6 hWJ-MSCs.*

6.3.4 Gene expression analysis

The gene expression analysis was performed using qRT-PCR. The expression of macrophage type 1 (M1) – related genes (*Irf5, Cd86*), M2-related genes (*Mrc1, Cd163*), astrogliosis (*Gfap*) and apoptosis (*Casp3*), was analysed at 4 and 9 weeks after the cell transplantation (Fig. 20).

No significant changes in gene expression were found after 4 weeks in cell treated groups and control group.

On the other hand, significant downregulation of *Irf5, Cd86, Mrc1* and *Cd163* was found after transplantation of 3x 1.5 x 10^6 hWJ-MSCs at 9 weeks when compared to the saline treated controls (Fig. 20).

Significant downregulation of expression of *Gfap* was found only in the group 3x 1.5 x 10^6 hWJ-MSCs at 9 weeks after the cell implantation, which corresponds with the immunohistochemical analysis of astrogliosis that was decreased in this group (Fig. 20).

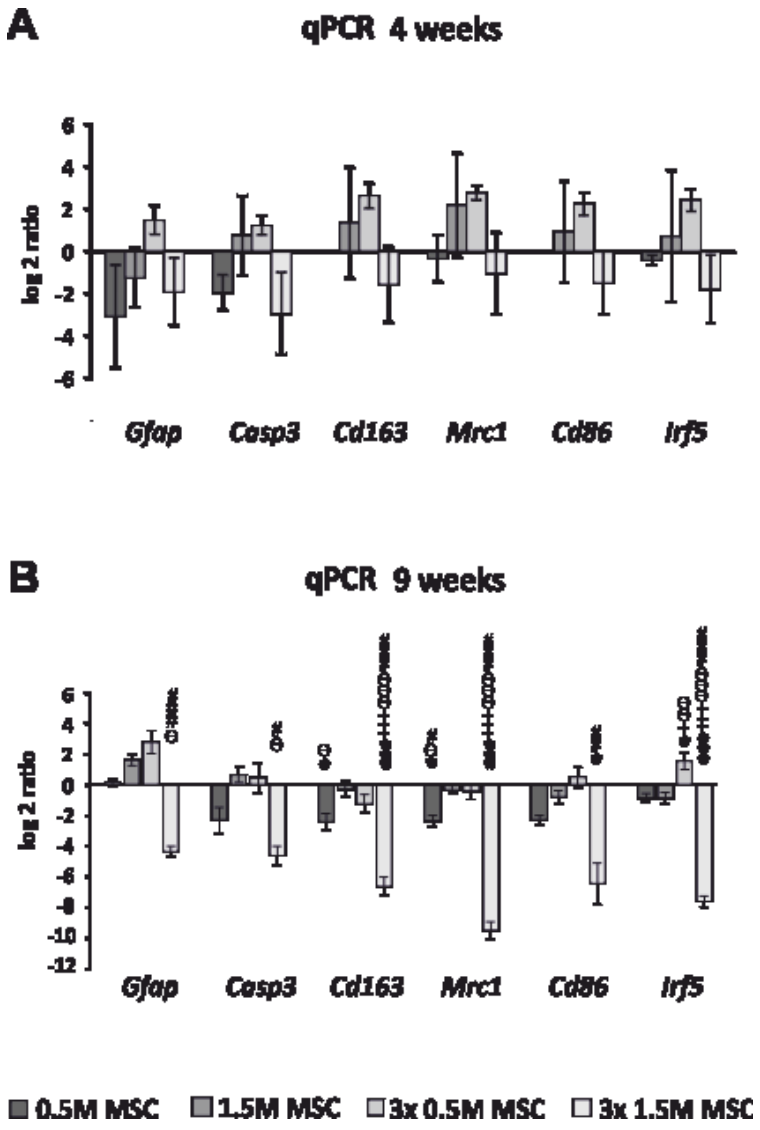

*Fig. 20. Messenger ribonucleic acid (mRNA) expression of selected genes (A) 4 and (B) 9 weeks after human Wharton´s jelly mesenchymal stromal cells (hWJ-MSCs) transplantation into the spinal cord injury (SCI). The graphs show the log2-fold changes of the ΔΔCt values of the indicated genes in comparison to the animals treated with the saline. Gfap, glial fibrillary acidic protein; Casp3, caspase 3; Cd163, macrophage scavenger receptor; Mrc1, mannose receptor C-type 1; Irf5, interferon regulatory factor 5. Data are shown as mean ± standard error mean. Statistical analysis using one-way ANOVA was used to compare ΔCt values, * $p<0.05$ versus saline; *** $p<0.001$ versus saline; + $p<0.05$ versus 0.5 x 10^6 hWJ-MSCs; +++ $p<0.001$ versus 0.5 x 10^6 hWJ-MSCs; # $p<0.05$ versus 3x 0.5 x 10^6 hWJ-MSCs; ## $p<0.01$ versus 3x 0.5 x 10^6 hWJ-MSCs; ### $p<0.001$ versus 3x 0.5 x 10^6 hWJ-MSCs; ɵ $p<0.05$ versus 1.5 x 10^6 hWJ-MSCs; ɵɵ $p<0.01$ versus 1.5 x 10^6 hWJ-MSCs; ɵɵɵ $p<0.001$ versus 1.5 x 10^6 hWJ-MSCs.*

6.3.5 Cell survival

Survival of the transplanted cells (0.5 and 1.5 x 10^6 hWJ-MSCs) was evaluated at 2 weeks after the transplantation. Surviving cells were detected as green clusters. Most of the cells remained at the site of the implantation – caught between the folds of arachnoidea in the cauda equina. There was, however, a difference in the number of cells present. While after 0.5 x 10^6 hWJ-MSCs implantation only a few cells were detected, the application of 1.5 x 10^6 hWJ-MSCs resulted in a greater number of trapped cells. No homing into the lesion site was observed.

6.4 Conclusion

Implantation of a single dose of 1.5 x 10^6 hWJ-MSCs or repeated application (3x) of 0.5 x 10^6 and 1.5 x 10^6 hWJ-MSCs improved functional outcome after SCI. Significant recovery of functional outcome was observed in all of the treated groups except for the single application of the low number of cells. Histochemical analysis revealed gradually increasing effect of grafted cells resulting in significant increase in number of GAP43+ fibers, higher amount of spared grey matter and reduced astrogliosis. mRNA expression of macrophage markers and apoptosis was down-regulated after the repeated application of 1.5 x 10^6 cells. We concluded that the effect of hWJ-MSCs on spinal cord regeneration is dose-dependent and potentiated by repeated application.

7 Part 3: ECM Preparation and Characterisation

7.1 Introduction

In SCI treatment, biomaterials are utilized mainly to bridge the cavity. Newly introduced prospect of using biological scaffolds, *e.g.* ECM, allows not only structural support for the lesioned site; but through releasing biological cues it activates endogenous restorative mechanisms and/or enables the engraftment of transplanted cells (Kubinova 2015; Kubinova and Sykova 2012).

ECM hydrogels prepared by decellularisation were previously reported as natural injectable materials suitable for neural tissue repair (Crapo et al. 2012; Medberry et al. 2013). Both allogeneic and xenogeneic biological ECM materials are currently being transplanted for tissue and organ replacement.

Human derived biomaterials could be more desirable as they avoid concerns related to potential immune responses by anti-Gal and anti-nonGal antibodies (Galili 2015) as well as xenogeneic diseases transfer. In contrast to adult tissue, the ECM from foetal or neonatal tissue is composed from more immature collagen with less crosslinks, which promotes more effective tissue remodelling (Badylak 2014). It is therefore conceivable that ECM derived from foetal or neonatal tissue would induce more efficient and constructive tissue remodelling than ECM derived from adult or old tissues.

In this context, umbilical cord (UC) represents the suitable neonatal tissue source, which is easily accessible in sufficient amounts without any ethical constraints. However, to the best of our knowledge there is no study that compares the properties of human UC-ECM to previously reported porcine ECM.

7.2 Aim of the study

In this study, we prepared and characterized ECM hydrogel derived from human umbilical cord (UC) and evaluated its composition and mechanical and biological properties in comparison with the previously described ECM hydrogels, derived from porcine urinary bladder (UB), brain (B) and spinal cord (SC).

7.3 Results

7.3.1 Structure of ECM hydrogels

B-ECM, SC-ECM and UB-ECM hydrogels were prepared by decellularisation protocols as described previously (Crapo et al. 2012; Medberry et al. 2013). Due to a high amount of hyaluronic acid which causes massive tissue swelling in water, the decellularisation procedure of UC-ECM required more washing steps in dH_2O and PBS to thoroughly remove the cells from the ECM. Importantly, we found that agitation of the tissue in trypsin/EDTA was a necessary step to achieve gelation of the resultant ECM hydrogel (Fig. 21A, B).

The fibre network topology of different ECM hydrogels was examined on SEM images (Fig. 21C). Microscopic comparison of these gels shows that fibre width of UC-ECM (60.47 ± 2.73 nm) and SC-ECM (68.23 ± 43.61 nm) was significantly smaller in comparison to UB-ECM (99.00 ± 3.37 nm) and B-ECM (86.57 ± 4.53 nm, Fig. 21D). To extract quantitative data on fibril orientation, circular statistics were used, which are adapted to directional data, to analyse the properties of the tangent direction over the region of interest. The circular variance of the tangent direction defines the score and determines whether the fibrils are well ordered (fibril array anisotropy, Fig. 21E). With regard to the anisotropy score, the following conventions were used: 0 for no order (purely isotropic arrays) and 1 for perfectly ordered, *i.e.*, parallel fibrils (purely anisotropic arrays) (Boudaoud et al. 2014). Indeed, there was no difference with regard to the anisotropy score between all types of the ECM.

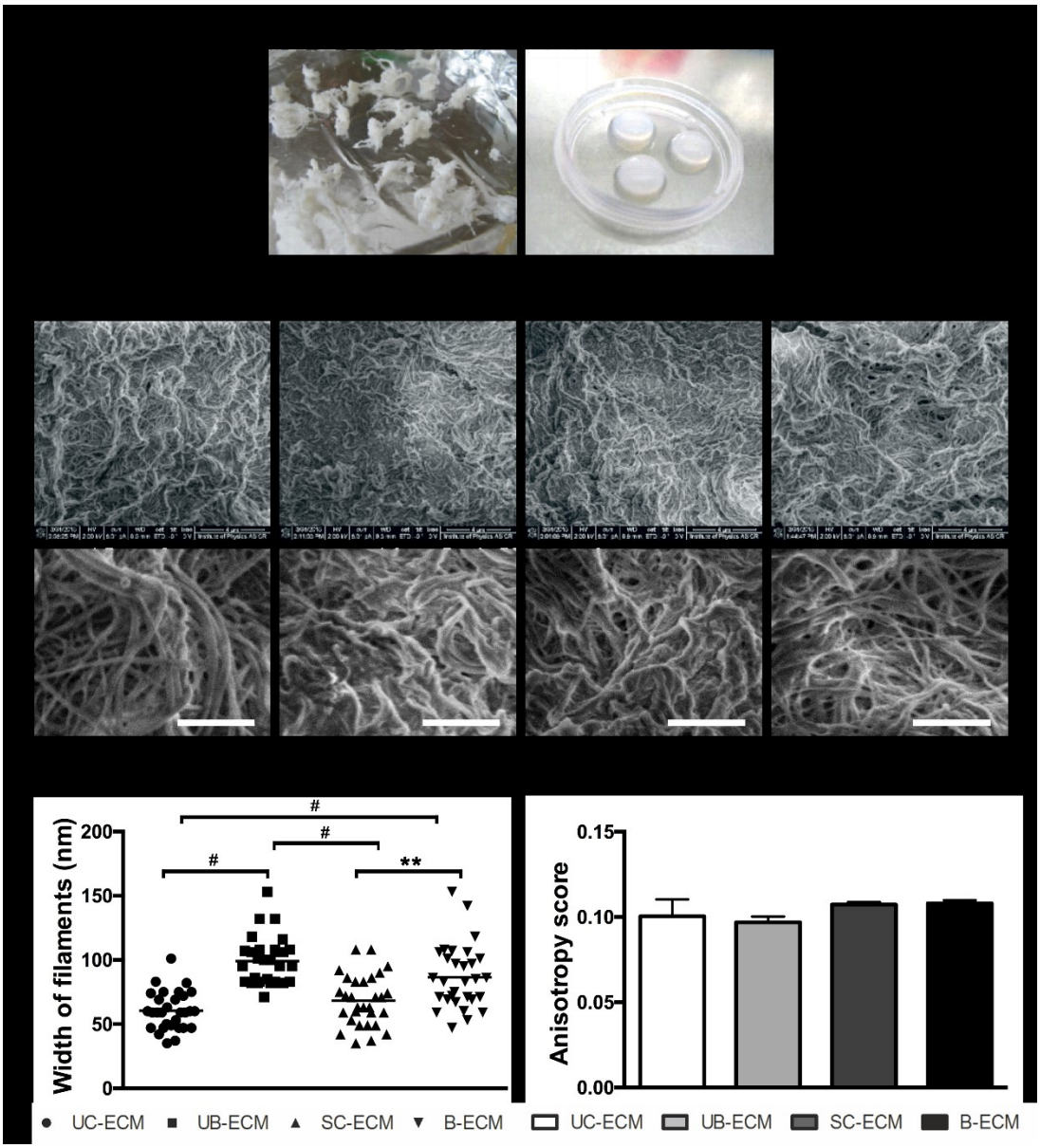

*Fig. 21. (A) Umbilical cord extracellular matrix (UC-ECM) after the decellularisation process, (B) UC-ECM in a form of hydrogel. (C) Representative scanning electron micrograph of UC-ECM, urinary bladder (UB-ECM), spinal cord (SC-ECM) and brain (B- ECM). Scale bars represent 1 μm. (D) Fibre diameter distribution and (E) anisotropy score in UC-ECM, UB-ECM, SC-ECM and B-ECM. UC-ECM and SC-ECM have a smaller fibre width when compared to UB-ECM and B-ECM. No difference in anisotropy score was found between the ECM hydrogels. Data are shown as mean ± standard error mean. Statistical analysis using one-way ANOVA, n = 30, **p<0.01, #p<0.001.*

7.3.2 Composition of ECM hydrogels

Similarly to porcine ECMs, UC-ECM was successfully decellularized with minimal cellular content within the scaffold (Fig. 22). H&E and DAPI staining confirmed the absence of residual cell nuclei (Fig. 22A). Quantification of dsDNA showed that in all ECM samples, the residual dsDNA was less than 50 ng per mg dry ECM (Fig. 22B, C). Previous studies (Crapo et al. 2011; Crapo et al. 2014; Ghuman et al. 2016) show that DNA contained in ECM should not exceed

50 ng/mg of the tissue, in order not to elicit an immune-reaction on the recipient´s site. Our protocol of UC decellularisation ensured efficient cell removal, and resulting UC-ECM contained < 50 ng or no residual dsDNA, and therefore met the basic requirement for clinical application.

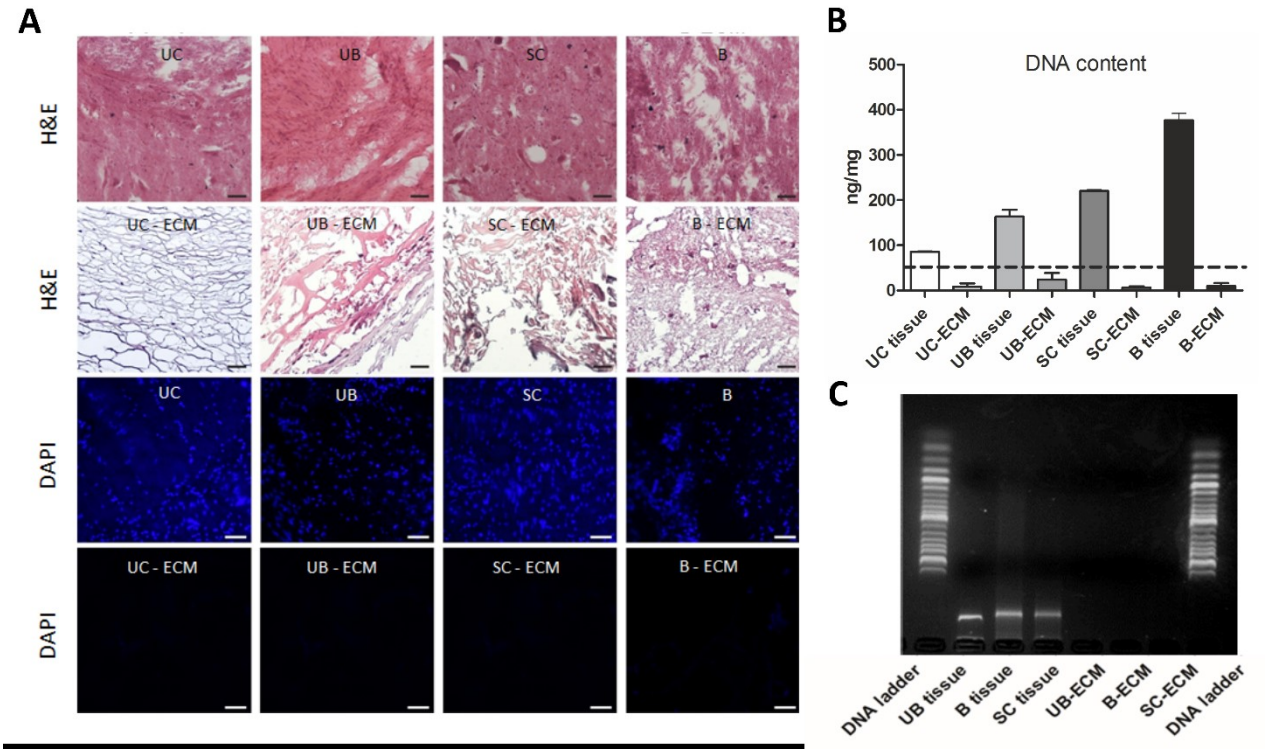

Fig. 22. (A) First row: haematoxylin and eosin (H&E) staining of (from left to right): umbilical cord (UC), urinary bladder (UB), spinal cord (SC) and brain (B) tissue sections before decellularisation. Second row: H&E staining of UC extracellular matrix (UC-ECM), UB-ECM, SC-ECM and B-ECM after decellularisation. Third row: 4′,6-diamidino-2-phenylindole (DAPI) staining for DNA of (from left to right): UC, UB, SC, and B sections of tissue before decellularisation. Fourth row: DAPI staining for residual DNA content in UC- ECM, UB-ECM, SC-ECM, B-ECM. Scale bars represent 50 µm. (B) Double - strain DNA (dsDNA) quantification. The dotted line shows the maximum allowed amount of dsDNA (50 ng/mg) per mg of dry weight – this amount could be transplanted from a different source without causing an immune reaction. Data are shown as mean ± standard error mean, n = 3. (C) DNA base pairs (bp) quantification using electrophoresis. On the left and the right side of the gel is a DNA ladder depicting 50-1500 bp.

An important parameter which shows efficacy of ECM harvesting is the ECM yield, expressed as the percentage of dry weight of ECM to wet weight of the initial source tissue (Table 6). The highest ECM yield was found for UB-ECM 8.06 ± 4.66 % (n = 6), followed by UC-ECM 0.96 ± 0.51 % (n = 6). In contrast, the decellularisation of CNS tissues, which requires more complex decellularisation procedures due to the high amount of myelin, resulted in a very low ECM yield; 0.25 ± 0.14 % for SC-ECM (n = 6) and 0.12 ± 0.07 % for B-ECM (n = 6) respectively.

Physical properties of ECM				
	UC-ECM	UB-ECM	SC-ECM	B-ECM
Number of batches	6	6	6	6
ECM yield (%)	0.96 ± 0.51	8.06 ± 4.66	0.25 ± 0.14	0.12 ± 0.07
t_{lag} (min)	0.20 ± 0.57	30.78 ± 0.98	19.77 ± 0.98	22.88 ± 1.98
$t_{1/2}$ (min)	12.00 ± 0.75	43.70 ± 0.48	28.19 ± 1.92	32.31 ± 1.26
t_{95} (min)	40.06 ± 5.15	79.00 ± 5.92	55.30 ± 6.77	60.00 ± 3.64
S (min^{-1})	0.10 ± 0.01	0.09 ± 0.01	0.13 ± 0.02	0.10 ± 0.01

Table 6. Extracellular matrix (ECM) yield and the time required to reach lag phase (t_{lag}), half of the final turbidity ($t_{1/2}$), 95 % of the final turbidity (t_{95}), and gelation rate (S) of extracellular matrix derived from human umbilical cord (UC-ECM), porcine urinary bladder (UB-ECM), porcine spinal cord (SC-ECM), and porcine brain (B-ECM). ECM yield is expressed as a percentage of the dry weight of ECM to the wet weight of the initial tissue ± standard error mean.

Alcian blue was used to stain acid polysaccharides such as glycosaminoglycans (Fig. 23A). Immunohistochemical staining showed that ECM scaffolds are composed of collagen (Fig. 23B), laminin (Fig. 23C) and fibronectin (Fig. 23D).

Collagen concentration did not significantly differ among all the ECM types. The highest amount of collagen was found for UC-ECM (542.6 ± 1.78 µg/mg of dry ECM weight), then for UB-ECM (476.1 ± 45.38 µg/mg), B-ECM (408.1 ± 141.0 µg/mg) and SC-ECM (384.7 ± 147.6 µg/mg) (Fig. 23E).

It has been shown that the concentration of hyaluronic acid within ECM is high in foetal and new-born tissues, including umbilical cords (Leung et al. 2012). Here, the significantly highest amount of sGAG was found in UC-ECM (6.59 ± 1.24 µg/mg), when compared to UB-ECM (3.46 ± 0.99 µg/mg), SC-ECM (1.84 ± 1.26 µg/mg) and B-ECM (1.47 ± 0.79 µg/mg of dry ECM weight) (Fig. 23F).

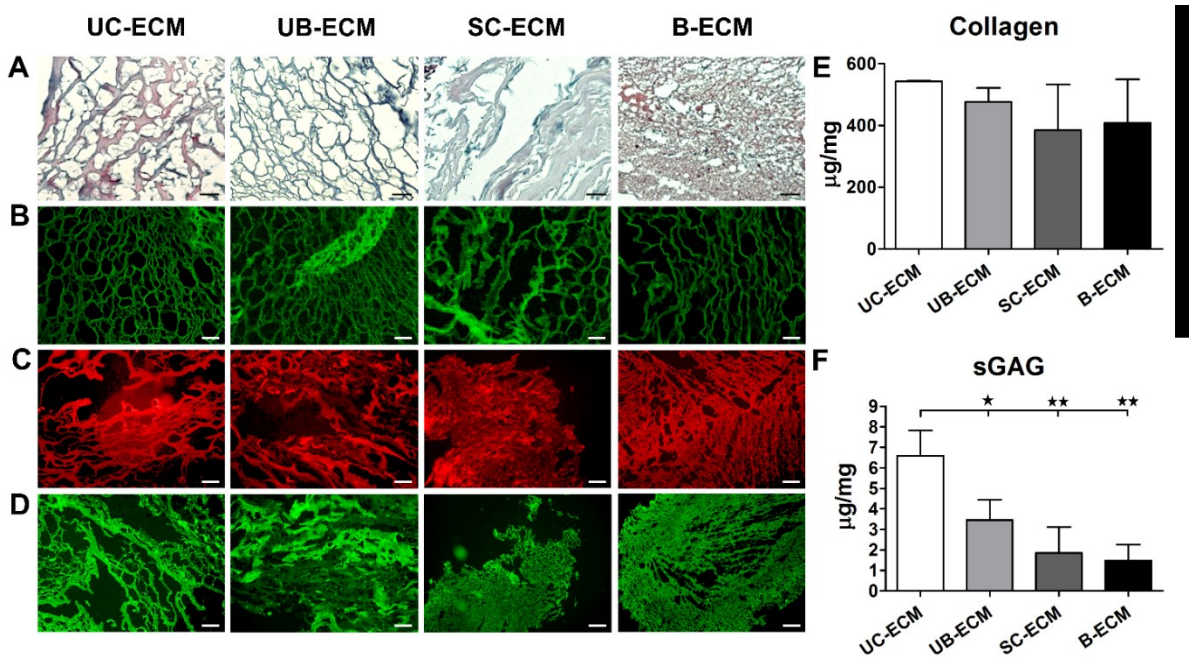

*Fig. 23. (A) Alcian blue staining for acid mucopolysaccharides in extracellular matrix hydrogels derived from human umbilical cord (UC-ECM), porcine urinary bladder (UB-ECM), porcine spinal cord (SC-ECM), and porcine brain (B-ECM) (B) Immunohistochemical localization of collagen, (C) laminin, and (D) fibronectin. Scale bars represent 100 µm. (E) Collagen and (F) sulphated glycosaminoglycans (sGAG) content per mg of dry weight of individual ECM using colorimetric assay. Data are shown as mean ± standard error mean. Statistical analysis using one-way ANOVA, *p<0.05, ** p<0.01, n = 3.*

7.3.3 Proteomic analysis

The native UC tissue and UC-ECM were subjected to mass spectrometry analysis to determine the precise composition of ECM, ECM associated and non-ECM proteins. Proteomic analysis showed that the most abundant proteins in native as well as decellularized UC are from collagen protein family, followed by transgelin, actin and other non-ECM proteins (Table 7). The most abundant cell-adhesive glycoprotein was fibronectin. Decellularisation process led to decrease of ECM-associated proteins such as lumican, decorin and plexin-B1 as well as non-ECM proteins such as transgelin, immunoglobulins (Ig) and TGF-β induced protein Ig-h3.

Core ECM protein	UC (ppm)	UC-ECM (ppm)
Collagen alpha-2(I) chain	121210	260669
Collagen alpha-1(I) chain	101666	396521
Collagen alpha-1(III) chain	39022	195378
Collagen alpha-1(V) chain	18230	14552
Collagen alpha-1(II) chain	17415	80283
Collagen alpha-3(VI) chain	16742	2842
Collagen alpha-1(VI) chain	12143	1558
Collagen alpha-1(XI) chain	12002	4807
Collagen alpha-2(V) chain	9535	7349
Collagen alpha-2(VI) chain	9260	2338

Fibronectin	7808	1793
Collagen alpha-2(XI) chain	6954	6655
Collagen alpha-1(IV) chain	6839	3562
Fibrillin-1	6265	2542
Collagen alpha-2(IV) chain	5663	4172
Collagen alpha-1(XII) chain	4358	1088
Fibrillin-2	3305	1218
Tenascin	2575	397

ECM associated protein	**UC (ppm)**	**UC-ECM (ppm)**
Lumican	22316	0
Decorin	20839	0
Plexin-B1	14904	0

Non ECM proteins	**UC (ppm)**	**UC-ECM (ppm)**
Transgelin	24242	0
Actin. aortic smooth muscle	57420	2028
Actin. cytoplasmic 2	36727	1992
Ig gamma-1 chain C region	17634	0
Hemoglobin subunit beta	15895	58
Hemoglobin subunit alpha	13077	0
Mimecan	12846	0
Filamin-A	9728	144
Ig gamma-3 chain C region	9716	117
Immunoglobulin kappa constant	9459	20
TGF-β induced protein Ig-h3	8913	0
Ig gamma-4 chain C region	8665	0
Ig gamma-2 chain C region	7346	0
Tropomyosin beta chain	6720	1061
Tropomyosin alpha-1 chain	6718	1059
Tropomyosin alpha-4 chain	6647	1128
Myosin-11	6095	892
Serotransferrin	1987	237
Caveolin-1	1532	310
Caveolin-2	389	205
CD70 antigen	238	576
Neutrophil defensin 1	108	602

Table 7. Mass spectrometry analysis of the most abundant proteins of native umbilical cord (UC) tissue and UC extracellular matrix (ECM).

7.3.4 Properties of ECM hydrogel

ECM hydrogel properties were evaluated using rheological and turbidimetric measurements. In rheological experiments, we determined the flow and mechanical properties of ECM hydrogels. Increasing the strain, G´ of ECM hydrogels, started a decline of 10% amplitude, when they became more viscose, which was observed for all ECM hydrogels, irrespective of their origin (Fig. 24A). The storage modulus of the matrix was found to be the highest for UB-ECM, while the softest material was B-ECM.

Turbidimetric gelation kinetic curves showed a sigmoidal shape for UC-ECM, whereas other ECMs had an exponential shape (Fig. 24B). A significantly longer lag phase, as well as the longer time required to reach half of the final turbidity ($t_{1/2}$) and 95 % of the final turbidity (t_{95}) was found for UB-ECM than for other ECM hydrogels, while the shortest gelation time was found for UC-ECM (Fig. 24B-E). However, the velocity to complete gelation or gelation rate (S) was significantly higher for SC-ECM when compared to UB-ECM (Fig. 24F). These results suggest that hydrogel assembly was the fastest for UC-ECM, followed by SC-ECM and B-ECM, while the UB-ECM hydrogels had the longest gelation time.

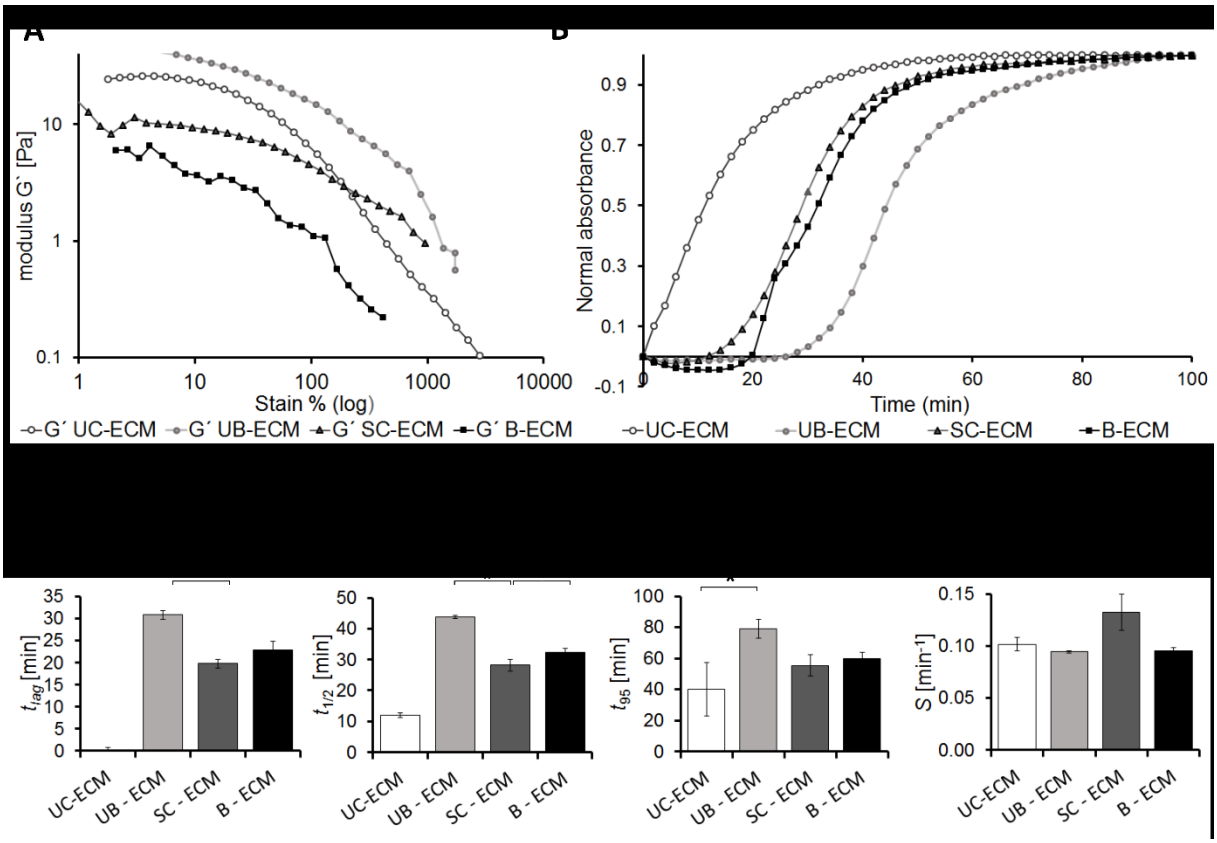

Fig. 24. (A) Dynamic oscillatory shear test for viscoelastic properties analysis of extracellular matrix hydrogels derived from human umbilical cord (UC-ECM), porcine urinary bladder (UB-ECM), porcine spinal cord (SC-ECM), and porcine brain (B-ECM). Strain is depicted on the x

*axis and storage modulus (G′) on the y axis. (B) Representative curve for turbidimetric gelation kinetics of UC-ECM, UB-ECM, SC-ECM and B-ECM. (C) Lag time (t_{lag}) of ECM hydrogels determined as an intercept point of the slope at log $t_{1/2}$ and turbidimetry baseline with 0 % absorbance. (D) Time to reach 50 % ($t_{1/2}$) and (E) 95 % (t_{95}) maximal absorbance. (F) The gelation rate S defined as the slope of the linear region of the gelation curve. Data are shown as mean ± standard error mean. Statistical analysis using one-way ANOVA, *p<0.05, ** p<0.01, # p<0.001, n = 3.*

7.3.5 Cell growth, proliferation and migration on the ECM hydrogels

Proliferation of hBM-MSC, hASCs and hWJ-MSC on ECM hydrogels was determined using WST-1 assay after 1, 3, 7 and 14 days of the culture. While hBM-MSCs on UC-ECM proliferated similarly as in the control tissue culture well, lower proliferation of hBM-MSC was found on all porcine-derived hydrogels, UB-ECM, SC-ECM and B-ECM. On the other hand, proliferation of hASCs on all types of ECM hydrogels did not significantly differ from controls. Notably, proliferation of hWJ-MSCs at 14 days was significantly higher on tissue specific UC-ECM than on other ECM hydrogels or even in controls (Fig. 25).

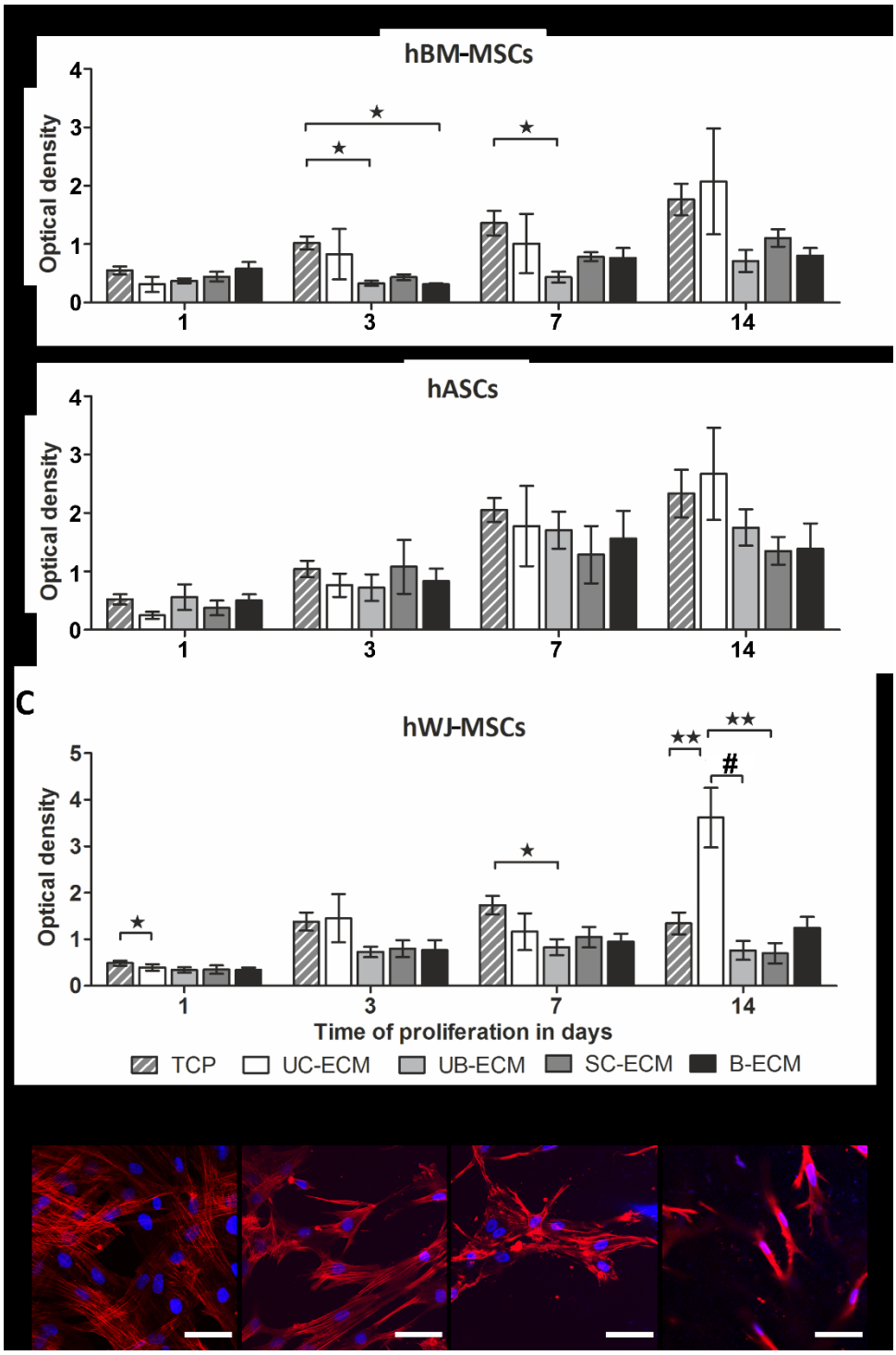

*Fig. 25. (A) Comparison of proliferation of human mesenchymal stromal cells isolated from human bone marrow (hBM-MSCs), B) human adipose tissue (hASCs), (C) and human Wharton's jelly (hWJ-MSCs), on extracellular matrix hydrogels derived from human umbilical cord (UC-ECM), porcine urinary bladder (UB-ECM), porcine spinal cord (SC-ECM), porcine brain (B-ECM) and control tissue culture plastic (TCP) on 1, 3, 7 and 14 days using WST-1 reagent. The proliferation rate was assessed on a spectrophotometer and illustrated as optical density. (D) The morphology of proliferating hWJ-MSCs on UC-ECM, (E) UB-ECM, (F) SC-ECM and (G) B-ECM was depicted after 14 days. Data are shown as mean ± standard error mean. Statistical analysis using one-way ANOVA, Scale bars represent 50 µm. *p<0.05, ** p<0.01, # p<0.001, n = 6.*

Using migration assay, all ECM hydrogels revealed chemotactic properties and stimulated the migration of all types of hMSCs, which was significantly higher when compared to the cell migration to the control culture medium alone (Fig. 26A-C).

The ability of ECM hydrogels to support neurite outgrowth was observed using DRG explant cultures. After 7 days of culture, neurites densely extended from DRG bodies with no significant differences in neurite length, or neurite area between individual hydrogels and Matrigel, which served as a positive control (Fig. 26D-F).

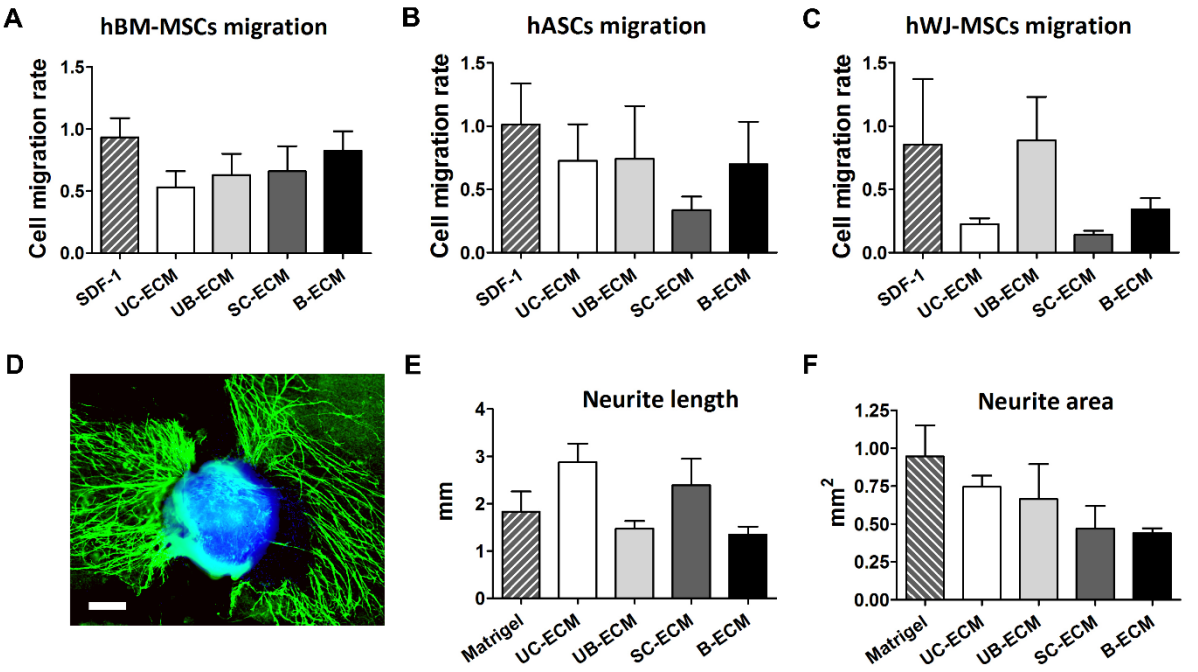

Fig. 26. (A-C) Chemotactic properties of ECM hydrogels investigated using xCELLigence® RTCA DP Cell Invasion and Migration Assay showing migration of (A) human bone marrow mesenchymal stromal cells (hBM-MSCs), (B) human adipose tissue-derived stromal cells (hASCs) and (C) human Wharton's jelly mesenchymal stromal cells (WJ-MSCs), towards extracellular matrix (ECM) hydrogel derived from umbilical cord (UC-ECM), urinary bladder (UC-ECM), spinal cord (SC-ECM), and brain (B-ECM) at 6 hours after seeding. Results are normalized to the control (media without supplements) (n = 5). (D) Dorsal root ganglion (DRG,) explant culture on UC-ECM hydrogel stained with DAPI and NF160. DRGs were cultivated for 7 days on the Matrigel, or ECM hydrogels and the longest neurite length (E) and neurite area (F) were determined using NeuriteJ ImageJ plug-in Data are shown as mean ± standard error mean. Statistical analysis using one-way ANOVA, n = 3. Scale bars represent 200 µm.

It is well known that the unique compositions and microstructural features of ECM have been shown to be influential in directing cell fate or morphology (Bonnans et al. 2014). To reveal the neurotrophic properties of ECM hydrogels, we determined neural differentiation of NSC culture. NSCs grew on all ECM hydrogels, and after 7 days displayed an expression of the early neuronal marker NF70 (Fig. 27). Of note, in contrast to the dispersed NSC cultured on laminin

coated glass coverslips, the NSCs grown on the ECM hydrogels tend to grow in distinct clusters with delimitated borders. After 14 days in culture, NSCs proliferated and differentiated into neuronal cells positive for neuronal marker MAP2, without any remarkable differences between particular ECM hydrogels.

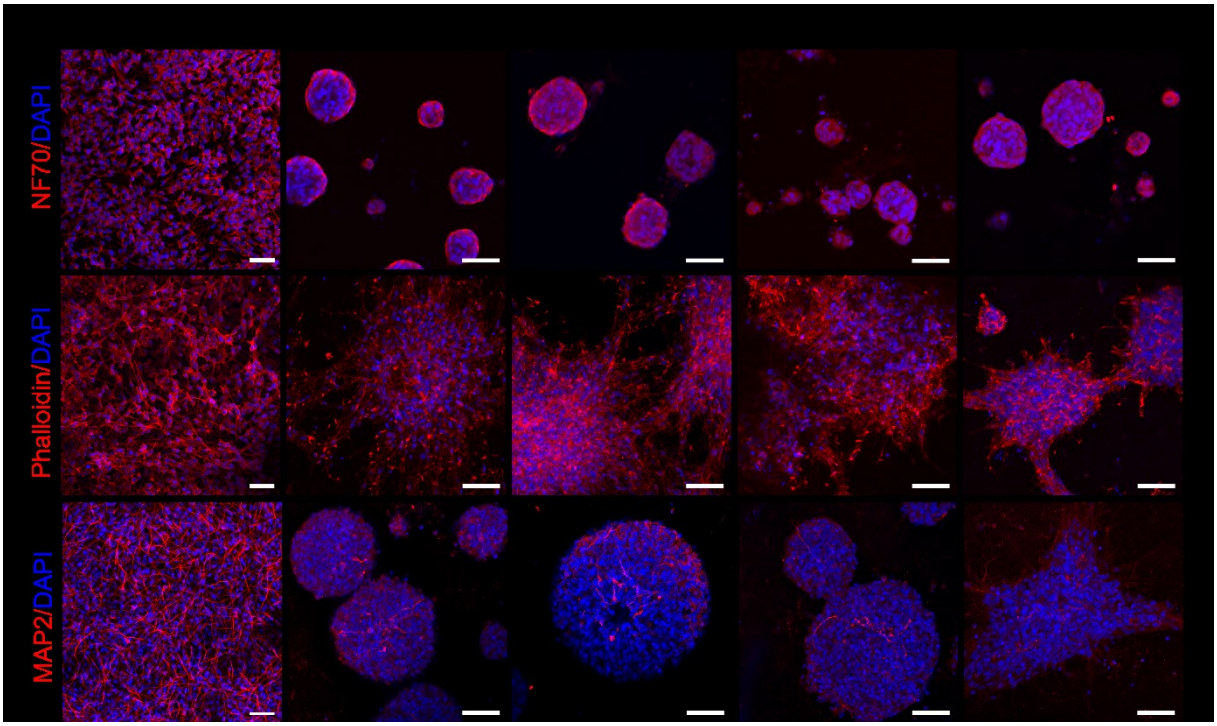

Fig. 27. (A) Growth and differentiation of human neural stem cell line SPC-01 (NSCs) on laminin coated glass coverslips (control), and on extracellular matrix (ECM) hydrogel derived from umbilical cord (UC-ECM), urinary bladder (UB-ECM), spinal cord (SC-ECM), and brain (B-ECM). Immunostaining for neurofilaments NF70 and DAPI after 1 week (1w) in culture, (B) phalloidin and DAPI after 2w in culture, and (C) MAP2 and DAPI after 2w in culture. Scale bars represent 50 µm.

7.3.6 Evaluation of ECM hydrogels *in vivo*

To prove the *in vivo* gelation and biocompatibility of UC-ECM, the hydrogel was injected into the model of focal cerebral ischaemia – a photothrombotic lesion created in the rat motor cortex. As is illustrated in Fig. 28 on collagen and DAPI staining after 24 hours, the UC-ECM formed a compact hydrogel within the lesion which was highly populated by endogenous cells. The host macrophages were the prevalent cell type present within the lesion, and also infiltrating the hydrogel (75.7 ± 5.0 % of all infiltrating cells in the gel, n = 3). As is apparent from Fig. 28C, the macrophages detected within the UC-ECM hydrogel revealed predominant positivity for marker of M2 macrophages (CD206+ cells), which represented 77.1 ± 6.5 % of all macrophages within the hydrogel.

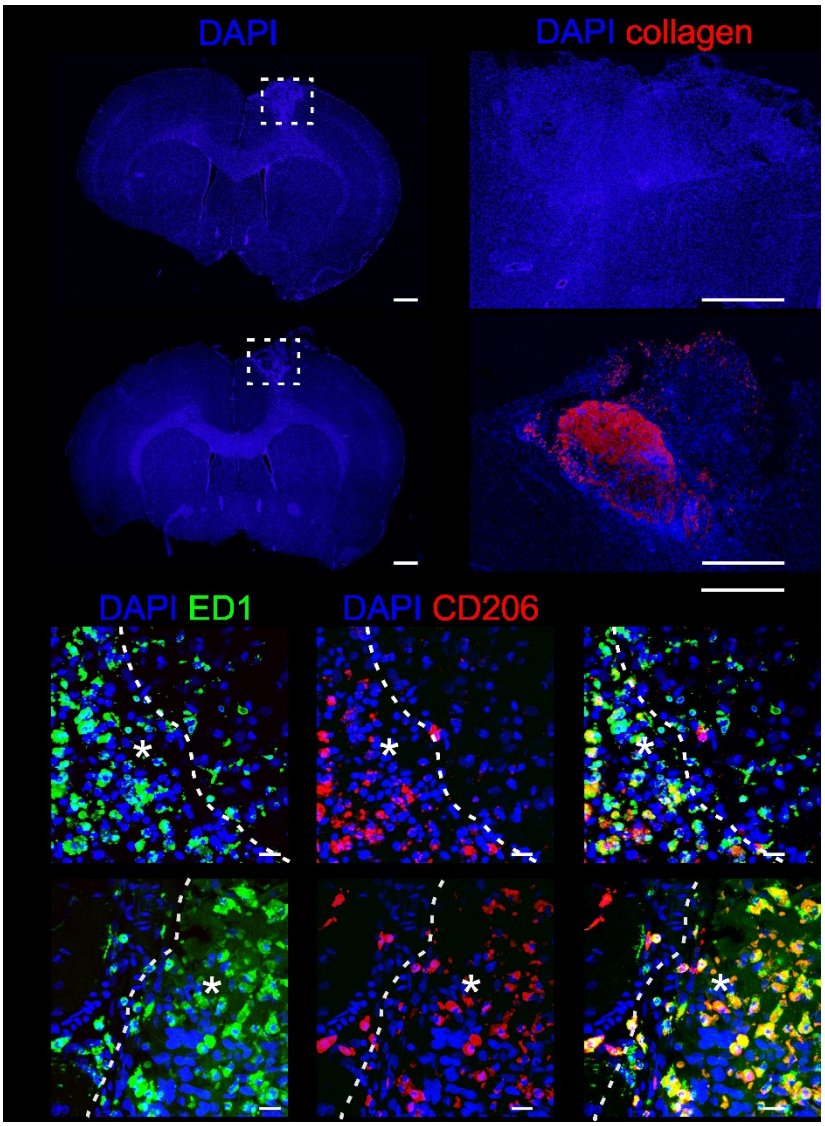

Fig. 28. Coronal brain sections illustrating in vivo gelation and cellular infiltration of umbilical cord extracellular matrix (UC-ECM) hydrogel, 24 hours after the implantation into the photothrombotic lesion in the rat motor cortex. (A, B) Saline (control lesion, first row) and UC-ECM hydrogel (second row) were injected into the lesion site 7 days after the lesion induction. (A) Staining for cell nuclei (DAPI). Scale bars represent 1 mm. (B) Staining for DAPI (blue) and collagen I (red). Scale bars represent 500 µm. (C) The infiltration of macrophages into the control lesion and UC-ECM hydrogel was depicted by ED1 (green) and CD206 (red) staining. Cell nuclei were stained for DAPI (blue). The dotted line shows the border of the lesion and intact brain tissue, the asterisk represents the lesion site. Scale bars represent 20 µm.

7.4 Conclusion

In this study, we prepared injectable ECM hydrogel by decellularisation of human UC tissue and compared its properties to CNS and non-CNS ECM hydrogels derived from porcine UB, B and SC. The fibre width of UC-ECM was significantly smaller in comparison to porcine tissue-derived ECM. UC-ECM contained significantly higher amounts of sGAG when compared to other ECM hydrogels. The shortest gelation time was found also for UC-ECM. The elastic modulus was then found to be the highest for UB-ECM.

All ECM revealed similar *in vitro* neurotrophic properties, which does not indicate a benefit of tissue specific ECM for neural tissue repair. After injection into the cortical photothrombotic lesion in rats, the UC-ECM formed a hydrogel *in situ* and was densely populated by host macrophages. UC-ECM presents an easily accessible material of human origin that provides the appropriate mechanical and bioactive properties suitable for CNS repair. Further *in vivo* studies are needed to consider the potential of ECM hydrogels for clinical translation.

8 Part 4: *In Vivo* Evaluation of ECM Biomaterials

8.1 Introduction

ECM hydrogels as injectable scaffolds enable targeted delivery by minimally invasive techniques - they quickly fill even irregularly shaped space and polymerize to form a support suitable for host infiltration (Wolf et al. 2012).

We (Chapter 7), and others (Crapo et al. 2012; Crapo et al. 2014), have previously shown that both CNS and non-CNS ECM hydrogels have neurotrophic potential *in vitro,* as well as *in vivo*.

However, some studies suggest that ECM scaffolds derived from the same tissue type as that of the injury site may have a unique composition of molecular constituents to induce constructive tissue specific remodelling. For instance, cardiac ECM has demonstrated the capacity to provide tissue specific cues for cardiac cell growth and differentiation (Wang and Christman 2016). Tissue- specific skeletal muscle ECM revealed better outcomes for critical limb ischaemia treatment compared to UC-ECM (Ungerleider et al. 2016). Also, the B-ECM hydrogel, being the tissue specific matrix, unlike the SC-ECM and UB-ECM, increased the length of neurite extensions of the neuroblastoma cell line (Medberry et al. 2013). In our previous study we reported tissue specific effect only when UC-ECM selectively promoted proliferation of hWJ-MSCs.

According to these results, CNS-ECM hydrogels might be advantageous for providing supportive environment for the *in vivo* CNS repair.

8.2 Aim of the study

Current data are contradictory in terms of tissue specificity of ECM hydrogels. Therefore, in this study, we compared the neuro-regenerative properties of CNS and non-CNS derived ECM hydrogels *in vivo,* in a model of SCI.

To limit differences caused by different tissue origin, we considered porcine tissue as a feasible source for both, CNS and non-CNS derived ECM hydrogels. As a representative of CNS derived tissue, SC-ECM hydrogel was chosen and compared to a UB-ECM hydrogel – a representative of non-CNS derived tissue.

8.3 Results

8.3.1 Histological evaluation after ECM hydrogel injection

Both, UB-ECM and SC-ECM hydrogels, were injected into the cavity of the spinal cord hemisection and examined at 2, 4 and 8 weeks. The tissue response to the scaffolds was histologically evaluated by analysing of axonal ingrowth, vascularization, and infiltration of macrophages/microglia, astrocytes and oligodendrocytes within the injury site.

At 2 weeks after injury, H&E staining of longitudinal spinal cord sections demonstrated that both hydrogel types were biocompatible with the surrounding host tissue and filled the lesion cavity with no signs of any adverse effects (Fig. 29A, B). The hydrogels were detectable in the lesion area, and were densely populated with the host cells. By 4 weeks after injury, small areas of the original hydrogel were still detectable by the histologic evaluation (Fig. 29E), while the newly formed tissue interconnected with the host tissue bridged the lesion centre. Macrophages massively infiltrated preferably the periphery of the lesion where several small cysts were developed due to the rapid graft degradation. Similar tissue response was found at 8 weeks, when the hydrogels were fully degraded, which was followed by the further progression in cyst formation. In contrast to the tissue remodelling process observed in the lesion after hydrogel injection, large pseudocysts were formed in the control sham-treated lesion (Fig. 29C, F, I).

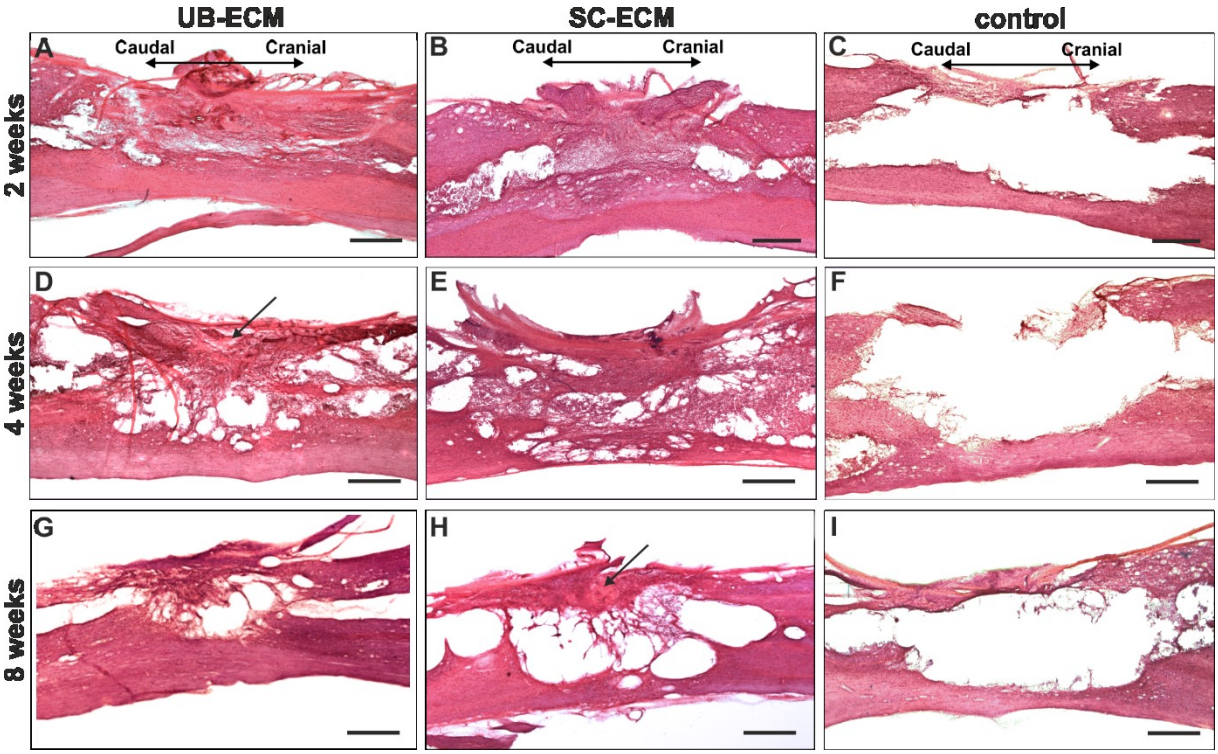

Fig. 29. Haematoxylin-eosin staining of the longitudinal sections of the spinal cord lesion (A-C) 2 weeks, (D-F) 4 weeks and (F-I) 8 weeks after injection of (A, D, G) urinary bladder

extracellular matrix (UB-ECM) hydrogels; (B, E, H) spinal cord (SC-) ECM hydrogels. (C, F, I) represent sham-operated control lesion. The arrow shows the nondegraded part of the hydrogel. Scale bar: 500 µm.

To evaluate axonal ingrowth into the hydrogels, a neurofilament marker (NF160) was used (Fig. 30). Robust ingrowth of NF-positive fibres into the hydrogel treated lesion was observed from both, the rostral and caudal stumps of the lesion, while the dense infiltration of NF was also found in the centre of the lesion.

Quantification analysis expressed the relative value of NF160 immunopositive area as percentage of the lesion area. The ingrowth of NF was maximal at 2 weeks in the both hydrogel groups, and did not further increase in later time points. No differences in the NF area were found between SC-ECM and UB-ECM hydrogels in all time points (Fig. 30G). Despite the isotropic structure of the ECM hydrogels, the ingrowing axons linearly bridged the SCI lesion while forming multiple bundles organized in the longitudinal direction along the spinal cord (Fig. 30B). Astrocytes, evaluated by immunofluorescent staining for GFAP, did not migrate inside the lesion and thus served to reveal a clear demarcation of the lesion area (Fig. 30C, F). Only few astrocytic processes grew into the graft from the lesion border (Fig. 30F).

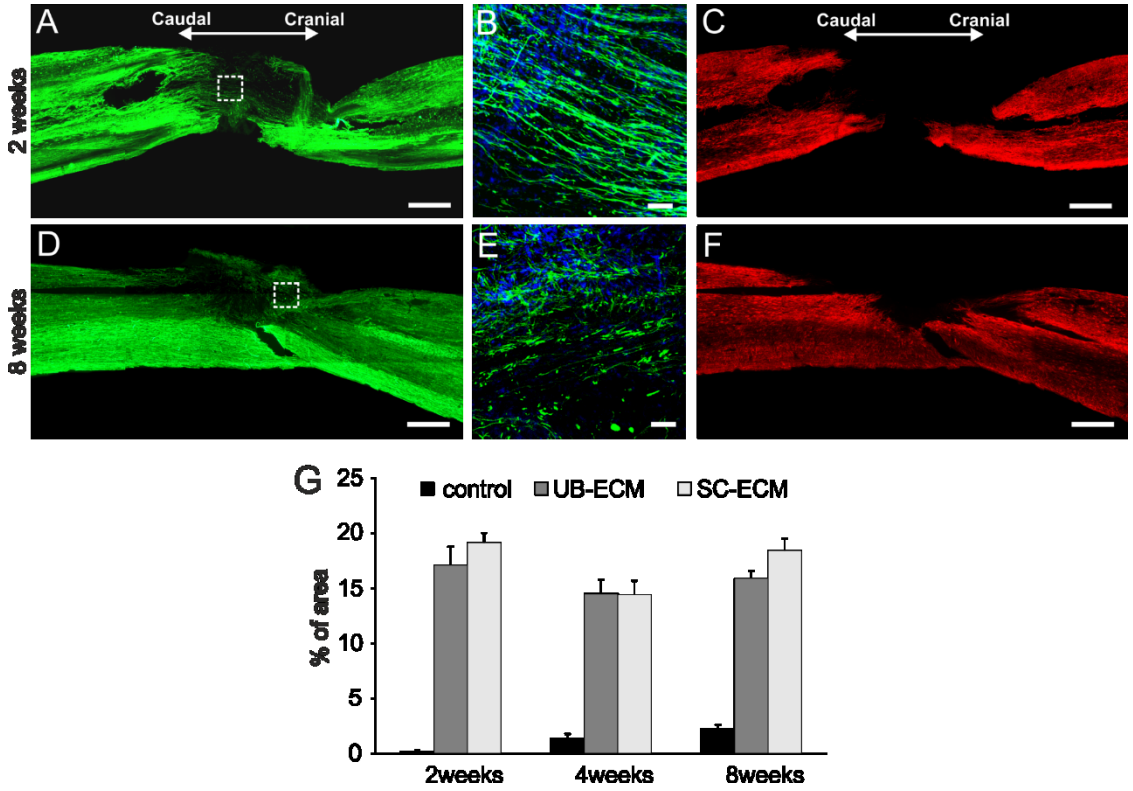

Fig. 30. Representative images of the spinal cord lesion (A-C) 2 and (D-F) 8 weeks after injection of SC-ECM hydrogels. Immunofluorescent staining for (A, B, D, E) neurofilaments (NF160), (C, F) astrocytes (GFAP) and (B, E) cell nuclei (DAPI, blue). Dashed squares in (A, D) represent the area magnified on the right (B, E). (G) The effect of extracellular matrix

(ECM) hydrogels on the ingrowth of NF. A significantly higher ingrowth of NF was found in both ECM hydrogel groups when compared to the control lesion in all time points. Data are shown as mean ± standard error mean. Scale bar: (A, C, D, F) 500 µm; (B, E) 50 µm.

In terms of neo-vascularization, a number of blood vessels (RECA staining) grew into the hydrogel treated lesions and formed a dense network (Fig. 31A-D). The relative area of blood vessels gradually increased in time, but no differences in blood vessel density were found between the UB-ECM and SC-ECM hydrogels in all time points (Fig. 31E).

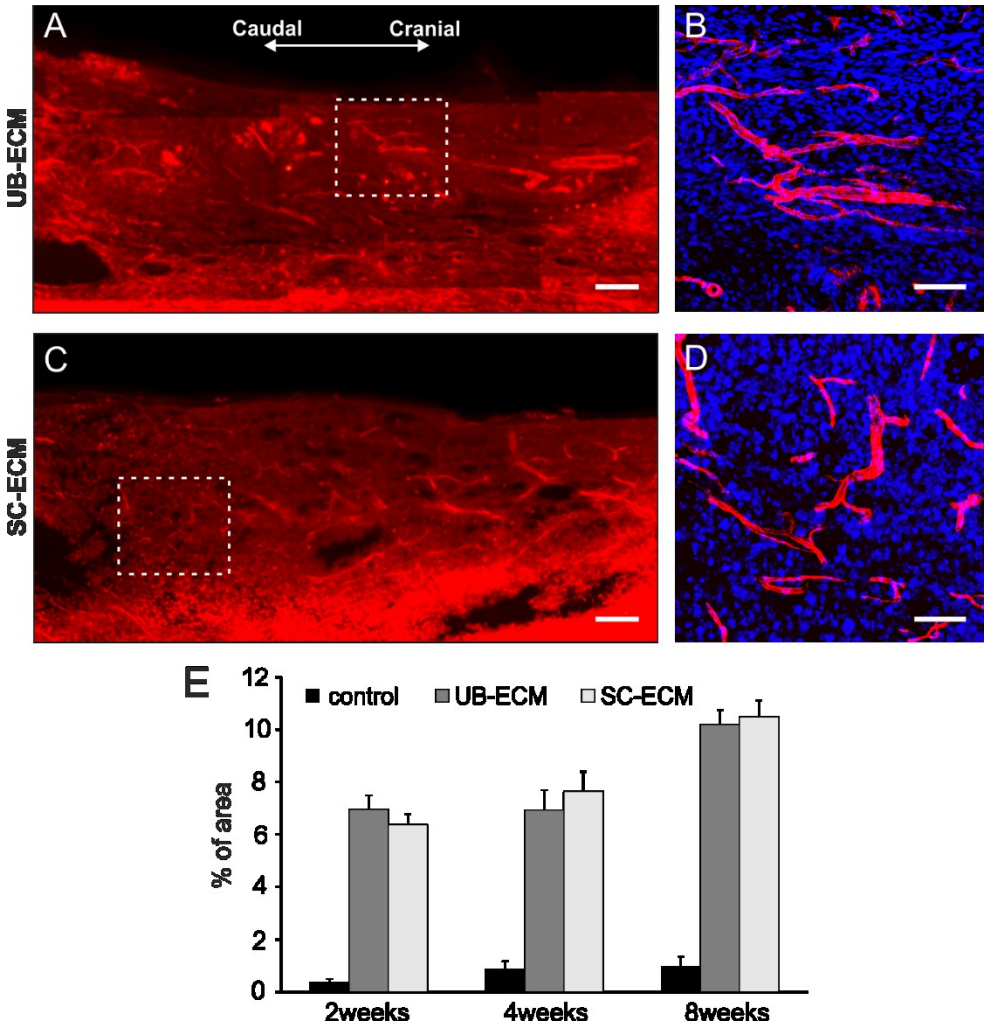

Fig. 31. Representative images of the spinal cord lesion at 2 weeks after injection of (A, B) urinary bladder extracellular matrix (UB-ECM) and (C, D) spinal cord (SC-)ECM hydrogels. Immunofluorescent staining for blood vessels (RECA) and (B, D) cell nuclei (DAPI). Dashed squares in (A, C) represent the area magnified on the right (B, D). (E) An effect of ECM hydrogels on the vascularization. A significantly higher ingrowth of blood vessels was found in both ECM hydrogel groups when compared to the control lesion in all time points. Data are shown as mean ± standard error mean. Scale bar: (A) 500 µm; (B) 100 µm, (C, D) 50 µm.

The host tissue remodelling response was characterized by robust infiltration of CD68+ cell throughout the entire lesion area (Fig. 32A, B), which populated the hydrogels at all time points, and remained in the lesion site after the hydrogel had degraded. As is apparent from the staining for M1 and M2 macrophages in Fig. 32E, macrophages at the interface of the ECM hydrogel and the host tissue were predominantly of the M1 phenotype (CD86 staining), while M2 phenotype macrophages (CD206 staining) were mostly present within the hydrogel area. Infiltration of serotonin-positive axons (Fig. 32D) was observed from the rostral part of the hydrogels, but these axons did not spread across the lesion. Infiltration of oligodendrocytes (OSP staining, Fig. 32F) within the lesion site indicated that myelination occurred in some regenerating axons. Numerous endogenous Schwann cells that migrated from the nerve roots were detected within the lesion site as well as in the surrounding tissue (Fig. 32H).

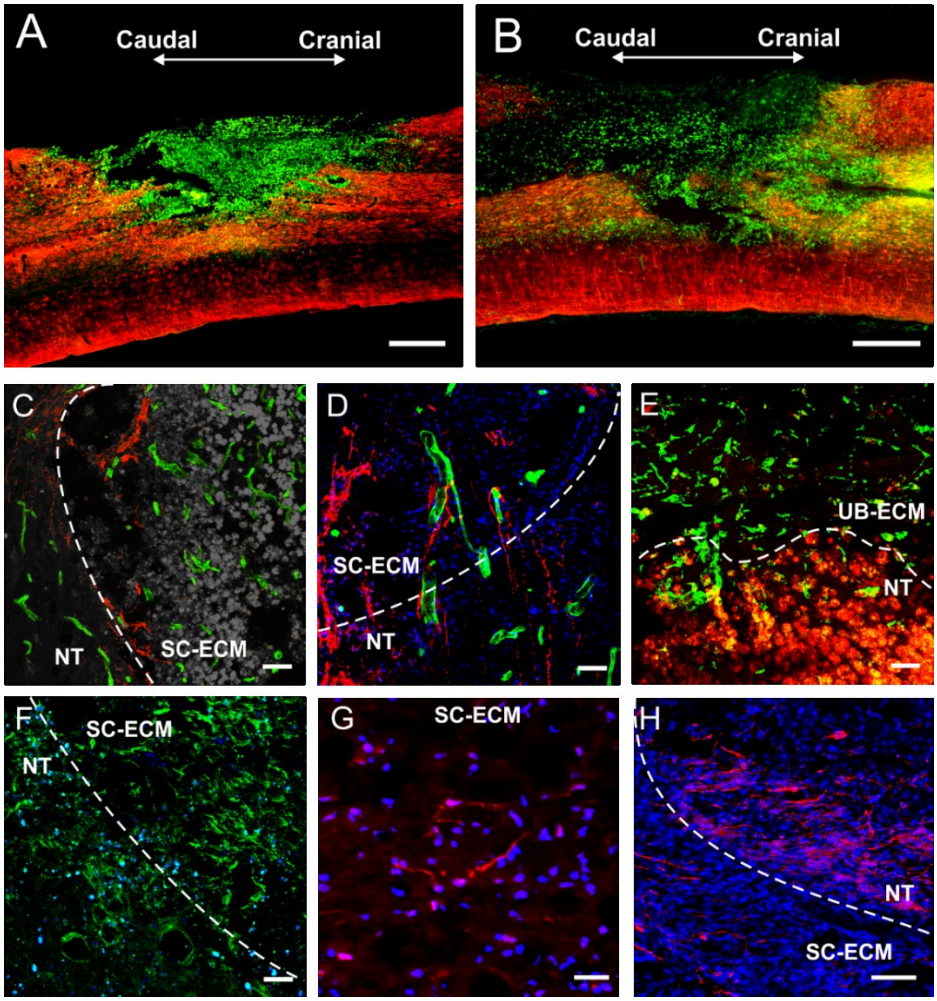

Fig. 32. Representative immunofluorescent staining for (A, B) macrophages (ED1, green) and astrocytes (GFAP, red) in (A) urinary bladder extracellular matrix (UB-ECM) at 2 weeks and (B) spinal cord (SC-) ECM seeded with WJ-MSCs at 4 weeks. Confocal micrographs of the staining for (C) serotonin-positive axons (5-HT, red) and blood vessels (RECA, green) in SC-ECM at 4 weeks, (D) serotonin-positive axons (5-HT, red), blood vessels (RECA, green) and cell nuclei (DAPI, blue) in SC-ECM seeded with WJ-MSCs at 4 weeks, (E) M1 macrophages

(CD86, green) and M2 macrophages (CD206, red) in UB-ECM hydrogel at 2 weeks; (F) oligodendrocytes (OSP, green) and cell nuclei (DAPI, blue) in SC-ECM at 4 weeks; (G) neuronal growth cones (GAP 43, red) and cell nuclei (DAPI, blue) in SC-ECM at 4 weeks; (H) Schwann cells (p75, red) and cell nuclei (DAPI, blue) in SC-ECM at 4 weeks. The dotted line in (C, D, E, F, H) describes the border between ECM hydrogel and neural tissue (NT). Scale bar: (A, B) 500 µm; (C, H) 100 µm; (D, E, F) 50 µm; (G) 25 µm.

8.3.2 Histological evaluation of implanted ECM hydrogels combined with hWJ-MSCs

To evaluate the potential of ECM hydrogels as cell vehicle, the SC-ECM hydrogels were mixed with hWJ-MSCs (0.5 x 10^6 cells per 0.2 mL), and the cell-hydrogel constructs containing ~ 1.5 x 10^3 cells were implanted into the hemisection cavity. Four weeks after the surgery, grafts were densely infiltrated with endogenous tissue, while cysts were developed at the graft-tissue interface. Only very few surviving cells, positive for marker of human mitochondria MTCO2, were detected in the lesion (Fig. 33B). Transplanted cells did not further increase the ingrowth of NF-positive fibres as well as blood vessels, but increased relative area of NF-positive fibres was found in the groups of animals that received immunosuppression (Fig. 33F, G). As in empty ECM hydrogels, M2 phenotype macrophages were mostly present within the hydrogel area (Fig. 33E).

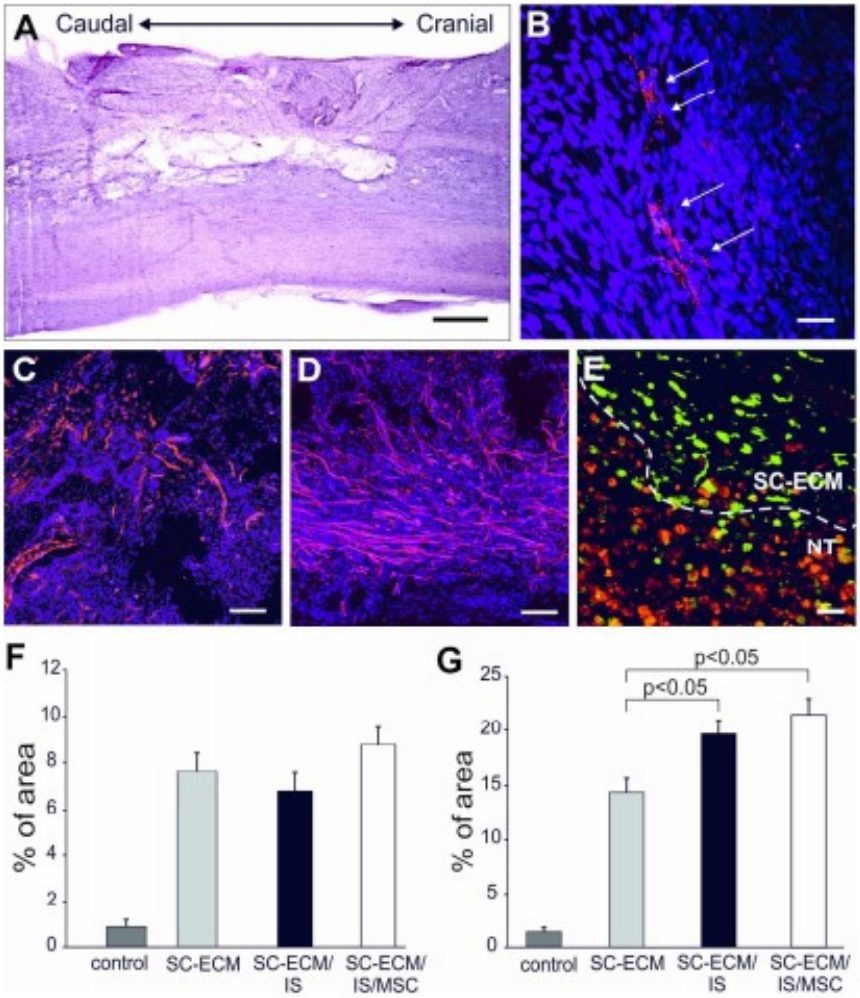

Fig. 33. Representative images of the spinal cord lesion after implantation of spinal cord extracellular matrix (SC-ECM) seeded with human Wharton´s jelly mesenchymal stromal cells (hWJ-MSCs) at 4 weeks. (A) Haematoxylin-eosin staining. Confocal micrographs of the staining for (B) human mitochondria (MTCO2); (C) blood vessels (RECA); (D) neurofilaments (NF160) and (B - D) cell nuclei (DAPI, blue); E) M1 macrophages (CD86, red) and M2 macrophages (CD206, green). The dotted line in E describes the border between ECM hydrogel and neural tissue (NT). An effect of the SC-CM hydrogels seeded with hWJ-MSCs on the ingrowth of (F) blood vessels and (G) neurofilaments. (IS) - animal groups that received immunosuppression. Data are shown as mean ± standard error mean. Statistical analysis using one-way ANOVA, Scale bar: (A) 500µm, (B) 100µm, (C) 50µm, (D) 25µm.

8.3.3 Gene expression analysis induced by ECM hydrogels

Changes in the mRNA expression of genes related to inflammation (*Ptgs2, Ccl3, Ccl5, Il2, Il6, Il12b*), M1 macrophages (*Irf5, Cd86, Nos2*), M2 macrophages (*Mrc1, Cd163, Arg1*), growth factors (*Nt-3, Fgf2*), axonal sprouting (*Gap43*), astrogliosis (*Gfap*), angiogenesis (*Vegfa*) and apoptosis (*Casp3*) were determined at 2, 4 and 8 weeks after hydrogel injection and compared to the control SCI lesion. The most profound host tissue response to the ECM hydrogels was observed 2 weeks after injury, when significant downregulation was found in expression of *Fgf2, CD163, Irf5, Ccl5* and *Gap43* in both hydrogel groups; and of *Gfap* in the UB-ECM hydrogel group only, when compared to the control SCI lesion (Fig. 34). At 4 weeks, no significant changes were detected between both hydrogel groups and control group, except for significant upregulation of *Arg1* in UB-ECM hydrogel group compared to SC-ECM. A potential tissue specific effect of SC-ECM was observed at 8 weeks, when significant upregulation of mRNA expression was detected for *Nt-3, Fgf2, Irf5* and *Casp3*. Expression of pro-inflammatory cytokines *IL-2, IL-6, Il12b* and *Nos2* was undetectable in all group (data not shown).

The effect of hWJ-MSCs combined with SC-ECM hydrogels was determined 4 weeks after the scaffold implantation. The animals received immunosuppression to prevent rejection of the xenogeneic cells. Interestingly, the immunosuppression significantly decreased the mRNA expression of *Gfap* in both, empty and cell seeded hydrogels, and of *Fgf2, Casp3, Ccl3* and *Cd86* in empty hydrogels, when compared to the control lesion (Fig. 34). Moreover, significant increase of expressions *Vegfa* and *Gap43* was also found in cell-seeded hydrogels when compared to the empty hydrogels.

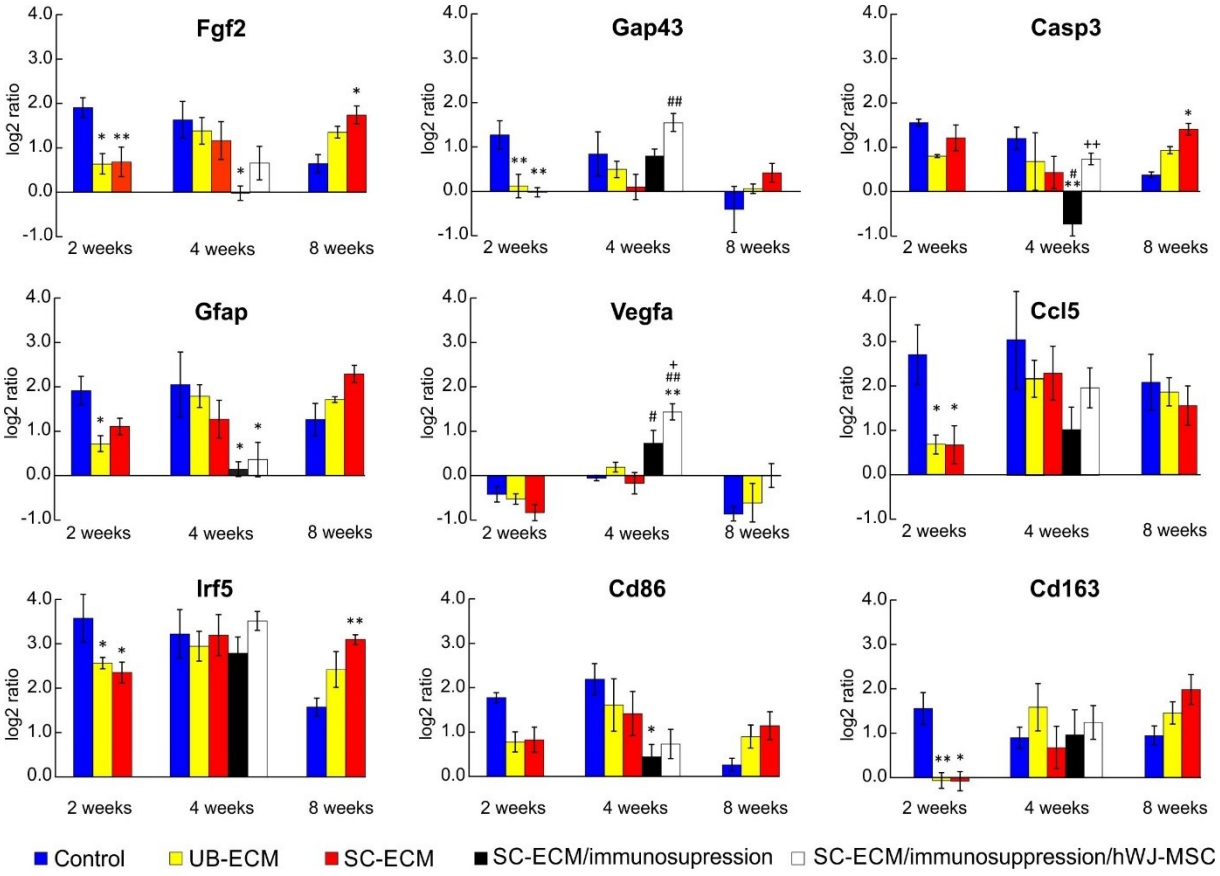

*Fig. 34. Analysis of messenger ribonucleic acid (mRNA) gene expression of several genes involved in inflammatory and reparative processes following spinal cord injury (SCI) treated with extracellular matrix (ECM) hydrogels. The graphs show the log2 fold changes of the ΔΔCt values of the indicated genes in comparison to the intact spinal cord tissue. Data are shown as mean ± standard error mean. Statistical analysis using two-way repeated measurement ANOVA, * p<0.05, ** p<0.01 ΔCt values of ECM hydrogel vs control lesion, # p<0.05, ## p<0.01 ΔCt values of SC-ECM hydrogel with immunosuppression vs SC-ECM, + p<0.05, ++ p<0.01 ΔCt values of SC-ECM hydrogel with immunosuppression and hWJ-MSCs vs empty SC-ECM with immunosuppression.*

8.4 Conclusion

Both, CNS-derived and non-CNS derived ECM hydrogels showed significant immunomodulatory and neuro-regenerative effects and provided the substrate for tissue bridging after SCI. Both types of hydrogels integrated into the lesion and stimulated neovascularization and axonal ingrowth into the lesion. On the other hand, massive macrophage infiltration and rapid hydrogel degradation did not prevent cyst formation, which progressively developed over 8 weeks. No significant differences were found between SC-ECM and UB-ECM. Gene expression analysis revealed significant down-regulation of genes related to immune response and inflammation in both hydrogel types at 2 weeks post-SCI. A combination of hWJ-MSCs with SC-ECM did not further promote ingrowth of axons and blood vessels into the lesion, when compared with the SC-ECM hydrogel alone. Fast hydrogel degradation might be a limiting factor for the use of native ECM hydrogels in the treatment of acute SCI and should be addressed in the future research.

9 DISCUSSION

Following neural injury, numerous obstacles such as loss of the neural tissue, formation of the cavity, inflammation, glial scarring, demyelinization, loss of neural excitation and function must be overcome. Given the complexity, successful neural tissue regeneration requires a combinatorial approach. In this thesis, we addressed cell transplantation and biomaterial implantation and their combination as promising treatments for SCI repair.

9.1 MSCs isolation, expansion and *in vitro* characterization

Cell therapy has emerged as a promising treatment for neural repair in order to replace and/or protect damaged tissue and provide physical as well as trophic support for axonal regrowth.

In the first part of this thesis, we compared hMSCs from three different tissue sources and demonstrated that all cell types comply with ISCT minimal criteria for hMSCs (Dominici et al. 2006). When compared to hBM-MSCs and hASCs, we proved hWJ-MSCs as the cells with the highest cell yield and proliferation rate, production of high amounts of cytokines, neurotrophic growth factors, chemokines and cell adhesion molecules, and therefore, we suggest these cells as a possible candidate for stem cell therapy in neural tissue regeneration.

With regard to hMSCs clinical application, the cell yield and proliferation capacity is important for the achievement of the sufficient cell number in the short time period. We confirmed the findings of other authors (Hass et al. 2011; Huang et al. 2010; Pittenger et al. 1999) and demonstrated that hWJ-MSCs and hASCs were isolated in significantly higher amounts and proliferated better and with shorter PDT when compared to hBM-MSCs. The mean PDT in 1P was found about 29.5 hours for the hWJ-MSCs, while (Lu et al. (2006) reported 24 hours, and about 43.7 hours for the hASCs, while Peng et al. (2008) reported 45 hours, and remained almost same up to the 11P. In contrast, the mean PDT for hBM-MSCs was 68.3 hours, while Peng et al (2008) reported 61 hours, and increased considerably with number of passage. Besides the higher proliferative activity of hWJ-MSCs and hASCs, these cells showed no sign of senescence over several passages (up to 11P), as is well documented by increasing their cPD. Some authors report that hBM-MSCs start to demonstrate senescence from 7P (Kern et al. 2006), which is in line with our results that showed a plateau in hBM-MSCs cPD in 8P.

In terms of the phenotype, both, hBM-MSCs and hASCs express CD29, CD44, CD73, CD90 and CD105 and differ in expression of CD34, CD49d and CD106 (De Ugarte et al. 2003; Zuk et al. 2001). These are in accordance with our results where we showed a similar expression of

all observed markers except of expression of CD106 which was found in hBM-MSCs, but not in hASCs or hWJ-MSCs. CD106, also known as VCAM-1 is a cell adhesion molecule which is related to leukocyte extravasation. CD106+ hMSCs were reported to have enhanced immunomodulatory properties (Yang et al. 2013). Expression of VCAM-1 can be induced by inflammatory cytokines (Yang et al. 2013), which was confirmed also in our experiments in secretome analysis.

hWJ-MSCs showed moderate expression of CD146 and CD235a that was in contrast to the absence of their expression in the other cell types. Expression of CD146 is associated with higher multipotency and genuine stemness of hWJ-MSCs. CD235a is expressed by erythroid precursors and mature circulating red cells. Its higher expression in hWJ-MSCs might be attributed to their participation in embryonic haematopoiesis and was shown by other reports as well (Conconi et al. 2011).

It is generally accepted that hMSCs secrete a number of bioactive factors and the therapeutic potential of hMSCs secretome has become recently increasingly acknowledged (Pawitan 2014). The application of secreted molecules is appealing as it might replace the stem cell therapy and therefore minimize biological variability, allow precise dosing, overcome stem cell limitations and lead to development of standard, safe and effective therapy with possibly predictable outcomes (Skalnikova 2013). In general, the secreted factors in CM differed with regards to the hMSCs type.

Pawitan (2014) reviewed 39 studies that used CM in various indications and reported that there is a lack of standard in terms of cell passage, media, cell number and culture condition and that these parameters determine the quality and quantity of the secretome content. In our study, we also observed differences in cell secretomes when using different cell numbers, cell passage or culture conditions. For final evaluation, therefore, we selected these standard conditions: 5 x 10^6 cells were seeded into one compartment of 6-well plate and cultured under normoxic conditions (O_2 level 20-21%) with ITS supplement alone or with an addition of inflammatory cytokines.

In line with Pawitan (2014), we detected proinflammatory cytokines as IL-6, IL-12, and IFNα, anti-inflammatory cytokine IL-1RA, growth factors such as VEGF, EGF, HGF, bFGF, BDNF, chemokines such as MCP1, SDF-1, IP-10 and RANTES and cell adhesion molecules such as ICAM-1 and VCAM-1.

Importantly, stimulation by inflammatory cytokines led to considerable increase of IL-6, IL-12, IL-1RA and IFNα in all cell types. While IL-1RA is an anti-inflammatory cytokine, the IL-6, IL-12 and IFNα are considered to have pro-inflammatory effect. This suggest that when exposed to inflammatory environment, the final effect of MSCs might be ambivalent and depends on the complex interactions of exogenous and endogenous factors.

Chemokines MCP1, IP-10, RANTES and cell adhesion molecules ICAM-1, VCAM-1 were also upregulated after stimulation with inflammatory cytokines. ICAM- 1 and VCAM-1 regulate leukocyte and hematopoietic cell migration across blood walls and provide attachment points for developing endothelium during angiogenesis (Imhof 1995), thus it can be hypothesized that these molecules have a role in hMSCs trafficking.

VEGF plays a key role in angiogenesis (Sadat et al. 2007) and may prevent apoptosis under hypoxic conditions (Bhang et al. 2014) such as after SCI. Amable et al. (2014) reported that hWJ-MSC secreted very low concentrations of VEGF, which was four times lower than hBM-MSCs and hASC respectively; our study shows a similar trend. This suggests that hWJ-MSC might have a lower angiogenic effect than hBM-MSCs and hASCs.

In terms of neural tissue repair, all cell types secreted neurotrophic growth factors that play a role in neuroprotection and neurogenesis, such as BDNF, HGF, bFGF and EGF.

Secretion of BDNF and HGF was found to be higher in hWJ-MSC when compared to other cell types. BDNF is neuroprotective – it not only promotes cell survival but also reduces the glial scaring (Cantinieaux et al. 2013). Similarly, HGF has also been found to support neural cell survival and axonal regeneration (Wong et al. 2014) and to contribute to neurogenesis and angiogenesis (Di Santo et al. 2009; Ho et al. 2012). bFGF stimulates angiogenesis and proliferation of fibroblast, preadipocytes, endothelial, epithelial and neural stem cells, migration and differentiation of precursors into mature neurons and glial cells (Yun et al. 2010). EGF contributes to regeneration of mesenchymal, glial and epithelial cells (Oki and Ando 2008). While BDNF and HGF were present in all cell types CM, bFGF and EGF were found in CM only after inflammatory stimulation and in small amounts only.

Notably, there is a big difference between the cell sources in terms of the application. While hBM-MSCs and hASCs can be used for both autologous and allogeneic administration, hWJ-MSCs are prevalently intended for allogeneic cell therapy with the advantage that they can be expanded in a high number and used off the shelf. Moreover, hWJ-MSCs can be obtained in large amounts non-invasively and without ethical constrains. On the downside, despite proven

immunomodulatory properties, allogeneic hMSCs might be rejected in the recipient which might limit the time period for which they can execute their paracrine effect.

However, despite these drawbacks that still need to be addressed at basic and preclinical levels, hWJ-MSCs are increasingly used in clinical trials.

9.2 Transplantation of hWJ-MSCs into SCI

The second part of this thesis aimed to determine the effect and optimal dosage of transplanted stem cells derived from WJ into SCI.

We compared single and triple repeated i.t. delivery of hWJ-MSCs with a low and high cell dose (0.5 and 1.5 x 10^6) in each application. Since cell survival in the vertebral canal is rather low (Antonic et al. 2013; Ruzicka et al. 2017; Urdzikova et al. 2014), we hypothesized that by repeated application, the trophic and immunomodulatory effect of the cells can be substantially increased.

Analysis of behavioural tests revealed that functional recovery of hind limb motion in treated rats was dependent on the cell dose and repeated application, which was in line with findings of other authors (Antonic et al. 2013; Li 2010; Pal et al. 2010). Whereas the single dose of 0.5 x 10^6 hWJ-MSCs showed no significant difference in BBB test score when compared to control animals, the other treatment groups (high cell dose and repeated application) achieved significantly higher scores. The beneficial effect of repeated injections was then visible in the advanced motor function testing, such as beam walking. No effect was, however, detected in the rotarod test, which requires a higher level of motor coordination and stepping.

Improvement in both, locomotor and sensory behavioural scores was reported by Pal et al. (2010), who tested single administration of 0.5 and 1.5 x 10^6 of hBM-MSCs applied i.t. or directly into the site of SCI 3rd or 14th day after the lesion. For the whole study period (4 weeks), no differences in BBB test score were observed between the lower and higher cell dose. Contrary to these findings, we observed significant improvement in BBB test score from the 4th week post SCI, after single application of higher dose of hWJ-MSCs. Similar to our results, in the study of Pal et al, more advanced motor tests distinguished between the cell dose. When compared with the lower cell dose, the transplantation of 1.5 x 10^6 hBM-MSCs showed significantly fewer foot slips while performing grid walk and almost recovered their score in the inclined plane test to pre-SCI level. In addition, only the group implanted with higher cell dose recovered their sensitivity on plantar test to pre-SCI levels. In terms of timing of the cell

transplantation, no differences were noted in the recovery pattern between the group of animals treated 3rd and 14th day.

A systematic review and meta-analysis by Antonic et al. (2013) reported dose-response relationship for sensory outcomes in 473 animals with SCI. However, regarding motor improvement, no dose-dependency was observed. The response increasingly correlated only in doses starting from as low as 10^3 implanted cells (Zhao et al. 2010).

Most studies employ acute or subacute timing for MSCs implantation, while studies investigating treatments of chronic SCI are rare and often fail to provide functional recovery (Tetzlaff et al. 2011).

To increase the chances of good timing along with increasing the cell survival, some studies employ repeated application. Li et al. (2010) applied 10^6 of allogeneic Hoechst-labelled BM-MSCs into a rat SCI once, one week post injury and then repeatedly (twice, three-times and five-times post injury). All cell treated groups improved in BBB test when compared to control group. At later time points, repeated administration (three- and five-times) significantly increased BBB test score compared to single and double administration. At 3 weeks post injury, BM-MSCs were detected in all cell-treated groups. At the end of the study, *i.e.* at 12 weeks post injury, surviving cells were detected only in groups with repeated administration. Also, axonal growth indicated by NF-200 positive fibres was maximal in groups with triple and 5-times repeated administration.

The reports on cell survival and migration into the SCI are divergent, but in general it is considered low. While some authors report cell survival after 4 weeks post-SCI and migration of hBM-MSCs into the site of the injury (Pal et al. 2010), in our study we detected only few surviving hWJ-MSCs two weeks post-SCI. And these cells were localized in the site of injection without apparent homing into the lesion site. Similarly in a longer follow-up study, Urdzikova et al. (2014) found no living cells 8 weeks after the surgery.

In terms of trans-differentiation, no β-III tubulin, O4 or GFAP positive staining was detected by Pal et al. (2010), thus confirming the theory that MSCs do not differentiate in the host tissue.

The route of administration is another important factor that should be taken into account. In our study, only i.t. route of administration was applied also due to the fact that repeated administration inside the lesion is technically demanding. Different ways such as i.v.

(Urdzikova et al. 2006), i.t. and administration into the lesion site (Pal et al. 2010; Ruzicka et al. 2017) has been demonstrated as having beneficial effect on SCI treatment. Pal et al. (2010) reported that while both i.t. and intraspinal transplantation showed improvement in histological evaluation, only the i.t. transplanted group performed better in all behavioural tests. In addition to improved functional recovery, i.t. administration is much safer and is clinically more suitable.

Immunohistochemical analysis showed, that transplantation of hWJ-MSC facilitates axonal sprouting and plays a role in decreasing the glial scar formation. Astrogliosis, which is closely bound up with reactive astrocytes was significantly less present in cell-treated rats. Axonal sprouting was gradually enhanced with the increased number of transplanted cells. The same trend was present in the measuring of the white and grey matter preservation, which revealed a strong neuroprotective effect in grey matter, mainly in the centre of the lesion and only in groups with the highest number of treated cells. A significant effect on tissue sparing was observed only in animals treated by single or triple implantation of 1.5 x 10^6 hWJ-MSCs. All these findings was supported by behavioural analysis, where significant improvement in BBB test score was found after single high cell dose and repeated application of both low and single cell dose. No differences in BBB test score was then found between single application of 0.5 x 10^6 hWJ-MSCs and control animals. It is evident that for the simple locomotor test, such as the BBB test, a threshold of a minimum number of cells is required to trigger functional improvement. However, closer analysis of tissue microstructure has shown that an increased number of cells applied repeatedly, further enhanced the neuroprotective and neuroregenerative effect of the hWJ-MSC on SCI.

It is generally accepted that due to the low ability of hMSCs to survive in the donor tissue (Antonic et al. 2013), as confirmed in our study, and their limited *in vivo* differentiation (Pal et al. 2010), the main therapeutic effect of MSC lies in their ability to secrete trophic factors. We (in Chapter 5) and others (Bollini et al. 2013; Crigler et al. 2006; Neuhuber et al. 2005) have previously shown that MSCs secrete a number of neurotrophic and other cytokines that stimulate nerve growth, promote local neovascularization, inhibit cell death and suppress the immune response.

In this study, we propose hWJ-MSCs as suitable source for cell therapy of SCI. Since hWJ-MSCs are allogenic, can be easily up-scaled, prepared in advance, cryopreserved and ready for use in a relatively short time. Repeated application of hWJ-MSCs could even enhance their therapeutic potential for neural repair.

9.3 ECM preparation and characterization

Acellular tissue specific ECM matrices can be utilized as biological scaffolds for reconstruction of neural tissues. ECM in the form of hydrogels are clinically more acceptable as these materials retain biologic activity, with the advantage of injectability and *in situ* polymerization which offer minimally invasive delivery techniques. Indeed, injectable ECM hydrogels derived from different tissue sources have been previously demonstrated for the treatment of stroke (Freytes et al. 2008), post-myocardial infarction (Singelyn and Christman 2010), critical limb ischaemia (Ungerleider et al. 2016), and new adipose tissue development (Young et al. 2011).

In the third part of this thesis, we optimized the decellularisation protocol as described by Badylak et al. (2015), to prepare an injectable hydrogel from human UC tissue, which combines the advantages of neonatal tissue of human origin with the ease of availability, without any ethical or regulatory constraints. Our data showed that decellularisation process preserved the core ECM proteins, mainly collagen and fibronectin as well as non-ECM proteins. In contrast to other previously used ECMs extracted from the porcine UB, B or SC, UC-ECM contained a significantly higher amount of sGAG, which is generally high in foetal and new-born tissues, including the UC (Kato et al. 2004). Moreover, the sGAGs present in ECM include chondroitin sulphates, heparin, heparan sulphate and, these structures can bind cytokines and growth factors, such as bFGF and contribute to neural tissue repair (Badylak 2004; Crapo et al. 2012; Horn et al. 2007; Seif-Naraghi et al. 2012; Wang and Spector 2009).

The concentration of sGAGs has been shown to alter gelation kinetics and mechanical properties of ECM hydrogels (Medberry et al. 2013). Indeed, UC-ECM revealed the fastest gelation rate when compared to the porcine ECMs with lower sGAGs. Notably, even if the B-ECM, SC-ECM and UB-ECM were prepared by the same decellularisation protocols, they displayed slight differences in collagen and sGAG concentrations as well as in gelation time and rheologic properties, when compared to those described by Medberry et al. (2013). These differences might result from different origin as well as the age of porcine tissues used for decellularisation.

Despite dissimilarities in nano-scale topography, sGAG content, mechanical properties and the speed of gelation, we did not observe any significant differences in chemotactic or neurotrophic properties between the CNS- and non-CNS derived ECM materials of human or porcine origin, which does not indicate an advantage of tissue specificity for ECM hydrogels in neural tissue repair. Of note, to achieve effective cell removal, CNS-derived tissues required the more

complex decellularisation procedures compared with *e.g.* UB-ECM or UC-ECM, which may result in the removal of neurosupportive proteins and growth factors, and consequent loss of CNS tissue specific bioactivity.

On the other hand, we found a tissue specific effect of UC-ECM which selectively promoted proliferation of hWJ-MSC when compared to the other types of ECMs and MSCs. We assumed that UC-ECM preserved distinct cues and provides original environment specifically designed for hWJ-MSC.

Finally, we proved *in vivo* UC-ECM gelation and biocompatibility using a rat model of photothrombotic lesion. The UC-ECM was densely infiltrated by resident macrophages with a predominating M2 phenotype. An M2-like macrophage phenotype was also found after UB-ECM injection into rat middle cerebral ischemia lesion cavities (Ghuman et al. 2016). An M2-positive macrophage infiltration in response to acellular ECM has been positively correlated to constructive host tissue remodelling, while M1 phenotype resulted in the deposition of dense connective tissue and scarring (Badylak 2014; Brown et al. 2009). Nevertheless, future work is needed to determine the *in vivo* UC-ECM degradation and its replacement by the host tissue in a longer time period.

9.4 *In vivo* evaluation of ECM biomaterials

In the last part of this thesis, we evaluated *in vivo* neuro-regenerative potential of two types of ECM hydrogels - CNS and non-CNS derived - in the rat acute SCI. The ECM matrices were derived from porcine SC and UB and processed to injectable hydrogel form as was described previously (Medberry et al. 2013; Wolf et al. 2012). Regarding different tissue source, SC-ECM and UB-ECM hydrogels were prepared by a different decellularisation methods and differed in composition and as well as in physical and biologic properties (as shown in Chapter 7).

When injected into SCI, both hydrogel types were well integrated with the surrounding tissue with persisting massive cell infiltration and neovascularization. A potentially important factor for the tissue regeneration is tissue specificity of the ECM hydrogel source. In this study, however, no significant differences were found between CNS-derived SC-ECM and non-CNS UB-ECM hydrogels with regards to ingrowth of NF and neovascularization in all observed time points. This confirmed our previous results where we did not observe any differences in neurotrophic properties between various ECM hydrogel types.

Macrophages were the predominant infiltrating cells within the grafts that participated in the ECM degradation. As was shown by other authors, degradation of ECM scaffolds is essential

for constructive tissue remodelling process by which a degradable biomaterial serves as a temporary inductive niche which is gradually replaced by anatomically appropriate and functional tissue as opposed to scar tissue (Badylak et al. 2009; Tottey et al. 2011; Valentin et al. 2009). Moreover, degradation of ECM scaffolds stimulates the release of matricryptic molecules; which possess a variety of bioactive properties such as recruitment of endogenous stem and progenitor cells, antimicrobial activity, and angiogenic effects (Valentin et al. 2009).

In this study, however, despite the fact that the lesion cavity was filled with endogenous cell populated ECM hydrogels 2 weeks after their injection, further progression in matrix degradation at the later time points was not followed by the full neural tissue replacement, but rather resulted into the formation of the sparse network of tissue containing axons, blood vessels as well as other neural tissue elements interrupted by a number of small cysts.

According to gene expression analysis, *in vivo* ECM degradation was associated with significant decrease in mRNA expression of markers for pro-inflammatory/M1 macrophages (*Irf5*) and regulatory/M2 macrophages (*Cd163*), inflammation (*Ccl5/Rantes*) as well as genes for growth factor *Fgf2*, astrogliosis (*Gfap*) and neuronal growth cones (*Gap43*). Expression of other markers related to immune response, such as *Cd86, Mrc1* and *Ptgs2* was also decreased, but these changes were not found to be significant. Interestingly, these effects were detected during the early phase after injury, but decreased or even reversed in the later time points, suggesting that ECM hydrogel degradation have played significant role in the transient modulation of the innate immune and tissue repair response.

As evidenced in the literature (Badylak and Gilbert 2008; Brown et al. 2012), *in vivo* degradation of ECM was associated with increased numbers of M2 macrophages and constructive tissue remodelling. In this study, the expression of genes related to both, M1 and M2 macrophages decreased at 2 weeks, which reflects that both inflammatory, as well as anti-inflammatory responses were inhibited after ECM hydrogel treatment.

ECM molecules, such as laminin, fibronectin, collagen and heparan sulphate proteoglycans as well as their degradation products play the significant role in the regulation of growth cone motility and axon guidance (Myers et al. 2011). *Gap43*, which is expressed at high levels in neuronal growth cones during axonal regeneration, is considered a crucial component of an effective regenerative response in the nervous system. Contradictorily, decreased mRNA expression of *Gap43* in both hydrogel groups at 2 weeks did not correlate with a robust axonal ingrowth into the lesion as revealed by the histological analysis. It is likely that axonal sprouting

might culminate throughout an earlier period after injury (Hsu and Xu 2005), but undoubtedly, further work to prove the protein synthesis during the repair process need be done to elucidate *Gap43* as a sufficient marker of promotion of axonal outgrowth. On the other hand, significant increase in mRNA expression of *Gap43* was found in the hydrogels seeded with hWJ-MSCs at 4 weeks, together with an elevated axonal ingrowth into the lesion.

Many studies indicate that cell-seeded biomaterial scaffolds lead to greater axonal regrowth than biomaterial scaffolds alone (Gao et al. 2013; Li et al. 2013; Liu et al. 2017; Teng et al. 2002; Wang et al. 2017; Zeng et al. 2015). To test the potential of ECM hydrogels as supportive cell carriers, they were combined with hWJ-MSCs prior implantation into a rat hemisection. The inflammatory milieu of the acute lesion together with the massive infiltration of macrophages, however, were not supportive for the cell survival, and only few cells were detected within the lesion 4 weeks after the implantation. On the other hand, due to the limited volume of the implanted scaffold, the total number of implanted cells within the hydrogel was relatively small (~3 x 10^4). For higher *in vivo* cell surviving rate, increased number of implanted cells would be needed.

Notably, immunosuppression significantly promoted axonal ingrowth, decreased expression of *Gfap, Fgf2, Casp3, Ccl3* and *CD86*, and increased expression of *Vefga*, which confirmed the neurotrophic effect of immunosuppressive agents (Sosa et al. 2005).

ECM hydrogels are undoubtedly advantageous biomaterials in terms of their injectability, degradability, as well as biologic activity which enables them to modulate immune response and stimulate vascularization and axonal ingrowth. However, one impediment that limits using of ECM hydrogels in their current form as optimal materials for CNS is their rapid *in vivo* degradation, which was too fast to be followed with the full tissue reconstruction in the lesion cavity.

10 EVALUATION OF HYPOTHESES AND STUDY AIMS

1) Human mesenchymal stromal cells (hMSCs) isolated from human Wharton´s jelly are comparable with other cell types, such as hASCs and hBM-MSCs.

- hWJ-MSCs were successfully isolated from human Wharton´s jelly and displayed comparable properties as hASCs and hBM-MSCs in terms of expression of surface markers, migration capacity, differentiation and secretion of growth factors, cytokines, chemokines and cell adhesion molecules. hWJ-MSCs had higher cell yield, proliferation, cPD and shorter PDT when compared to hBM-MSCs. Our data showed that in comparison to adult hMSCs, hWJ-MSCs secreted lower amounts of angiogenic factor VEGF but higher levels of neurotrophic factors HGF and BDNF.

2) i.t. transplantation of hWJ-MSCs has beneficial effects on SCI repair in rats and their effect is dose-dependent.

- We confirmed that i.t. transplantation of hWJ-MSCs has beneficial effects on SCI repair in rats. Moreover, we demonstrated that the effect was dose-dependent and further potentiated by repeated administration. Based on the dose (0.5 or 1.5 x 10^6), the cell application led to gradually increased axonal ingrowth, higher amount of spared grey matter and reduced astrogliosis. Gene expression analysis showed downregulation of markers for both M1- and M2-like macrophages and apoptosis only after repeated administration of higher dose of hWJ-MSCs (1.5 x 10^6). Better immunohistochemical and histological results after repeated administration of higher dose of hWJ-MSCs corresponded with functional recovery that showed improved locomotor function mainly in advanced coordination skills.

3) Extracellular matrix (ECM) can be isolated from the human umbilical cord (UC), solubilized to form a hydrogel and used for neural tissue repair.

- We successfully prepared ECM from human umbilical cord that was solubilized to form an injectable hydrogel suitable for neural repair. Human UC-ECM, and porcine UB-ECM, B-SCM and SC-ECM were characterized in terms of fibre width, collagen and sGAG content, protein composition, gelation time and elastic modulus. UC-ECM contained significantly higher amounts of sGAG, displayed shortest gelation time and showed tissue specific enhancement in hWJ-MSCs proliferation when compared to other MSCs types. Despite some differences in structure and physical properties, all ECM revealed similar *in vitro* neurotrophic properties.

CNS –derived ECM scaffolds are suitable for spinal cord injury (SCI) repair and reveal tissue specific effect.

- We proved that both CNS- as well as non-CNS derived hydrogels are suitable materials for SCI repair. After injection into spinal cord hemisection, both hydrogel types revealed immunomodulatory and neuro-regenerative effects as shown by increased neovascularization and axonal ingrowth into the SCI lesion and down-regulation of genes related to immune response and inflammation. However, no tissue specific effect of CNS-derived ECM hydrogels was observed when compared to non-CNS derived ECM hydrogels in vivo. A combination of ECM hydrogels with hWJ-MSCs did not show improvement of SCI repair when compared to ECM hydrogel alone.

11 SUMMARY

In the first part of this thesis we showed that hWJ-MSCs meet the criteria for MSC and among adult hMSCs cell types, represent a cell source with several advantages, such as easy accessibility (umbilical cord is waste material) and non-invasive isolation, high cell yield and proliferation rate without cell senescence until high passage. Production of cytokines, growth factors and chemokines suggests that these cells have pro-regenerative neurotrophic paracrine effects and may thus represent a promising tool for regeneration of neural tissue.

The high therapeutic potential of hWJ-MSCs was then confirmed *in vivo* in a rat SCI model. The transplantation of hWJ-MSCs promoted axonal sprouting, preserved higher amounts of grey matter, reduced inflammation, apoptosis and improved locomotor functions of rats after SCI. The effect of hWJ-MSCs was found to be dose-dependent and potentiated by repeated application. This study confirmed the paracrine effect of the cells after i.t. transplantation, as no homing of transplanted cells into the lesion as well as no long-term cell survival was observed.

In the third part of this thesis, injectable ECM hydrogels were prepared by decellularisation of CNS and non-CNS tissues of both human and porcine origin. All ECM hydrogels retained their biologic activity and possessed mechanical properties suitable for the application into the soft neural tissue.

When injected into the SCI, porcine CNS- and non-CNS derived ECM hydrogels showed significant immunomodulatory and neuro-regenerative effects and provided a substrate for tissue bridging. Both types of hydrogels integrated into the lesion and stimulated the neovascularization and axonal ingrowth into the lesion. However, no benefit of tissue specific effect of CNS-derived ECM was observed when compared with non CNS derived ECM hydrogel.

Of note, the limiting factor of using ECM hydrogels both alone or in combination with the cells is their fast *in vivo* degradation which may be enhanced in the inflammatory environment of the lesion.

In conclusion, both, hWJ-MSCs and ECM biological scaffolds were proved as efficient approaches for the SCI repair. The results of our studies indicate that a combination of repeated i.t. transplantation of a high dose of hWJ-MSCs and the injection of acellular UC-ECM hydrogel into the lesion might further potentiate their regenerative effect.

12 SOUHRN

V první části této práce jsme ukázali, že hWJ-MSCs splňují minimální kritéria pro MSCs a mají vzhledem k hMSCs z kostní dřeně a tukové tkáně několik výhod, jako je snadná dostupnost (pupečník je odpadní materiál), neinvazivní izolace, vysoký výtěžek buněk a vysoká míra proliferace bez senescence buněk i ve vyšších pasážích. Produkce cytokinů, růstových faktorů, chemokinů a buněčných adhezních molekul naznačuje, že tyto buňky mají proregenerativní neurotrofické parakrinní účinky a mohou tak představovat slibný nástroj pro regeneraci nervové tkáně.

Vysoký terapeutický potenciál hWJ-MSC byl pak potvrzen v *in vivo* na modelu míšního poranění u laboratorního potkana. Transplantace hWJ-MSC podporovala axonální růst, měla neuroprotektivní a protizánětlivý efekt, a zlepšila lokomotorické schopnosti potkanů po míšním poranění. Účinek hWJ-MSC byl závislý na počtu transplantovaných buněk a byl potencován opakovaným použitím. Studie potvrdila parakrinní účinek buněk po jejich intratekální transplantaci, neboť nebyla pozorována migrace transplantovaných buněk do léze ani jejich dlouhodobé přežití v hostitelské tkáni.

Ve třetí části této práce byly připraveny injektabilní ECM hydrogely pomocí decelularizace CNS a non-CNS tkání lidského i prasečího původu. ECM hydrogely vykazovaly biologickou aktivitu a vhodné mechanické vlastnosti pro aplikace do měkké neurální tkáně.

Aplikace ECM hydrogelů odvozených z CNS (mícha) a non-CNS (močový měchýř) tkání do míšní léze měla významné imunomodulační a neuroregenerativní účinky a injikované ECM hydrogely poskytly vhodný substrát pro přemostění léze. Oba typy hydrogelů se integrovaly do tkáně a stimulovaly tvorbu nových cév a prorůstání axonů do léze. Nicméně benefit účinku u tkáňově specifického ECM hydrogelu derivovaného z míšní tkáně nebyl prokázán.

Je třeba poznamenat, že omezujícím faktorem při použití ECM hydrogelů jak samotných, tak v kombinaci s buňkami, je jejich rychlá *in vivo* degradace, která může být zvýšena v zánětlivém prostředí léze.

Závěrem lze zhodnotit, že transplantace hWJ-MSC i implantace ECM hydrogelů jsou účinné metody pro reparaci nervové tkáně. Výsledky naších studií ukazují že vhodná kombinace léčby míšního poranění může zahrnovat opakovanou i.t. transplantaci vysoké dávky hWJ-MSC a implantaci bezbuněčného UC-ECM hydrogelu do místa léze.

13 BIBLIOGRAPHY

Acquistapace, A., Bru, T., Lesault, P. F., Figeac, F., Coudert, A. E., le Coz, O., Christov, C., Baudin, X., Auber, F., Yiou, R., Dubois-Rande, J. L.and Rodriguez, A. M. Human mesenchymal stem cells reprogram adult cardiomyocytes toward a progenitor-like state through partial cell fusion and mitochondria transfer. Stem Cells, May 2011, 29(5), 812-824.

Allen, A. R. Surgical experimental lesion of spinal cord. Equivalent to crush injury of fracture dislocation of spinal column. J Am Med Assoc, 1911, 57, 878-880.

Altman, J. Are new neurons formed in the brains of adult mammals? Science, Mar 30 1962, 135(3509), 1127-1128.

Altman, J.and Chorover, S. L. Autoradiographic Investigation of the Distribution and Utilization of Intraventricularly Injected Adenine-3h, Uracil-3h and Thymidine-3h in the Brains of Cats. J Physiol, Dec 1963, 169, 770-779.

Alvarez-Buylla, A., Kohwi, M., Nguyen, T. M.andMerkle, F. T. The heterogeneity of adult neural stem cells and the emerging complexity of their niche. Cold Spring Harb Symp Quant Biol, 2008, 73, 357-365.

Amable, P. R., Teixeira, M. V., Carias, R. B., Granjeiro, J. M.and Borojevic, R. Protein synthesis and secretion in human mesenchymal cells derived from bone marrow, adipose tissue and Wharton's jelly. Stem Cell Res Ther, Apr 16 2014, 5(2), 53.

Anderova, M., Kubinova, S., Jelitai, M., Neprasova, H., Glogarova, K., Prajerova, I., Urdzikova, L., Chvatal, A.and Sykova, E. Transplantation of embryonic neuroectodermal progenitor cells into the site of a photochemical lesion: immunohistochemical and electrophysiological analysis. J Neurobiol, Sep 01 2006, 66(10), 1084-1100.

Anderson, K. D., Borisoff, J. F., Johnson, R. D., Stiens, S. A.and Elliott, S. L. Long-term effects of spinal cord injury on sexual function in men: implications for neuroplasticity. Spinal Cord, May 2007, 45(5), 338-348.

Anderson, K. D., Sharp, K. G.and Steward, O. Bilateral cervical contusion spinal cord injury in rats. Exp Neurol, Nov 2009, 220(1), 9-22.

Annabi, N., Tamayol, A., Uquillas, J. A., Akbari, M., Bertassoni, L. E., Cha, C., Camci-Unal, G., Dokmeci, M. R., Peppas, N. A.and Khademhosseini, A. 25th anniversary article: Rational design and applications of hydrogels in regenerative medicine. Adv Mater, Jan 08 2014, 26(1), 85-123.

Antonic, A., Sena, E. S., Lees, J. S., Wills, T. E., Skeers, P., Batchelor, P. E., Macleod, M. R.and Howells, D. W. Stem cell transplantation in traumatic spinal cord injury: a systematic review and meta-analysis of animal studies. PLoS Biol, Dec 2013, 11(12), e1001738.

Arboleda, D., Forostyak, S., Jendelova, P., Marekova, D., Amemori, T., Pivonkova, H., Masinova, K.and Sykova, E. Transplantation of predifferentiated adipose-derived stromal cells for the treatment of spinal cord injury. Cell Mol Neurobiol, Oct 2011, 31(7), 1113-1122.

Badylak, S. F. Xenogeneic extracellular matrix as a scaffold for tissue reconstruction. Transplant Immunology, Apr 2004, 12(3-4), 367-377.

Badylak, S. F. Decellularized allogeneic and xenogeneic tissue as a bioscaffold for regenerative medicine: factors that influence the host response. Ann Biomed Eng, Jul 2014, 42(7), 1517-1527.

Badylak, S. F., Freytes, D. O.and Gilbert, T. W. Extracellular matrix as a biological scaffold material: Structure and function. Acta Biomater, Jan 2009, 5(1), 1-13.

Badylak, S. F.and Gilbert, T. W. Immune response to biologic scaffold materials. Semin Immunol, Apr 2008, 20(2), 109-116.

Badylak, S. F., Lantz, G. C., Coffey, A.and Geddes, L. A. Small intestinal submucosa as a large diameter vascular graft in the dog. J Surg Res, Jul 1989, 47(1), 74-80.

Baptiste, D. C.and Fehlings, M. G. Update on the treatment of spinal cord injury. Prog Brain Res, 2007, 161, 217-233.

Barros, C. S., Franco, S. J.and Muller, U. Extracellular matrix: functions in the nervous system. Cold Spring Harb Perspect Biol, Jan 01 2011, 3(1), a005108.

Basso, D. M., Beattie, M. S.and Bresnahan, J. C. A sensitive and reliable locomotor rating scale for open field testing in rats. J Neurotrauma, Feb 1995, 12(1), 1-21.

Bayer, S. A. Changes in the total number of dentate granule cells in juvenile and adult rats: a correlated volumetric and 3H-thymidine autoradiographic study. Exp Brain Res, 1982, 46(3), 315-323.

Behrmann, D. L., Bresnahan, J. C., Beattie, M. S.and Shah, B. R. Spinal cord injury produced by consistent mechanical displacement of the cord in rats: behavioral and histologic analysis. J Neurotrauma, Fall 1992, 9(3), 197-217.

Bhang, S. H., Lee, S., Shin, J. Y., Lee, T. J., Jang, H. K.and Kim, B. S. Efficacious and clinically relevant conditioned medium of human adipose-derived stem cells for therapeutic angiogenesis. Mol Ther, Apr 2014, 22(4), 862-872.

Bignami, A., Hosley, M.and Dahl, D. Hyaluronic acid and hyaluronic acid-binding proteins in brain extracellular matrix. Anat Embryol (Berl), Nov 1993, 188(5), 419-433.

Blesch, A.and Tuszynski, M. H. Spinal cord injury: plasticity, regeneration and the challenge of translational drug development. Trends Neurosci, Jan 2009, 32(1), 41-47.

Bollini, S., Gentili, C., Tasso, R.and Cancedda, R. The Regenerative Role of the Fetal and Adult Stem Cell Secretome. J Clin Med, Dec 17 2013, 2(4), 302-327.

Bonnans, C., Chou, J.and Werb, Z. Remodelling the extracellular matrix in development and disease. Nat Rev Mol Cell Biol, Dec 2014, 15(12), 786-801.

Borrie, S. C., Baeumer, B. E.and Bandtlow, C. E. The Nogo-66 receptor family in the intact and diseased CNS. Cell Tissue Res, Jul 2012, 349(1), 105-117.

Boudaoud, A., Burian, A., Borowska-Wykret, D., Uyttewaal, M., Wrzalik, R., Kwiatkowska, D. and Hamant, O. FibrilTool, an ImageJ plug-in to quantify fibrillar structures in raw microscopy images. Nat Protoc, Feb 2014, 9(2), 457-463.

Bouhadir, K. H.and Mooney, D. J. In vitro and in vivo models for the reconstruction of intercellular signaling. Ann N Y Acad Sci, Apr 15 1998, 842, 188-194.

Bozkurt, G., Mothe, A. J., Zahir, T., Kim, H., Shoichet, M. S.and Tator, C. H. Chitosan channels containing spinal cord-derived stem/progenitor cells for repair of subacute spinal cord injury in the rat. Neurosurgery, Dec 2010, 67(6), 1733-1744.

Bracken, M. B., Shepard, M. J., Collins, W. F., Holford, T. R., Young, W., Baskin, D. S., Eisenberg, H. M., Flamm, E., Leo-Summers, L., and Maroon, J. A randomized, controlled trial of methylprednisolone or naloxone in the treatment of acute spinal-cord injury. Results of the Second National Acute Spinal Cord Injury Study. N Engl J Med, May 17 1990, 322(20), 1405-1411.

Bracken, M. B., Shepard, M. J., Holford, T. R., Leo-Summers, L., Aldrich, E. F., Fazl, M., Fehlings, M., Herr, D. L., Hitchon, P. W., Marshall, L. F., Nockels, R. P., Pascale, V., Perot, P. L., Jr., Piepmeier, J., Sonntag, V. K., Wagner, F., Wilberger, J. E., Winn, H. R.and Young, W. Administration of methylprednisolone for 24 or 48 hours or tirilazad mesylate for 48 hours in the treatment of acute spinal cord injury. Results of the Third National Acute Spinal Cord Injury Randomized Controlled Trial. National Acute Spinal Cord Injury Study. JAMA, May 28 1997, 277(20), 1597-1604.

Breslin, K.and Agrawal, D. The use of methylprednisolone in acute spinal cord injury: a review of the evidence, controversies, and recommendations. Pediatr Emerg Care, Nov 2012, 28(11), 1238-1245; quiz 1246-1238.

Brown, B. N., Ratner, B. D., Goodman, S. B., Amar, S.and Badylak, S. F. Macrophage polarization: an opportunity for improved outcomes in biomaterials and regenerative medicine. Biomaterials, May 2012, 33(15), 3792-3802.

Brown, B. N., Valentin, J. E., Stewart-Akers, A. M., McCabe, G. P.and Badylak, S. F. Macrophage phenotype and remodeling outcomes in response to biologic scaffolds with and without a cellular component. Biomaterials, Mar 2009, 30(8), 1482-1491.

Callera, F.and do Nascimento, R. X. Delivery of autologous bone marrow precursor cells into the spinal cord via lumbar puncture technique in patients with spinal cord injury: a preliminary safety study. Exp Hematol, Feb 2006, 34(2), 130-131.

Cantinieaux, D., Quertainmont, R., Blacher, S., Rossi, L., Wanet, T., Noel, A., Brook, G., Schoenen, J.and Franzen, R. Conditioned medium from bone marrow-derived mesenchymal stem cells improves recovery after spinal cord injury in rats: an original strategy to avoid cell transplantation. PLoS One, 2013, 8(8), e69515.

Caplan, A. I. Mesenchymal Stem-Cells. Journal of Orthopaedic Research, Sep 1991, 9(5), 641-650.

Caplan, A. I. Adult mesenchymal stem cells for tissue engineering versus regenerative medicine. J Cell Physiol, Nov 2007, 213(2), 341-347.

Caplan, A. I. Why are MSCs therapeutic? New data: new insight. J Pathol, Jan 2009, 217(2), 318-324.

Caplan, A. I. Mesenchymal Stem Cells: Time to Change the Name! Stem Cells Transl Med, Jun 2017, 6(6), 1445-1451.

Caplan, A. I.and Dennis, J. E. Mesenchymal stem cells as trophic mediators. J Cell Biochem, Aug 01 2006, 98(5), 1076-1084.

Casha, S., Zygun, D., McGowan, M. D., Bains, I., Yong, V. W.and Hurlbert, R. J. Results of a phase II placebo-controlled randomized trial of minocycline in acute spinal cord injury. Brain, Apr 2012, 135(Pt 4), 1224-1236.

Cizkova, D., Kakinohana, O., Kucharova, K., Marsala, S., Johe, K., Hazel, T., Hefferan, M. P.and Marsala, M. Functional recovery in rats with ischemic paraplegia after spinal grafting of human spinal stem cells. Neuroscience, Jun 29 2007, 147(2), 546-560.

Conconi, M. T., Di Liddo, R., Tommasini, M., Calore, C.and Parnigotto, P. P. Phenotype and Differentiation Potential of Stromal Populations Obtained from Various Zones of Human Umbilical Cord: An Overview. The Open Tissue Engineering and Regenerative Medicine Journal, 2011, 4, 6-20.

Crapo, P. M., Gilbert, T. W.and Badylak, S. F. An overview of tissue and whole organ decellularization processes. Biomaterials, Apr 2011, 32(12), 3233-3243.

Crapo, P. M., Medberry, C. J., Reing, J. E., Tottey, S., van der Merwe, Y., Jones, K. E.and Badylak, S. F. Biologic scaffolds composed of central nervous system extracellular matrix. Biomaterials, May 2012, 33(13), 3539-3547.

Crapo, P. M., Tottey, S., Slivka, P. F.and Badylak, S. F. Effects of biologic scaffolds on human stem cells and implications for CNS tissue engineering. Tissue Eng Part A, Jan 2014, 20(1-2), 313-323.

Crigler, L., Robey, R. C., Asawachaicharn, A., Gaupp, D.and Phinney, D. G. Human mesenchymal stem cell subpopulations express a variety of neuro-regulatory molecules and promote neuronal cell survival and neuritogenesis. Exp Neurol, Mar 2006, 198(1), 54-64.

De Ugarte, D. A., Alfonso, Z., Zuk, P. A., Elbarbary, A., Zhu, M., Ashjian, P., Benhaim, P., Hedrick, M. H.and Fraser, J. K. Differential expression of stem cell mobilization-associated molecules on multi-lineage cells from adipose tissue and bone marrow. Immunol Lett, Oct 31 2003, 89(2-3), 267-270.

Deda, H., Inci, M. C., Kurekci, A. E., Kayihan, K., Ozgun, E., Ustunsoy, G. E.and Kocabay, S. Treatment of chronic spinal cord injured patients with autologous bone marrow-derived hematopoietic stem cell transplantation: 1-year follow-up. Cytotherapy, 2008, 10(6), 565-574.

DeQuach, J. A., Yuan, S. H., Goldstein, L. S.and Christman, K. L. Decellularized porcine brain matrix for cell culture and tissue engineering scaffolds. Tissue Eng Part A, Nov 2011, 17(21-22), 2583-2592.

Devine, S. M.and Hoffman, R. Role of mesenchymal stem cells in hematopoietic stem cell transplantation. Curr Opin Hematol, Nov 2000, 7(6), 358-363.

Dezawa, M., Ishikawa, H., Itokazu, Y., Yoshihara, T., Hoshino, M., Takeda, S., Ide, C.and Nabeshima, Y. Bone marrow stromal cells generate muscle cells and repair muscle degeneration. Science, Jul 08 2005, 309(5732), 314-317.

Di Nicola, M., Carlo-Stella, C., Magni, M., Milanesi, M., Longoni, P. D., Matteucci, P., Grisanti, S.and Gianni, A. M. Human bone marrow stromal cells suppress T-lymphocyte proliferation induced by cellular or nonspecific mitogenic stimuli. Blood, May 15 2002, 99(10), 3838-3843.

Di Santo, S., Yang, Z., Wyler von Ballmoos, M., Voelzmann, J., Diehm, N., Baumgartner, I.and Kalka, C. Novel cell-free strategy for therapeutic angiogenesis: in vitro generated conditioned medium can replace progenitor cell transplantation. PLoS One, May 21 2009, 4(5), e5643.

Ding, D. C., Shyu, W. C., Chiang, M. F., Lin, S. Z., Chang, Y. C., Wang, H. J., Su, C. Y.and Li, H. Enhancement of neuroplasticity through upregulation of beta1-integrin in human umbilical cord-derived stromal cell implanted stroke model. Neurobiol Dis, Sep 2007, 27(3), 339-353.

Djerbal, L., Lortat-Jacob, H.and Kwok, J. C. F. Chondroitin sulfates and their binding molecules in the central nervous system. Glycoconjugate Journal, Jun 2017, 34(3), 363-376.

Dominici, M., Le Blanc, K., Mueller, I., Slaper-Cortenbach, I., Marini, F., Krause, D., Deans, R., Keating, A., Prockop, D.and Horwitz, E. Minimal criteria for defining multipotent mesenchymal stromal cells. The International Society for Cellular Therapy position statement. Cytotherapy, 2006, 8(4), 315-317.

Dubsky, M., Jirkovska, A., Bem, R., Fejfarova, V., Pagacova, L., Nemcova, A., Sixta, B., Chlupac, J., Peregrin, J. H., Sykova, E.and Jude, E. B. Comparison of the effect of stem cell therapy and percutaneous transluminal angioplasty on diabetic foot disease in patients with critical limb ischemia. Cytotherapy, Dec 2014, 16(12), 1733-1738.

Dunlop, S. A. Activity-dependent plasticity: implications for recovery after spinal cord injury. Trends Neurosci, Aug 2008, 31(8), 410-418.

Erickson, A. C.and Couchman, J. R. Still more complexity in mammalian basement membranes. J Histochem Cytochem, Oct 2000, 48(10), 1291-1306.

Eva, R.and Fawcett, J. Integrin signalling and traffic during axon growth and regeneration. Curr Opin Neurobiol, Aug 2014, 27, 179-185.

Fahmy, G. H.and Moftah, M. Z. Fgf-2 in astroglial cells during vertebrate spinal cord recovery. Front Cell Neurosci, 2010, 4, 129.

Fawcett, J. W.and Asher, R. A. The glial scar and central nervous system repair. Brain Res Bull, Aug 1999, 49(6), 377-391.

Filbin, M. T. Myelin-associated inhibitors of axonal regeneration in the adult mammalian CNS. Nat Rev Neurosci, Sep 2003, 4(9), 703-713.

Flamm, E. S., Young, W., Collins, W. F., Piepmeier, J., Clifton, G. L.and Fischer, B. A phase I trial of naloxone treatment in acute spinal cord injury. J Neurosurg, Sep 1985, 63(3), 390-397.

Frankenberger, Z. De formatione granulosa in nervis aliisque úartibus organismi animalis - a comment. edited by J.E. PURKYNĚ. Edtion ed. Prague: State Medical Publishing, 1954.

Freytes, D. O., Martin, J., Velankar, S. S., Lee, A. S.and Badylak, S. F. Preparation and rheological characterization of a gel form of the porcine urinary bladder matrix. Biomaterials, Apr 2008, 29(11), 1630-1637.

Friedenstein, A. J., Petrakova, K. V., Kurolesova, A. I.and Frolova, G. P. Heterotopic of bone marrow. Analysis of precursor cells for osteogenic and hematopoietic tissues. Transplantation, Mar 1968, 6(2), 230-247.

Galili, U. Avoiding detrimental human immune response against Mammalian extracellular matrix implants. Tissue Eng Part B Rev, Apr 2015, 21(2), 231-241.

Gao, M., Lu, P., Bednark, B., Lynam, D., Conner, J. M., Sakamoto, J.and Tuszynski, M. H. Templated agarose scaffolds for the support of motor axon regeneration into sites of complete spinal cord transection. Biomaterials, Feb 2013, 34(5), 1529-1536.

Geffner, L. F., Santacruz, P., Izurieta, M., Flor, L., Maldonado, B., Auad, A. H., Montenegro, X., Gonzalez, R.and Silva, F. Administration of autologous bone marrow stem cells into spinal cord injury patients via multiple routes is safe and improves their quality of life: comprehensive case studies. Cell Transplant, 2008, 17(12), 1277-1293.

Gelman, R. A., Williams, B. R.and Piez, K. A. Collagen fibril formation. Evidence for a multistep process. J Biol Chem, Jan 10 1979, 254(1), 180-186.

Ghuman, H., Massensini, A. R., Donnelly, J., Kim, S. M., Medberry, C. J., Badylak, S. F.and Modo, M. ECM hydrogel for the treatment of stroke: Characterization of the host cell infiltrate. Biomaterials, Jun 2016, 91, 166-181.

Glennie, S., Soeiro, I., Dyson, P. J., Lam, E. W.and Dazzi, F. Bone marrow mesenchymal stem cells induce division arrest anergy of activated T cells. Blood, Apr 01 2005, 105(7), 2821-2827.

Gomes, M. E., Rodrigues, M. T., Domingues, R. M. A.and Reis, R. L. Tissue Engineering and Regenerative Medicine: New Trends and Directions-A Year in Review. Tissue Eng Part B Rev, Jun 2017, 23(3), 211-224.

Gronthos, S., Franklin, D. M., Leddy, H. A., Robey, P. G., Storms, R. W.and Gimble, J. M. Surface protein characterization of human adipose tissue-derived stromal cells. J Cell Physiol, Oct 2001, 189(1), 54-63.

Gros, T., Sakamoto, J. S., Blesch, A., Havton, L. A.and Tuszynski, M. H. Regeneration of long-tract axons through sites of spinal cord injury using templated agarose scaffolds. Biomaterials, Sep 2010, 31(26), 6719-6729.

Gruner, J. A. A monitored contusion model of spinal cord injury in the rat. J Neurotrauma, Summer 1992, 9(2), 123-126; discussion 126-128.

Gunn, J. W., Turner, S. D.and Mann, B. K. Adhesive and mechanical properties of hydrogels influence neurite extension. J Biomed Mater Res A, Jan 01 2005, 72(1), 91-97.

Hass, R., Kasper, C., Bohm, S.and Jacobs, R. Different populations and sources of human mesenchymal stem cells (MSC): A comparison of adult and neonatal tissue-derived MSC. Cell Commun Signal, May 14 2011, 9, 12.

Haynesworth, S. E., Baber, M. A.and Caplan, A. I. Cytokine expression by human marrow-derived mesenchymal progenitor cells in vitro: effects of dexamethasone and IL-1 alpha. J Cell Physiol, Mar 1996, 166(3), 585-592.

Hejcl, A., Lesny, P., Pradny, M., Michalek, J., Jendelova, P., Stulik, J.and Sykova, E. Biocompatible hydrogels in spinal cord injury repair. Physiol Res, 2008, 57 Suppl 3, S121-132.

Hejcl, A., Lesny, P., Pradny, M., Sedy, J., Zamecnik, J., Jendelova, P., Michalek, J.and Sykova, E. Macroporous hydrogels based on 2-hydroxyethyl methacrylate. Part 6: 3D hydrogels with positive and negative surface charges and polyelectrolyte complexes in spinal cord injury repair. J Mater Sci Mater Med, Jul 2009, 20(7), 1571-1577.

Hirano, Y.and Mooney, D. J. Peptide and protein presenting materials for tissue engineering. Advanced Materials, Jan 5 2004, 16(1), 17-25.

Hirbec, H., Gaviria, M.and Vignon, J. Gacyclidine: a new neuroprotective agent acting at the N-methyl-D-aspartate receptor. CNS Drug Rev, Summer 2001, 7(2), 172-198.

Ho, J. C., Lai, W. H., Li, M. F., Au, K. W., Yip, M. C., Wong, N. L., Ng, E. S., Lam, F. F., Siu, C. W.and Tse, H. F. Reversal of endothelial progenitor cell dysfunction in patients with type 2 diabetes using a conditioned medium of human embryonic stem cell-derived endothelial cells. Diabetes Metab Res Rev, Jul 2012, 28(5), 462-473.

Hoffmann, A., Czichos, S., Kaps, C., Bachner, D., Mayer, H., Kurkalli, B. G., Zilberman, Y., Turgeman, G., Pelled, G., Gross, G.and Gazit, D. The T-box transcription factor Brachyury mediates cartilage development in mesenchymal stem cell line C3H10T1/2. J Cell Sci, Feb 15 2002, 115(Pt 4), 769-781.

Holmes, B. B., Devos, S. L., Kfoury, N., Li, M., Jacks, R., Yanamandra, K., Ouidja, M. O., Brodsky, F. M., Marasa, J., Bagchi, D. P., Kotzbauer, P. T., Miller, T. M., Papy-Garcia, D.and Diamond, M. I. Heparan sulfate proteoglycans mediate internalization and propagation of specific proteopathic seeds. Proceedings of the National Academy of Sciences of the United States of America, Aug 13 2013, 110(33), E3138-E3147.

Horn, E. M., Beaumont, M., Shu, X. Z., Harvey, A., Prestwich, G. D., Horn, K. M., Gibson, A. R., Preul, M. C.and Panitch, A. Influence of cross-linked hyaluronic acid hydrogels on neurite outgrowth and recovery from spinal cord injury. J Neurosurg Spine, Feb 2007, 6(2), 133-140.

Hsu, J. Y.and Xu, X. M. Early profiles of axonal growth and astroglial response after spinal cord hemisection and implantation of Schwann cell-seeded guidance channels in adult rats. J Neurosci Res, Nov 15 2005, 82(4), 472-483.

Huang, P., Lin, L. M., Wu, X. Y., Tang, Q. L., Feng, X. Y., Lin, G. Y., Lin, X., Wang, H. W., Huang, T. H.and Ma, L. Differentiation of human umbilical cord Wharton's jelly-derived mesenchymal stem cells into germ-like cells in vitro. J Cell Biochem, Mar 1 2010, 109(4), 747-754.

Huebner, E. A.and Strittmatter, S. M. Axon regeneration in the peripheral and central nervous systems. Results Probl Cell Differ, 2009, 48, 339-351.

Hugnot, J. P.and Franzen, R. The spinal cord ependymal region: a stem cell niche in the caudal central nervous system. Front Biosci (Landmark Ed), Jan 01 2011, 16, 1044-1059.

Hultborn, H.and Malmsten, J. Changes in Segmental Reflexes Following Chronic Spinal-Cord Hemisection in the Cat .2. Conditioned Mono-Synaptic Test Reflexes. Acta Physiol Scand, 1983, 119(4), 423-433.

Chan, T. M., Harn, H. J., Lin, H. P., Chou, P. W., Chen, J. Y., Ho, T. J., Chiou, T. W., Chuang, H. M., Chiu, S. C., Chen, Y. C., Yen, S. Y., Huang, M. H., Liang, B. C.and Lin, S. Z. Improved human mesenchymal stem cell isolation. Cell Transplant, 2014, 23(4-5), 399-406.

Chen, J. L., Li, Y., Wang, L., Lu, M., Zhang, X. H.and Chopp, M. Therapeutic benefit of intracerebral transplantation of bone marrow stromal cells after cerebral ischemia in rats. J Neurol Sci, Aug 15 2001, 189(1-2), 49-57.

Cheng, H., Liu, X., Hua, R., Dai, G., Wang, X., Gao, J.and An, Y. Clinical observation of umbilical cord mesenchymal stem cell transplantation in treatment for sequelae of thoracolumbar spinal cord injury. J Transl Med, Sep 12 2014, 12(1), 253.

Christensen, M. D.and Hulsebosch, C. E. Chronic central pain after spinal cord injury. J Neurotrauma, Aug 1997, 14(8), 517-537.

Chvatal, A. Revealing the structure of the nervous tissue II: Gabriel Gustav Valentin (1810-1883), Robert Remak (1815-1865) and Jan Evangelista Purkyně (1787-1869). Cesk Fysiol, 2014, 63(2), 56-73.

Imhof, B. A. D., D Adv. Immunol. Edtion ed., 1995.

Inostroza-Brito, K. E., Collin, E. C., Majkowska, A., Elsharkawy, S., Rice, A., Del Rio Hernandez, A. E., Xiao, X., Rodriguez-Cabello, J.and Mata, A. Cross-linking of a biopolymer-peptide co-assembling system. Acta Biomater, Aug 2017, 58, 80-89.

Jiang, X. X., Zhang, Y., Liu, B., Zhang, S. X., Wu, Y., Yu, X. D.and Mao, N. Human mesenchymal stem cells inhibit differentiation and function of monocyte-derived dendritic cells. Blood, May 15 2005, 105(10), 4120-4126.

Jones, L. L., Sajed, D.and Tuszynski, M. H. Axonal regeneration through regions of chondroitin sulfate proteoglycan deposition after spinal cord injury: a balance of permissiveness and inhibition. J Neurosci, Oct 15 2003, 23(28), 9276-9288.

Kadam, S. S., Tiwari, S.and Bhonde, R. R. Simultaneous isolation of vascular endothelial cells and mesenchymal stem cells from the human umbilical cord. In Vitro Cell Dev Biol Anim, Jan-Feb 2009, 45(1-2), 23-27.

Kaplan, J. M., Youd, M. E.and Lodie, T. A. Immunomodulatory activity of mesenchymal stem cells. Curr Stem Cell Res Ther, Dec 2011, 6(4), 297-316.

Karsy, M.and Hawryluk, G. Pharmacologic Management of Acute Spinal Cord Injury. Neurosurg Clin N Am, Jan 2017, 28(1), 49-62.

Kato, M., Yoshimura, S., Kokuzawa, J., Kitajima, H., Kaku, Y., Iwama, T., Shinoda, J., Kunisada, T.and Sakai, N. Hepatocyte growth factor promotes neuronal differentiation of neural stem cells derived from embryonic stem cells. Neuroreport, Jan 19 2004, 15(1), 5-8.

Keane, T. J., DeWard, A., Londono, R., Saldin, L. T., Castleton, A. A., Carey, L., Nieponice, A., Lagasse, E.and Badylak, S. F. Tissue-Specific Effects of Esophageal Extracellular Matrix. Tissue Eng Part A, Sep 2015, 21(17-18), 2293-2300.

Kern, S., Eichler, H., Stoeve, J., Kluter, H.and Bieback, K. Comparative analysis of mesenchymal stem cells from bone marrow, umbilical cord blood, or adipose tissue. Stem Cells, May 2006, 24(5), 1294-1301.

Kinnaird, T., Stabile, E., Burnett, M. S., Lee, C. W., Barr, S., Fuchs, S.and Epstein, S. E. Marrow-derived stromal cells express genes encoding a broad spectrum of arteriogenic cytokines and promote in vitro and in vivo arteriogenesis through paracrine mechanisms. Circ Res, Mar 19 2004, 94(5), 678-685.

Knerlich-Lukoschus, F., von der Ropp-Brenner, B., Lucius, R., Mehdorn, H. M.and Held-Feindt, J. Chemokine expression in the white matter spinal cord precursor niche after force-defined spinal cord contusion injuries in adult rats. Glia, Jun 2010, 58(8), 916-931.

Krampera, M., Marconi, S., Pasini, A., Galie, M., Rigotti, G., Mosna, F., Tinelli, M., Lovato, L., Anghileri, E., Andreini, A., Pizzolo, G., Sbarbati, A.and Bonetti, B. Induction of neural-like differentiation in human mesenchymal stem cells derived from bone marrow, fat, spleen and thymus. Bone, Feb 2007, 40(2), 382-390.

Kubinova, S. New trends in spinal cord tissue engineering. Future Neurol, 2015, 10, 129.

Kubinova, S., Horak, D.and Sykova, E. Cholesterol-modified superporous poly(2-hydroxyethyl methacrylate) scaffolds for tissue engineering. Biomaterials, Sep 2009, 30(27), 4601-4609.

Kubinova, S.and Sykova, E. Biomaterials combined with cell therapy for treatment of spinal cord injury. Regen Med, Mar 2012, 7(2), 207-224.

Kuo, C. K.and Tuan, R. S. Mechanoactive tenogenic differentiation of human mesenchymal stem cells. Tissue Eng Part A, Oct 2008, 14(10), 1615-1627.

Kwok, J. C., Afshari, F., Garcia-Alias, G.and Fawcett, J. W. Proteoglycans in the central nervous system: plasticity, regeneration and their stimulation with chondroitinase ABC. Restor Neurol Neurosci, 2008, 26(2-3), 131-145.

Kwok, J. C. F., Dick, G., Wang, D. F.and Fawcett, J. W. Extracellular Matrix and Perineuronal Nets in CNS Repair. Dev Neurobiol, Nov 2011, 71(11), 1073-1089.

Kwon, B. K., Tetzlaff, W., Grauer, J. N., Beiner, J.and Vaccaro, A. R. Pathophysiology and pharmacologic treatment of acute spinal cord injury. Spine J, Jul-Aug 2004, 4(4), 451-464.

Lai, R. C., Chen, T. S.and Lim, S. K. Mesenchymal stem cell exosome: a novel stem cell-based therapy for cardiovascular disease. Regen Med, Jul 2011, 6(4), 481-492.

Leung, A., Crombleholme, T. M.and Keswani, S. G. Fetal wound healing: implications for minimal scar formation. Curr Opin Pediatr, Jun 2012, 24(3), 371-378.

Li, H., Wen, Y., Luo, Y., Lan, X., Wang, D., Sun, Z. and Hu, L. Transplantation of bone marrow mesenchymal stem cells into spinal cord injury: a comparison of delivery different times. Chinese J of Reg and Recon Surg, 2010, 24(2), 180-184.

Li, X., Xiao, Z., Han, J., Chen, L., Xiao, H., Ma, F., Hou, X., Sun, J., Ding, W., Zhao, Y., Chen, B.and Dai, J. Promotion of neuronal differentiation of neural progenitor cells by using EGFR antibody functionalized collagen scaffolds for spinal cord injury repair. Biomaterials, Jul 2013, 34(21), 5107-5116.

Li, Y., Chen, J., Chen, X. G., Wang, L., Gautam, S. C., Xu, Y. X., Katakowski, M., Zhang, L. J., Lu, M., Janakiraman, N.and Chopp, M. Human marrow stromal cell therapy for stroke in rat: neurotrophins and functional recovery. Neurology, Aug 27 2002, 59(4), 514-523.

Liu, S., Schackel, T., Weidner, N.and Puttagunta, R. Biomaterial-Supported Cell Transplantation Treatments for Spinal Cord Injury: Challenges and Perspectives. Front Cell Neurosci, 2017, 11, 430.

Long, J. B., Kinney, R. C., Malcolm, D. S., Graeber, G. M.and Holaday, J. W. Intrathecal dynorphin A (1-13) and (3-13) reduce spinal cord blood flow by non-opioid mechanisms. NIDA Res Monogr, 1986, 75, 524-526.

Low, K., Culbertson, M., Bradke, F., Tessier-Lavigne, M.and Tuszynski, M. H. Netrin-1 is a novel myelin-associated inhibitor to axon growth. J Neurosci, Jan 30 2008, 28(5), 1099-1108.

Lu, L. L., Liu, Y. J., Yang, S. G., Zhao, Q. J., Wang, X., Gong, W., Han, Z. B., Xu, Z. S., Lu, Y. X., Liu, D., Chen, Z. Z.and Han, Z. C. Isolation and characterization of human umbilical cord mesenchymal stem cells with hematopoiesis-supportive function and other potentials. Haematologica, Aug 2006, 91(8), 1017-1026.

Lu, P., Jones, L. L.and Tuszynski, M. H. BDNF-expressing marrow stromal cells support extensive axonal growth at sites of spinal cord injury. Exp Neurol, Feb 2005, 191(2), 344-360.

Lysak, D., Koutova, L., Holubova, M., Vlas, T., Miklikova, M.and Jindra, P. The Quality Control of Mesenchymal Stromal Cells by in Vitro Testing of Their Immunomodulatory Effect on Allogeneic Lymphocytes. Folia Biol (Praha), 2016, 62(3), 120-130.

Ma, L., Feng, X. Y., Cui, B. L., Law, F., Jiang, X. W., Yang, L. Y., Xie, Q. D.and Huang, T. H. Human umbilical cord Wharton's Jelly-derived mesenchymal stem cells differentiation into nerve-like cells. Chin Med J (Engl), Dec 5 2005, 118(23), 1987-1993.

McDonald, J. W.and Belegu, V. Demyelination and remyelination after spinal cord injury. J Neurotrauma, Mar-Apr 2006, 23(3-4), 345-359.

McElreavey, K. D., Irvine, A. I., Ennis, K. T.and McLean, W. H. Isolation, culture and characterisation of fibroblast-like cells derived from the Wharton's jelly portion of human umbilical cord. Biochem Soc Trans, Feb 1991, 19(1), 29S.

Medberry, C. J., Crapo, P. M., Siu, B. F., Carruthers, C. A., Wolf, M. T., Nagarkar, S. P., Agrawal, V., Jones, K. E., Kelly, J., Johnson, S. A., Velankar, S. S., Watkins, S. C., Modo, M.and Badylak, S. F. Hydrogels derived from central nervous system extracellular matrix. Biomaterials, Jan 2013, 34(4), 1033-1040.

Medicine, U. S. N. L. o. Spinal Cord Trauma 2011.

Meezan, E., Hjelle, J. T., Brendel, K.and Carlson, E. C. A simple, versatile, nondisruptive method for the isolation of morphologically and chemically pure basement membranes from several tissues. Life Sci, Dec 01 1975, 17(11), 1721-1732.

Meirelles Lda, S., Fontes, A. M., Covas, D. T.and Caplan, A. I. Mechanisms involved in the therapeutic properties of mesenchymal stem cells. Cytokine Growth Factor Rev, Oct-Dec 2009, 20(5-6), 419-427.

Meletis, K., Barnabe-Heider, F., Carlen, M., Evergren, E., Tomilin, N., Shupliakov, O.and Frisen, J. Spinal cord injury reveals multilineage differentiation of ependymal cells. PLoS Biol, Jul 22 2008, 6(7), e182.

Menasche, P.and Vanneaux, V. Stem cells for the treatment of heart failure. Curr Res Transl Med, Apr-Jun 2016, 64(2), 97-106.

Meng, F., Modo, M.and Badylak, S. F. Biologic scaffold for CNS repair. Regen Med, May 2014, 9(3), 367-383.

Metz, G. A.and Whishaw, I. Q. The ladder rung walking task: a scoring system and its practical application. J Vis Exp, Jun 12 2009, (28).

Mitalipov, S.and Wolf, D. Totipotency, pluripotency and nuclear reprogramming. Adv Biochem Eng Biotechnol, 2009, 114, 185-199.

Muguruma, Y., Yahata, T., Miyatake, H., Sato, T., Uno, T., Itoh, J., Kato, S., Ito, M., Hotta, T.and Ando, K. Reconstitution of the functional human hematopoietic microenvironment derived from human mesenchymal stem cells in the murine bone marrow compartment. Blood, Mar 01 2006, 107(5), 1878-1887.

Murakami, T.and Ohtsuka, A. Perisynaptic barrier of proteoglycans in the mature brain and spinal cord. Arch Histol Cytol, Aug 2003, 66(3), 195-207.

Murphy, M. B., Moncivais, K.and Caplan, A. I. Mesenchymal stem cells: environmentally responsive therapeutics for regenerative medicine. Exp Mol Med, Nov 15 2013, 45, e54.

Myers, J. P., Santiago-Medina, M.and Gomez, T. M. Regulation of axonal outgrowth and pathfinding by integrin-ECM interactions. Dev Neurobiol, Nov 2011, 71(11), 901-923.

Naranjo, J. D., Scarritt, M. E., Huleihel, L., Ravindra, A., Torres, C. M.and Badylak, S. F. Regenerative Medicine: lessons from Mother Nature. Regen Med, Dec 2016, 11(8), 767-775.

Neuhuber, B., Timothy Himes, B., Shumsky, J. S., Gallo, G.and Fischer, I. Axon growth and recovery of function supported by human bone marrow stromal cells in the injured spinal cord exhibit donor variations. Brain Res, Feb 21 2005, 1035(1), 73-85.

Noiseux, N., Gnecchi, M., Lopez-Ilasaca, M., Zhang, L., Solomon, S. D., Deb, A., Dzau, V. J.and Pratt, R. E. Mesenchymal stem cells overexpressing Akt dramatically repair infarcted myocardium and improve cardiac function despite infrequent cellular fusion or differentiation. Mol Ther, Dec 2006, 14(6), 840-850.

Novikova, L. N., Pettersson, J., Brohlin, M., Wiberg, M.and Novikov, L. N. Biodegradable poly-beta-hydroxybutyrate scaffold seeded with Schwann cells to promote spinal cord repair. Biomaterials, Mar 2008, 29(9), 1198-1206.

Ohab, J. J., Fleming, S., Blesch, A.and Carmichael, S. T. A neurovascular niche for neurogenesis after stroke. J Neurosci, Dec 13 2006, 26(50), 13007-13016.

Oki, M.and Ando, K. [Hematopoietic growth factors, cytokines, and bone-marrow microenvironment]. Nihon Rinsho, Mar 2008, 66(3), 444-452.

Orlic, D., Kajstura, J., Chimenti, S., Jakoniuk, I., Anderson, S. M., Li, B., Pickel, J., McKay, R., Nadal-Ginard, B., Bodine, D. M., Leri, A.and Anversa, P. Bone marrow cells regenerate infarcted myocardium. Nature, Apr 05 2001, 410(6829), 701-705.

Oswald, J., Boxberger, S., Jorgensen, B., Feldmann, S., Ehninger, G., Bornhauser, M.and Werner, C. Mesenchymal stem cells can be differentiated into endothelial cells in vitro. Stem Cells, 2004, 22(3), 377-384.

Pal, R., Gopinath, C., Rao, N. M., Banerjee, P., Krishnamoorthy, V., Venkataramana, N. K.and Totey, S. Functional recovery after transplantation of bone marrow-derived human mesenchymal stromal cells in a rat model of spinal cord injury. Cytotherapy, Oct 2010, 12(6), 792-806.

Pan, H. C., Cheng, F. C., Lai, S. Z., Yang, D. Y., Wang, Y. C.and Lee, M. S. Enhanced regeneration in spinal cord injury by concomitant treatment with granulocyte colony-stimulating factor and neuronal stem cells. J Clin Neurosci, Jun 2008, 15(6), 656-664.

Park, H. C., Shim, Y. S., Ha, Y., Yoon, S. H., Park, S. R., Choi, B. H.and Park, H. S. Treatment of complete spinal cord injury patients by autologous bone marrow cell transplantation and administration of granulocyte-macrophage colony stimulating factor. Tissue Eng, May-Jun 2005, 11(5-6), 913-922.

Park, H. W., Lim, M. J., Jung, H., Lee, S. P., Paik, K. S.and Chang, M. S. Human mesenchymal stem cell-derived Schwann cell-like cells exhibit neurotrophic effects, via distinct growth factor production, in a model of spinal cord injury. Glia, Jul 2010a, 58(9), 1118-1132.

Park, J., Lim, E., Back, S., Na, H., Park, Y.and Sun, K. Nerve regeneration following spinal cord injury using matrix metalloproteinase-sensitive, hyaluronic acid-based biomimetic hydrogel scaffold containing brain-derived neurotrophic factor. J Biomed Mater Res A, Jun 01 2010b, 93(3), 1091-1099.

Parr, A. M., Tator, C. H.and Keating, A. Bone marrow-derived mesenchymal stromal cells for the repair of central nervous system injury. Bone Marrow Transplant, Oct 2007, 40(7), 609-619.

Paunescu, V., Deak, E., Herman, D., Siska, I. R., Tanasie, G., Bunu, C., Anghel, S., Tatu, C. A., Oprea, T. I., Henschler, R., Ruster, B., Bistrian, R.and Seifried, E. In vitro differentiation of human mesenchymal stem cells to epithelial lineage. J Cell Mol Med, May-Jun 2007, 11(3), 502-508.

Pawitan, J. A. Prospect of stem cell conditioned medium in regenerative medicine. Biomed Res Int, 2014, 2014, 965849.

Pego, A. P., Kubinova, S., Cizkova, D., Vanicky, I., Mar, F. M., Sousa, M. M.and Sykova, E. Regenerative medicine for the treatment of spinal cord injury: more than just promises? J Cell Mol Med, Nov 2012, 16(11), 2564-2582.

Peng, L., Jia, Z., Yin, X., Zhang, X., Liu, Y., Chen, P., Ma, K.and Zhou, C. Comparative analysis of mesenchymal stem cells from bone marrow, cartilage, and adipose tissue. Stem Cells Dev, Aug 2008, 17(4), 761-773.

Peng, X., Zhou, Z., Hu, J., Fink, D. J.and Mata, M. Soluble Nogo receptor down-regulates expression of neuronal Nogo-A to enhance axonal regeneration. J Biol Chem, Jan 22 2010, 285(4), 2783-2795.

Peran, M., Marchal, J. A., Rodriguez-Serrano, F., Alvarez, P.and Aranega, A. Transdifferentiation: why and how? Cell Biol Int, Apr 2011, 35(4), 373-379.

Pittenger, M. F., Mackay, A. M., Beck, S. C., Jaiswal, R. K., Douglas, R., Mosca, J. D., Moorman, M. A., Simonetti, D. W., Craig, S.and Marshak, D. R. Multilineage potential of adult human mesenchymal stem cells. Science, Apr 02 1999, 284(5411), 143-147.

Pitts, L. H., Ross, A., Chase, G. A.and Faden, A. I. Treatment with thyrotropin-releasing hormone (TRH) in patients with traumatic spinal cord injuries. J Neurotrauma, Jun 1995, 12(3), 235-243.

Pollock, K., Stroemer, P., Patel, S., Stevanato, L., Hope, A., Miljan, E., Dong, Z., Hodges, H., Price, J.and Sinden, J. D. A conditionally immortal clonal stem cell line from human cortical neuroepithelium for the treatment of ischemic stroke. Exp Neurol, May 2006, 199(1), 143-155.

Prang, P., Muller, R., Eljaouhari, A., Heckmann, K., Kunz, W., Weber, T., Faber, C., Vroemen, M., Bogdahn, U.and Weidner, N. The promotion of oriented axonal regrowth in the injured spinal cord by alginate-based anisotropic capillary hydrogels. Biomaterials, Jul 2006, 27(19), 3560-3569.

Profyris, C., Cheema, S. S., Zang, D., Azari, M. F., Boyle, K.and Petratos, S. Degenerative and regenerative mechanisms governing spinal cord injury. Neurobiol Dis, Apr 2004, 15(3), 415-436.

Puissant, B., Barreau, C., Bourin, P., Clavel, C., Corre, J., Bousquet, C., Taureau, C., Cousin, B., Abbal, M., Laharrague, P., Penicaud, L., Casteilla, L.and Blancher, A. Immunomodulatory effect of human adipose tissue-derived adult stem cells: comparison with bone marrow mesenchymal stem cells. Br J Haematol, Apr 2005, 129(1), 118-129.

Raposo, G.and Stoorvogel, W. Extracellular vesicles: exosomes, microvesicles, and friends. J Cell Biol, Feb 18 2013, 200(4), 373-383.

Rehman, J., Traktuev, D., Li, J., Merfeld-Clauss, S., Temm-Grove, C. J., Bovenkerk, J. E., Pell, C. L., Johnstone, B. H., Considine, R. V.and March, K. L. Secretion of angiogenic and antiapoptotic factors by human adipose stromal cells. Circulation, Mar 16 2004, 109(10), 1292-1298.

Reuss, B. and von Bohlen und Halbach, O. Fibroblast growth factors and their receptors in the central nervous system. Cell Tissue Res, Aug 2003, 313(2), 139-157.

Rivlin, A. S.and Tator, C. H. Effect of duration of acute spinal cord compression in a new acute cord injury model in the rat. Surg Neurol, Jul 1978, 10(1), 38-43.

Rogers, S. L., Letourneau, P. C.and Pech, I. V. The role of fibronectin in neural development. Dev Neurosci, 1989, 11(4-5), 248-265.

Rota, M., Kajstura, J., Hosoda, T., Bearzi, C., Vitale, S., Esposito, G., Iaffaldano, G., Padin-Iregas, M. E., Gonzalez, A., Rizzi, R., Small, N., Muraski, J., Alvarez, R., Chen, X. W., Urbanek, K., Bolli, R., Houser, S. R., Leri, A., Sussman, M. A.and Anversa, P. Bone marrow cells adopt the cardiomyogenic fate in vivo. Proc Natl Acad Sci U S A, Nov 6 2007, 104(45), 17783-17788.

Rowland, J. W., Hawryluk, G. W., Kwon, B.and Fehlings, M. G. Current status of acute spinal cord injury pathophysiology and emerging therapies: promise on the horizon. Neurosurg Focus, 2008, 25(5), E2.

Ruzicka, J., Machova-Urdzikova, L., Gillick, J., Amemori, T., Romanyuk, N., Karova, K., Zaviskova, K., Dubisova, J., Kubinova, S., Murali, R., Sykova, E., Jhanwar-Uniyal, M.and Jendelova, P. A Comparative Study of Three Different Types of Stem Cells for Treatment of Rat Spinal Cord Injury. Cell Transplant, Apr 13 2017, 26(4), 585-603.

Ruzicka, J., Romanyuk, N., Hejcl, A., Vetrik, M., Hruby, M., Cocks, G., Cihlar, J., Pradny, M., Price, J., Sykova, E.and Jendelova, P. Treating spinal cord injury in rats with a combination of human fetal

neural stem cells and hydrogels modified with serotonin. Acta Neurobiol Exp (Wars), 2013, 73(1), 102-115.

Sadat, S., Gehmert, S., Song, Y. H., Yen, Y., Bai, X., Gaiser, S., Klein, H.and Alt, E. The cardioprotective effect of mesenchymal stem cells is mediated by IGF-I and VEGF. Biochem Biophys Res Commun, Nov 23 2007, 363(3), 674-679.

Sadir, R., Forest, E.and Lortat-Jacob, H. The heparan sulfate binding sequence of interferon-gamma increased the on rate of the interferon-gamma-interferon-gamma receptor complex formation. J Biol Chem, May 01 1998, 273(18), 10919-10925.

Salazar, D. L., Uchida, N., Hamers, F. P., Cummings, B. J.and Anderson, A. J. Human neural stem cells differentiate and promote locomotor recovery in an early chronic spinal cord injury NOD-scid mouse model. PLoS One, Aug 18 2010, 5(8), e12272.

Sato, Y., Araki, H., Kato, J., Nakamura, K., Kawano, Y., Kobune, M., Sato, T., Miyanishi, K., Takayama, T., Takahashi, M., Takimoto, R., Iyama, S., Matsunaga, T., Ohtani, S., Matsuura, A., Hamada, H.and Niitsu, Y. Human mesenchymal stem cells xenografted directly to rat liver are differentiated into human hepatocytes without fusion. Blood, Jul 15 2005, 106(2), 756-763.

Seif-Naraghi, S. B., Horn, D., Schup-Magoffin, P. J.and Christman, K. L. Injectable extracellular matrix derived hydrogel provides a platform for enhanced retention and delivery of a heparin-binding growth factor. Acta Biomater, Oct 2012, 8(10), 3695-3703.

Shen, Y., Qian, Y., Zhang, H., Zuo, B., Lu, Z., Fan, Z., Zhang, P., Zhang, F.and Zhou, C. Guidance of olfactory ensheathing cell growth and migration on electrospun silk fibroin scaffolds. Cell Transplant, 2010, 19(2), 147-157.

Shim, W. S., Jiang, S., Wong, P., Tan, J., Chua, Y. L., Tan, Y. S., Sin, Y. K., Lim, C. H., Chua, T., Teh, M., Liu, T. C.and Sim, E. Ex vivo differentiation of human adult bone marrow stem cells into cardiomyocyte-like cells. Biochem Biophys Res Commun, Nov 12 2004, 324(2), 481-488.

Shiota, G.and Itaba, N. Progress in stem cell-based therapy for liver disease. Hepatol Res, May 18 2016.

Schwartz, G.and Fehlings, M. G. Evaluation of the neuroprotective effects of sodium channel blockers after spinal cord injury: improved behavioral and neuroanatomical recovery with riluzole. J Neurosurg, Apr 2001, 94(2 Suppl), 245-256.

Siegel, G., Schafer, R.and Dazzi, F. The immunosuppressive properties of mesenchymal stem cells. Transplantation, May 15 2009, 87(9 Suppl), S45-49.

Silver, J.and Miller, J. H. Regeneration beyond the glial scar. Nat Rev Neurosci, Feb 2004, 5(2), 146-156.

Singelyn, J. M.and Christman, K. L. Injectable materials for the treatment of myocardial infarction and heart failure: the promise of decellularized matrices. J Cardiovasc Transl Res, Oct 2010, 3(5), 478-486.

Skalnikova, H. K. Proteomic techniques for characterisation of mesenchymal stem cell secretome. Biochimie, Dec 2013, 95(12), 2196-2211.

Smith, P. D., Coulson-Thomas, V. J., Foscarin, S., Kwok, J. C.and Fawcett, J. W. "GAG-ing with the neuron": The role of glycosaminoglycan patterning in the central nervous system. Exp Neurol, Dec 2015, 274(Pt B), 100-114.

Sosa, I., Reyes, O.and Kuffler, D. P. Immunosuppressants: neuroprotection and promoting neurological recovery following peripheral nerve and spinal cord lesions. Exp Neurol, Sep 2005, 195(1), 7-15.

Sponer, P., Filip, S., Kucera, T., Brtkova, J., Urban, K., Palicka, V., Koci, Z., Syka, M., Bezrouk, A.and Sykova, E. Utilizing Autologous Multipotent Mesenchymal Stromal Cells and beta-Tricalcium Phosphate Scaffold in Human Bone Defects: A Prospective, Controlled Feasibility Trial. Biomed Res Int, 2016, 2016, 2076061.

Stenudd, M., Sabelstrom, H.and Frisen, J. Role of endogenous neural stem cells in spinal cord injury and repair. JAMA Neurol, Feb 2015, 72(2), 235-237.

Straley, K. S., Foo, C. W.and Heilshorn, S. C. Biomaterial design strategies for the treatment of spinal cord injuries. J Neurotrauma, Jan 2010, 27(1), 1-19.

Strioga, M., Viswanathan, S., Darinskas, A., Slaby, O.and Michalek, J. Same or not the same? Comparison of adipose tissue-derived versus bone marrow-derived mesenchymal stem and stromal cells. Stem Cells Dev, Sep 20 2012, 21(14), 2724-2752.

Sykova, E., Homola, A., Mazanec, R., Lachmann, H., Konradova, S. L., Kobylka, P., Padr, R., Neuwirth, J., Komrska, V., Vavra, V., Stulik, J.and Bojar, M. Autologous bone marrow transplantation in patients with subacute and chronic spinal cord injury. Cell Transplant, 2006, 15(8-9), 675-687.

Tadie, M. Multicenter study of patients with acute spinal cord injury. Bulletin De L Academie Nationale De Medecine, Jun 2005, 189(6), 1133-1134.

Takahashi, K., Tanabe, K., Ohnuki, M., Narita, M., Ichisaka, T., Tomoda, K.and Yamanaka, S. Induction of pluripotent stem cells from adult human fibroblasts by defined factors. Cell, Nov 30 2007, 131(5), 861-872.

Takahashi, K.and Yamanaka, S. Induction of pluripotent stem cells from mouse embryonic and adult fibroblast cultures by defined factors. Cell, Aug 25 2006, 126(4), 663-676.

Tang, X., Davies, J. E.and Davies, S. J. Changes in distribution, cell associations, and protein expression levels of NG2, neurocan, phosphacan, brevican, versican V2, and tenascin-C during acute to chronic maturation of spinal cord scar tissue. J Neurosci Res, Feb 01 2003, 71(3), 427-444.

Tator, C. H.and Fehlings, M. G. Review of the secondary injury theory of acute spinal cord trauma with emphasis on vascular mechanisms. J Neurosurg, Jul 1991, 75(1), 15-26.

Taylor, S. J., McDonald, J. W., 3rd and Sakiyama-Elbert, S. E. Controlled release of neurotrophin-3 from fibrin gels for spinal cord injury. J Control Release, Aug 11 2004, 98(2), 281-294.

Teng, Y. D., Lavik, E. B., Qu, X. L., Park, K. I., Ourednik, J., Zurakowski, D., Langer, R.and Snyder, E. Y. Functional recovery following traumatic spinal cord injury mediated by a unique polymer scaffold seeded with neural stem cells (vol 99, pg 3024, 2002). Proceedings of the National Academy of Sciences of the United States of America, Jul 9 2002, 99(14), 9606-9606.

Tester, N. J.and Howland, D. R. Chondroitinase ABC improves basic and skilled locomotion in spinal cord injured cats. Exp Neurol, Feb 2008, 209(2), 483-496.

Tetzlaff, W., Okon, E. B., Karimi-Abdolrezaee, S., Hill, C. E., Sparling, J. S., Plemel, J. R., Plunet, W. T., Tsai, E. C., Baptiste, D., Smithson, L. J., Kawaja, M. D., Fehlings, M. G.and Kwon, B. K. A Systematic Review of Cellular Transplantation Therapies for Spinal Cord Injury. Journal of Neurotrauma, Aug 2011, 28(8), 1611-1682.

Thiele, J., Varus, E., Wickenhauser, C., Kvasnicka, H. M., Lorenzen, J., Gramley, F., Metz, K. A., Rivero, F.and Beelen, D. W. Mixed chimerism of cardiomyocytes and vessels after allogeneic bone marrow and stem-cell transplantation in comparison with cardiac allografts. Transplantation, Jun 27 2004, 77(12), 1902-1905.

Timper, K., Seboek, D., Eberhardt, M., Linscheid, P., Christ-Crain, M., Keller, U., Muller, B.and Zulewski, H. Human adipose tissue-derived mesenchymal stem cells differentiate into insulin, somatostatin, and glucagon expressing cells. Biochem Biophys Res Commun, Mar 24 2006, 341(4), 1135-1140.

Torres-Espin, A., Santos, D., Gonzalez-Perez, F., del Valle, J.and Navarro, X. Neurite-J: an image-J plug-in for axonal growth analysis in organotypic cultures. J Neurosci Methods, Oct 30 2014, 236, 26-39.

Tottey, S., Corselli, M., Jeffries, E. M., Londono, R., Peault, B.and Badylak, S. F. Extracellular matrix degradation products and low-oxygen conditions enhance the regenerative potential of perivascular stem cells. Tissue Eng Part A, Jan 2011, 17(1-2), 37-44.

Tran, C.and Damaser, M. S. Stem cells as drug delivery methods: application of stem cell secretome for regeneration. Adv Drug Deliv Rev, Mar 2015, 82-83, 1-11.

Troyer, D. L.and Weiss, M. L. Wharton's jelly-derived cells are a primitive stromal cell population. Stem Cells, Mar 2008, 26(3), 591-599.

Tsai, E. C., Dalton, P. D., Shoichet, M. S.and Tator, C. H. Synthetic hydrogel guidance channels facilitate regeneration of adult rat brainstem motor axons after complete spinal cord transection. J Neurotrauma, Jun 2004, 21(6), 789-804.

Ungerleider, J. L., Johnson, T. D., Hernandez, M. J., Elhag, D. I., Braden, R. L., Dzieciatkowska, M., Osborn, K. G., Hansen, K. C., Mahmud, E.and Christman, K. L. Extracellular Matrix Hydrogel Promotes Tissue Remodeling, Arteriogenesis, and Perfusion in a Rat Hindlimb Ischemia Model. JACC Basic Transl Sci, Jan-Feb 2016, 1(1-2), 32-44.

Urdzikova, L., Jendelova, P., Glogarova, K., Burian, M., Hajek, M.and Sykova, E. Transplantation of bone marrow stem cells as well as mobilization by granulocyte-colony stimulating factor promotes recovery after spinal cord injury in rats. J Neurotrauma, Sep 2006, 23(9), 1379-1391.

Urdzikova, L. M., Ruzicka, J., LaBagnara, M., Karova, K., Kubinova, S., Jirakova, K., Murali, R., Sykova, E., Jhanwar-Uniyal, M.and Jendelova, P. Human Mesenchymal Stem Cells Modulate Inflammatory Cytokines after Spinal Cord Injury in Rat. International Journal of Molecular Sciences, Jul 2014, 15(7), 11275-11293.

Valentin, J. E., Stewart-Akers, A. M., Gilbert, T. W.and Badylak, S. F. Macrophage participation in the degradation and remodeling of extracellular matrix scaffolds. Tissue Eng Part A, Jul 2009, 15(7), 1687-1694.

Van Meeteren, N. L., Eggers, R., Lankhorst, A. J., Gispen, W. H.and Hamers, F. P. Locomotor recovery after spinal cord contusion injury in rats is improved by spontaneous exercise. J Neurotrauma, Oct 2003, 20(10), 1029-1037.

Vanicky, I., Urdzikova, L., Saganova, K., Cizkova, D.and Galik, J. A simple and reproducible model of spinal cord injury induced by epidural balloon inflation in the rat. J Neurotrauma, Dec 2001, 18(12), 1399-1407.

Verdu, E., Garcia-Alias, G., Fores, J., Vela, J. M., Cuadras, J., Lopez-Vales, R.and Navarro, X. Morphological characterization of photochemical graded spinal cord injury in the rat. J Neurotrauma, May 2003, 20(5), 483-499.

Wang, C., Sun, C., Hu, Z., Huo, X., Yang, Y., Liu, X., Botchway, B. O. A., Davies, H.andFang, M. Improved Neural Regeneration with Olfactory Ensheathing Cell Inoculated PLGA Scaffolds in Spinal Cord Injury Adult Rats. Neurosignals, 2017, 25(1), 1-14.

Wang, H., Lin, X. F., Wang, L. R., Lin, Y. Q., Wang, J. T., Liu, W. Y., Zhu, G. Q., Braddock, M., Zhong, M.and Zheng, M. H. Decellularization technology in CNS tissue repair. Expert Rev Neurother, May 2015, 15(5), 493-500.

Wang, R. M.and Christman, K. L. Decellularized myocardial matrix hydrogels: In basic research and preclinical studies. Adv Drug Deliv Rev, Jan 15 2016, 96, 77-82.

Wang, T. W.and Spector, M. Development of hyaluronic acid-based scaffolds for brain tissue engineering. Acta Biomater, Sep 2009, 5(7), 2371-2384.

Wisniewski, J. R., Zougman, A., Nagaraj, N.and Mann, M. Universal sample preparation method for proteome analysis. Nat Methods, May 2009, 6(5), 359-362.

Woerly, S., Fort, S., Pignot-Paintrand, I., Cottet, C., Carcenac, C.and Savasta, M. Development of a sialic acid-containing hydrogel of poly[N-(2-hydroxypropyl) methacrylamide]: characterization and implantation study. Biomacromolecules, Sep 2008, 9(9), 2329-2337.

Wolf, M. T., Daly, K. A., Brennan-Pierce, E. P., Johnson, S. A., Carruthers, C. A., D'Amore, A., Nagarkar, S. P., Velankar, S. S.and Badylak, S. F. A hydrogel derived from decellularized dermal extracellular matrix. Biomaterials, Oct 2012, 33(29), 7028-7038.

Wong, W. K., Cheung, A. W., Yu, S. W., Sha, O.and Cho, E. Y. Hepatocyte growth factor promotes long-term survival and axonal regeneration of retinal ganglion cells after optic nerve injury: comparison with CNTF and BDNF. CNS Neurosci Ther, Oct 2014, 20(10), 916-929.

Wu, Y., Chen, L., Scott, P. G.and Tredget, E. E. Mesenchymal stem cells enhance wound healing through differentiation and angiogenesis. Stem Cells, Oct 2007, 25(10), 2648-2659.

Yamaguchi, Y. Lecticans: organizers of the brain extracellular matrix. Cell Mol Life Sci, Feb 2000, 57(2), 276-289.

Yang, Z. X., Han, Z. B., Ji, Y. R., Wang, Y. W., Liang, L., Chi, Y., Yang, S. G., Li, L. N., Luo, W. F., Li, J. P., Chen, D. D., Du, W. J., Cao, X. C., Zhuo, G. S., Wang, T.and Han, Z. C. CD106 identifies a subpopulation of mesenchymal stem cells with unique immunomodulatory properties. PLoS One, 2013, 8(3), e59354.

Yezierski, R. P., Liu, S., Ruenes, G. L., Kajander, K. J.and Brewer, K. L. Excitotoxic spinal cord injury: behavioral and morphological characteristics of a central pain model. Pain, Mar 1998, 75(1), 141-155.

Yoon, S. H., Shim, Y. S., Park, Y. H., Chung, J. K., Nam, J. H., Kim, M. O., Park, H. C., Park, S. R., Min, B. H., Kim, E. Y., Choi, B. H., Park, H.and Ha, Y. Complete spinal cord injury treatment using autologous bone marrow cell transplantation and bone marrow stimulation with granulocyte macrophage-colony stimulating factor: Phase I/II clinical trial. Stem Cells, Aug 2007, 25(8), 2066-2073.

Yoshii, A.and Constantine-Paton, M. Postsynaptic BDNF-TrkB signaling in synapse maturation, plasticity, and disease. Dev Neurobiol, Apr 2010, 70(5), 304-322.

Young, D. A., Ibrahim, D. O., Hu, D.and Christman, K. L. Injectable hydrogel scaffold from decellularized human lipoaspirate. Acta Biomater, Mar 2011, 7(3), 1040-1049.

Yun, Y. R., Won, J. E., Jeon, E., Lee, S., Kang, W., Jo, H., Jang, J. H., Shin, U. S.and Kim, H. W. Fibroblast growth factors: biology, function, and application for tissue regeneration. J Tissue Eng, Nov 07 2010, 2010, 218142.

Zeng, X., Qiu, X. C., Ma, Y. H., Duan, J. J., Chen, Y. F., Gu, H. Y., Wang, J. M., Ling, E. A., Wu, J. L., Wu, W.and Zeng, Y. S. Integration of donor mesenchymal stem cell-derived neuron-like cells into host neural network after rat spinal cord transection. Biomaterials, Jun 2015, 53, 184-201.

Zhao, L. R., Duan, W. M., Reyes, M., Keene, C. D., Verfaillie, C. M.and Low, W. C. Human bone marrow stem cells exhibit neural phenotypes and ameliorate neurological deficits after grafting into the ischemic brain of rats. Exp Neurol, Mar 2002, 174(1), 11-20.

Zhao, P., Feng, S., Wang, Y. P. Z. and Feng, S. Q. Effect of different concentration of human umbilical cord mesenchymal stem cells in experimental spinal cord injury in rats. Orthop J of China, 2010, 18, 1817-1825.

Zhao, S., Wehner, R., Bornhauser, M., Wassmuth, R., Bachmann, M. and Schmitz, M. Immunomodulatory properties of mesenchymal stromal cells and their therapeutic consequences for immune-mediated disorders. Stem Cells Dev, May 2010, 19(5), 607-614.

Zhou, C., Yang, B., Tian, Y., Jiao, H., Zheng, W., Wang, J.and Guan, F. Immunomodulatory effect of human umbilical cord Wharton's jelly-derived mesenchymal stem cells on lymphocytes. Cell Immunol, 2011, 272(1), 33-38.

Zingale, A. An experimental model to study axonal regeneration of the rat spinal cord. J Neurosurg Sci, Oct-Dec 1989, 33(4), 329-331.

Zuk, P. A., Zhu, M., Mizuno, H., Huang, J., Futrell, J. W., Katz, A. J., Benhaim, P., Lorenz, H. P.and Hedrick, M. H. Multilineage cells from human adipose tissue: implications for cell-based therapies. Tissue Eng, Apr 2001, 7(2), 211-228.

14 AUTHOR´S PUBLICATIONS

Publications relevant to this Ph.D. thesis:

1. Krůpa P, Vacková I, Růžička J, Závisková K, Dubišová J, **Kočí Z**, Turnovcová K, Machova-Urdzíková L, Kubinová Š, Rehak S, Jendelova P. The Effect of Human Mesenchymal Stem Cells Derived from Wharton´s Jelly in Spinal Cord Injury Treatment is Dose-dependent and Can Be Facilitated by Repeated Application. Int J Mol Sci. 2018 May 17; 19(5). pii: E1503. doi: 10.3390/ijms19051503. IF 3.482
   Author contribution: 20%; cell isolation, cell culture, cell analysis, preparation of manuscript

2. Tukmachev D, Forostyak S, **Kočí Z**, Závišková K, Vacková I, Výborný K, Sandvig I, Sandvig A, Medberry Ch, Badylak S, Syková E, Kubinová Š. Injectable Extracellular Matrix Hydrogels as Scaffolds for Spinal Cord Injury Repair. Tissue Eng Part A. 2016 Feb;22(3-4):306-17. doi: 10.1089/ten.TEA.2015.0422. IF 4.92; 23 citations
   Author contribution: 30%; ECM extraction, cell culture, immunohistochemistry, microscopy, analysis of data, preparation of manuscript

3. **Kočí Z**, Výborný K, Dubišová J, Vacková I, Jäger A, Lunov O, Jiráková K, Kubinová Š. Extracellular Matrix Hydrogel Derived from Human Umbilical Cord as a Scaffold for Neural Tissue Repair and Its Comparison with Extracellular Matrix from Porcine Tissues. Tissue Eng Part C Methods. 2017 Jun; 23(6):333-345. doi: 10.1089/ten.TEC.2017.0089. IF 3.485; 4 citations
   Author contribution: 60%; biomaterial characterisation, dsDNA, sGAG, collagen quantification, cell isolation, cell culture, cell proliferation, migration, immunohistochemistry, microscopy, analysis of data, preparation of manuscript

Other publications:

1. **Kočí Z**, Boráň T, Krůpa P, Kubinová Š. The current state of Advanced Therapy Medicinal Products in the Czech Republic. Hum Gene Ther Clin Dev. 2018 Jun 5. doi: 10.1089/humc.2018.035. [Epub ahead of print]. IF 4.218
2. Školoudík L, Chrobok V, **Kočí Z**, Popelář J, Syka J, Laco J, Filipová A, Syková E, Filip S. The Transplantation of hBM-MSCs Increases Bone Neo-Formation and Preserves Hearing Function in the Treatment of Temporal Bone Defects- on the Experience of Two Month Follow Up. Stem Cell Rev. 2018 Jun 3. doi: 10.1007/s12015-018-9831-z. [Epub ahead of print]. IF 2.967
3. Tuček L, **Kočí Z**, Kárová K, Doležalová H, Suchánek J. The Osteogenic Potential of Human Non-differentiated and Pre-differentiated Mesenchymal Stem Cells Combined with an Osteoconductive Scaffold – Early Stage Healing. Acta Medica 2017; 60(1):12-18. doi:10.14712/18059694.2017 Mar 6. IF 0.67
4. Šponer P, Filip S, Kucera T, Brtková J, Urban K, Palička V, **Kočí Z**, Syka M, Bezrouk A, Syková E. Utilizing Autologous Multipotent Mesenchymal Stromal Cells and ß-Tricalcium Phosphate Scaffold in Human Bone Defects: A Prospective, Controlled Feasibility Trial. BioMed Res Int.2016. ;2016:2076061. doi: 10.1155/2016/2076061. Epub 2016 Apr 7. IF 3.169

5. Školoudík L, Chrobok V, Kalfert D, **Kočí Z**, Syková E, Chumak T, Popelář J, Syka J, Laco J, Dedková J, Dayanithi G, Filip S. Human Multipotent Mesenchymal Stromal Cells in the Treatment of Postoperative Temporal Bone Defect: an Animal Model. Cell Transplant. 2016;25(7):1405-14. doi: 10.3727/096368915X689730. Epub 2015 Oct 22. IF 3.127
6. Havlas V, Kotaška J, Koníček P, Trč T, Konrádová Š, **Kočí Z**, Syková E. Use of Cultured Human Autologous Bone Marrow Stem Cells in Repair of a Rotator Cuff Tear: Preliminary Results of a Safety Study. Acta Chir Orthop Traumatol Cech. 2015 Aug; 82(3):229-34. IF 0.39
7. **Kočí Z**, Turnovcová K, Dubský M, Baranovičová L, Holáň V, Chudíčková M, Syková E, Kubinová Š. Characterization of Human Adipose Tissue-derived Stromal Cells Isolated from Diabetic Patient's Distal Limbs with Critical Ischemia. Cell Biochem and Funct. 2014 Oct; 32(7): 597-604. doi:10.1002/cbf.3056. IF 2.01; 15 citations
8. Školoudík L, Chrobok V, Kalfert D, **Kočí Z**, Filip S. Multipotent Mesenchymal Stromal Cells in Otorhinolaryngology. Medical Hypotheses 2014 Jun; 82(6):769-773. doi:10.1016/j.mehy.2014.03.022. Epub 2014 Mar 27. Review. IF 1.07
9. Školoudík L, Chrobok V, Kalfert D, **Kočí Z**, Syková E, Filip S. Nové léčebné postupy s využitím mezenchymálních kmenových buněk (MSC) v otorinolaryngologii. Otolaryngologie a Foniatrie 2016; 65 (2): 97-101. IF 0.08
10. Stariat J, Šesták V, Vávrová K, Nobilis M, **Kollárová Z**, Klimeš J, Kalonowski S D, Richardson R D, Kovaříková P. LC-MS/MS Identification of the Principal *In vitro* and *In vivo* Phase I Metabolites of the Novel Thiosemicarbazone Anti-cancer Drug, Bp4eT. Anal Bioanal Chem 2012 APR; 403(1):309-21. doi:10.1007/s00216-012-5766-4. IF 3.44; 12 citations